Reviews in Mineralogy & Geochemistry
Vol. 83 pp. 469–533, 2017

Garnet: A Rock-Forming Mineral Petrochronometer

E.F. Baxter
Department of Earth and Environmental Sciences
Boston College
Chestnut Hill, Massachusetts 02467
USA
baxteret@bc.edu

M.J. Caddick
Department of Geosciences
Virginia Tech
Blacksburg, Virginia 24060
USA
caddick@vt.edu

B. Dragovic
Department of Geosciences
Virginia Tech
Blacksburg, Virginia 24060
USA
dragovic@vt.edu

INTRODUCTION

Garnet could be the ultimate petrochronometer. Not only can you date it directly (with an accuracy and precision that may surprise some), but it is also a common rock-forming and porphyroblast-forming mineral, with wide ranging—yet thermodynamically well understood—solid solution that provides direct and quantitative petrologic context. While accessory phase petrochronology is based largely upon establishing links to the growth or breakdown of key rock-forming pressure–temperature–composition (*P–T–X*) indicators (e.g., Rubatto 2002; Williams et al. 2007), garnet *is* one of those key indicator minerals. Garnet occurs in a great variety of rock types (see Baxter et al. 2013) and is frequently zoned (texturally, chemically) meaning that it contains more than just a snapshot of metamorphic conditions, but rather a semi-continuous history of evolving tectonometamorphic conditions during its often prolonged growth. In this way, garnet and its growth zonation have been likened to dendrochronology: garnet as the tree rings of evolving tectonometamorphic conditions (e.g., Pollington and Baxter 2010).

In some ways, the dream of 'petrochronology' all started with garnet (Fig. 1). When Atherton and Edmunds (1965) or Hollister (1966) recognized the chemical zonation in garnet, when Rosenfeld (1968) noted the spiral 'snowball' of inclusions in rotated garnet, or when Tracy et al. (1976) drew the first 2-D map of garnet chemical zonation, illuminating those 'tree-rings' for the first time, they could only imagine what is now a reality decades later—direct zoned garnet geochronology of those concentric rings of growth. Geoscientists soon thereafter attempted the first garnet geochronology (van Breemen and Hawkesworth 1980), though several factors severely limited the development and wider-spread use of

1529-6466/17/0083-0015$5.00 (print)
1943-2666/17/0083-0015$5.00 (online)
http://dx.doi.org/10.2138/rmg.2017.83.15

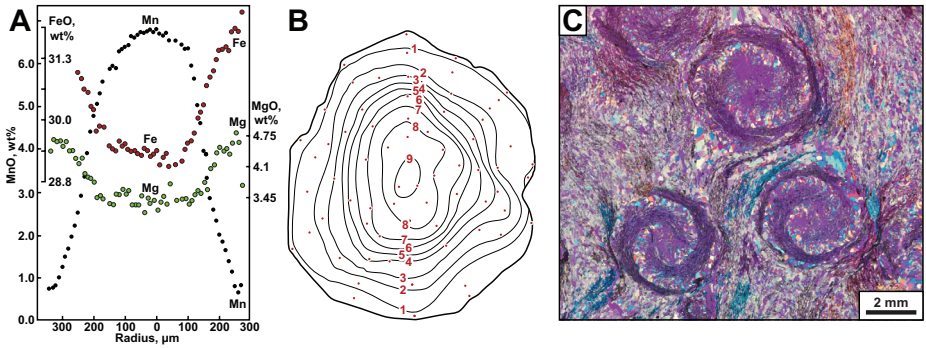

Figure 1. Important observations in the development of garnet petrochronology. **A.** Chemical zoning in a 1-D traverse across garnet from the Kwoiek area of British Columbia (redrawn from Hollister 1966). The 'bell-shaped' Mn zoning profile led to the now classic interpretation of garnet growth adhering to a Rayleigh fractionation model. **B.** 2-D zoning of Mn in garnet from central Massachusetts (redrawn from Tracy et al 1976, numbers equate to atomic percent Mn and dots indicate position of microprobe analyses). **C.** Spiral 'snowball' inclusions in rotated garnet described by Rosenfeld (1968); image shown is from thin section with first-order red filter provided by John Rosenfeld.

garnet geochronology from that point. These factors included 1) contamination of garnet by micro-mineral inclusions, 2) analytical limitations of small sample size, 3) the requirement of anchoring a garnet age analysis with another point on an isochron, and 4) the significant time and effort required for age determination. Even today, whether via MC-ICPMS or TIMS (e.g., Schoene and Baxter 2017, this volume), garnet geochronology requires weeks of time-consuming sample preparation. So, while petrologists boldly forged ahead in the use and development of garnet as probably the premier mineral recorder of evolving metamorphic and tectonic processes during the 1970's, 80's and 90's, garnet geochronology was mostly (though not completely) supplanted by the excitement, relative ease and undoubted utility of accessory phase geochronology (as reviewed by Engi 2017, this volume; Rubatto 2017, this volume). Then, because the petrology and thermodynamics of accessory phases had not been as well studied, the task of 'petrochronology' was to bring petrologic context to the age information accessible in phases such as zircon and monazite. Often, this endeavor came back to linking the growth of accessory phases with a key rock-forming mineral—garnet. The last 20 years have now seen the advancement of direct garnet geochronology driven by several factors, including 1) the addition of Lu–Hf to Sm–Nd as viable systems to date garnet (e.g., Duchene et al. 1997; Scherer et al. 2000), 2) robust methods to eliminate the effects of contaminating inclusions (e.g., Amato et al. 1999; Baxter et al. 2002; Anczkiewicz and Thirlwall 2003), 3) improved analytical techniques to reduce sample size limitations (e.g., Harvey and Baxter 2009; Bast et al. 2015), and 4) microsampling methods whereby those individual tree-rings can be sampled at higher and higher spatial resolution (e.g., Stowell et al. 2001; Ducea et al. 2003; Pollington and Baxter 2010, 2011). What this makes possible today is the introduction—or re-introduction—of garnet into the cadre of modern 'petrochronometers'.

Our purpose in this chapter is threefold. We begin with a review of the 'petro-' of garnet, followed by the '-chrono-' of garnet, setting us up for the modern possibilities—many yet to be fully explored—of garnet 'petrochronology'. First, we re-acquaint the reader with the myriad ways in which garnet has been used directly to reconstruct past tectonometamorphic conditions. Ranging from foundational thermodynamic *P–T* modeling and textural analysis to recent advances in inclusion barometry and trace element zonation, our aim is to illuminate for all readers the remarkable scope and potential for garnet as a recorder of tectonometamorphic context. It is not garnet per se that we are interested in, but rather the conditions and processes

that it records. Second, we bring the reader up to date on recent advances in direct chronology of garnet via Sm–Nd and Lu–Hf systems that have made it the robust and precise chronometer that it is. Our hope is to dispel the misconceptions that continue to limit the use and credence of garnet geochronology, and clearly lay out the wide-ranging opportunities for direct garnet geochronology, appropriately framed within the challenges and limitations which still exist for this (as with any!) geochronometer. This section on the 'chrono' of garnet also discusses diffusion geospeedometry of garnet, which provides complementary information on heating/cooling durations and rates. Finally, we bring the 'petro' and 'chrono' together and present several examples from the past decade of true garnet petrochronology wherein these methods are integrated in increasingly innovative ways. Figure 2 serves as both an outline of our chapter, and as our definition of garnet petrochronology: the effort to integrate any aspect(s) of garnet-based petrology (on the left of Fig. 2) with any aspect(s) of garnet geochronology, and in so doing, to gain insights about evolving tectonometamorphic conditions that complement what may be extracted from other methodologies. Perhaps the most important thing to emphasize is that garnet petrochronology is really still in its infancy. Many challenges have been overcome, and it is time now for creative petrologists to come back to garnet and try new ways of integrating the 'petro' and the 'chrono' (by choosing from the left and the right of Fig. 2) to make true advances in our understanding of petrologic and tectonic evolution of the crust-mantle system. Never before has the time been so ripe, and we hope the reader is inspired to take these next steps in creatively deploying garnet petrochronology in the future.

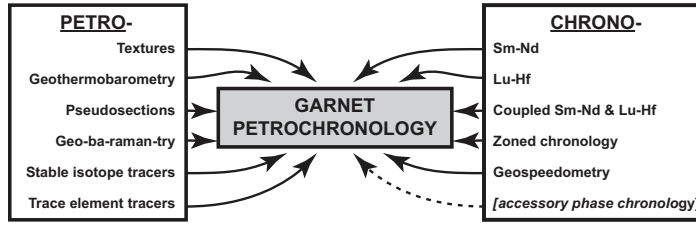

Figure 2. Outline of the chapter and definition of garnet petrochronology. Any "petro-" of garnet integrated with any "chrono" of garnet makes for garnet petrochronology. Accessory phase geochronology is included with a dashed line to note its integrative value, as valuable efforts have been made to link it to garnet.

PETRO- OF GARNET

Said the professor to their student: "*please try to collect some samples with garnet in them; there's not nearly as much we can do without it*". Although this statement is apocryphal, the sentiment will be familiar to many readers. Metamorphic petrology has been tied to the search for and study of garnet-bearing samples since soon after Barrow defined the 'garnet zone' in the eastern Scottish Highlands (Barrow 1893, 1912). Advancements in our ability to characterize the compositions and textures of metamorphic minerals, and in thermochemical models to describe the conditions of their evolution have commonly focused on garnet-bearing samples. In this section we review some of the reasons why garnet has been so central to the endeavor of reconstructing tectonometamorphic processes and conditions. We give an overview of some of the mechanisms that have been developed to infer pressure, temperature, deformation, mineral reaction or fluid–rock interaction, highlighting some of the recent and current developments that will aid this. Much has already been written about most of this, and we have thus made no attempt to be absolutely comprehensive, instead directing the reader to several of the other excellent reviews where each provide more detail about each technique. But by bringing all of this content together, our goal is to provide a comprehensive taste of what garnet has previously been used to quantify and constrain, with the expectation that these methods will increasingly be coupled with each other and with direct dating, as described later in the 'Chrono- of garnet'

section of this chapter. We will begin with the most easily observable (often at the hand sample scale) textural information locked in garnet, before reviewing its role in geothermobarometry and in tracing evolving petrologic reactions and open system fluid flow processes.

Textures of garnet—provider of tectonic context

Garnet's rigid porphyroblastic growth endows it with a propensity to retain and record its growth history in chemical as well as textural manifestations. This section provides several brief examples of how textural observations can provide valuable petrologic and tectonic context for garnet's growth span.

Garnet as a deformation and strain monitor. Garnet crystals are frequently riddled with cracks and inclusions of other minerals that can reveal a reaction history and the co-genetic evolution of tectonic stresses. For example Angiboust et al. (2011) interpreted cracks in UHP eclogite garnets as reflecting seismic brecciation during subduction to ~80 km depth in the Western Alps. Shear stress can also deform the matrix and cause garnet to rotate (Spry 1963; i.e., 'snowball garnets'; Rosenfeld 1968) or record changing metamorphic fabrics during porphyroblast growth (i.e., Ramsay 1962; Bell 1985). Controversy still exists between these two end-member interpretations (i.e., Johnson 1993; Ikeda et al. 2002; Stallard et al. 2002) but in any case, these common and often vivid patterns of inclusions inside garnets (e.g., Fig. 1c) clearly record rock deformation that may reflect localized structural—(e.g., Robyr et al. 2009) or regional tectonic-scale (e.g., Aerden et al. 2013; Sayab et al. 2016) processes. Beyond documentation of inclusion patterns in thin section, valuable textural information can be gleaned from additional methods of observation. Robyr et al. (2009) employed EBSD (electron backscattered diffraction) analysis to show that crystallographic orientations within single garnet porphyroblasts remained constant while the garnet was rotating. Then, those crystallographic orientations shifted to reflect surrounding phyllosilicate foliation when garnet grew during subsequent non-rotational regimes. Aerden et al. (2013) relate different textural generations of inclusions within garnets, each separated by a FIA (fold intersection axis) to major shifts in tectonic convergence vectors during the assembly and deformation of the Iberian Peninsula. These FIA are carefully mapped through analysis of radial sets of vertical thin sections and would not otherwise be readily apparent in a simple 2D thin section. Sayab et al. (2016) use similar methods to document tectonic convergence vectors in the Himalayan Orogen. Among the very first applications of true garnet petrochronology, Christensen et al. (1989) and Vance and Onions (1992) dated the cores and rims of such rotated snowball garnets to place constraints on the tectonic shear strain rate. Cases in which the identity or composition of the included minerals change from core to rim of the host garnet reveal additional, powerful information, as detailed below (e.g., St-Onge 1987).

Garnet resorption textures. As systems evolve and *P–T–X* changes, it is common for garnet to become unstable and start to break down by consumption from its rim inward (see Lanari et al. 2017 for additional examples). This resorption is driven by changes in *P–T–X* occurring during prograde metamorphism (e.g., Florence and Spear 1993), during retrograde metamorphism, due to chemical change related to influx of an external fluid, and sometimes due to polymetamorphism (when old garnet is introduced into a new orogenic cycle). Such resorbed surfaces often exhibit irregular morphologies, such as embayments, which often contrast with sharp original crystal growth faces. On the one hand, once a crystal (or its outermost portion) has been resorbed, there is little direct 'garnet petrochronology' that can be done to study that resorption event. However, if a resorption surface can be identified (texturally or chemically), the relative timing and conditions surrounding the resorption event may still be constrained. For example, if an element liberated during garnet resorption cannot be readily incorporated into product phases, a small amount of garnet might re-precipitate, preferentially incorporating that element, or the element itself might be reincorporated into any residual garnet (e.g., see discussion below relating to Y and HREE incorporation into

resorbed crystal rims). In general, such elements would be those that tend to be strongly partitioned into garnet over other matrix phases including Mn, Y, Lu and other HREE (e.g., Kohn and Spear 2000; Kelly et al. 2011; Gatewood et al. 2015). In some cases, secondary minerals may form at a garnet resorption surface driven by the sudden and proximal influx of those particular elements. Xenotime, for example, has been observed decorating the resorbed surfaces of garnets where localized flux of Y (from the resorbed garnet) promotes growth of xenotime (e.g., Gatewood et al. 2015). In this case, there is a useful textural link between resorbed garnet surface and neocrystallized accessory phase xenotime.

Textural evidence for polymetamorphism. We use the term 'polymetamorphic garnet' to describe crystals that grew during more than one tectonic 'event' separated by a significant hiatus that can be resolved texturally, chemically, or temporally with existing methods. Several examples of polymetamorphic garnet have been recognized in the Alpine-Himalayan system that grew during multiple orogenic cycles, separated by millions to hundreds of millions of years. Argles et al. (1999) dated fractions of garnet crystals, identifying that only crystal rims record Tertiary metamorphism, with crystal cores hundreds of millions of years older. Gaidies et al. (2006), Herwartz et al. (2011), Robyr et al. (2014) and (Lanari et al. 2017) recognized, garnet zonation textures in which Alpine overgrowths are vividly separated by prominent microstructural and chemical discontinuities from older Variscan cores. Manzotti and Ballevre (2013) recognized chemically heterogeneous detrital garnet cores—derived from multiple sources—that were overgrown by a homogeneous Alpine garnet rim. All of these examples serve to illustrate some of the textural and chemical means by which polymetamorphic garnet may be recognized. Of course, only by adding direct geochronology to each of these growth generations may we establish the absolute chronology and length of the hiatus between phases of garnet growth.

Porphyroblast nucleation and growth models. Metamorphic porphyroblastic minerals comprise vivid records of progressive nucleation and growth kinetics. Treated individually, each porphyroblast may record aspects of the rock's overall history colored by local chemical-textural features. Taken as a whole, porphyroblast crystal size distributions, their relative spatial disposition, and chemical zonation reveal information about the nucleation and growth process rock wide (e.g., Kretz 1973; Carlson et al. 1995; Chernoff and Carlson 1997; Meth and Carlson 2005). Several forward models have been developed to predict and interpret garnet CSD's and spatial dispositions within porphyroblastic rocks (Galwey and Jones 1966; Kretz 1966, 1974; Cashman and Ferry 1988; Carlson 1989, 2011; Spear and Daniel 2001; Gaidies et al. 2008b; Gaidies et al. 2011; Schwarz et al. 2011; Ketcham and Carlson 2012; Kelly et al. 2013a,b). These models offer testable predictions about the rate limiting processes for crystal growth and progressive metamorphism, including important implications for the attainment of local and rock-wide chemical equilibrium. Existing models make justified assumptions and interpretations about whether the rate-limiting step is breakdown of parent minerals (e.g., Schwarz et al. 2011), surface energetics of garnet (e.g., Gaidies et al. 2011), or transport of the least mobile nutrient (often aluminum) through the intergranular medium (e.g., Ketcham and Carlson 2012). The importance of Ostwald ripening (favoring growth of larger porphyroblasts at the expense of smaller porphyroblasts) has been debated (e.g., Carlson 1999), and some studies have cited heating rate as the key limitation. Each of these published cases shows persuasively that numerical simulations of one or several processes can successfully model natural crystal occurrences, suggesting that different rate-limiting processes may dominate under different circumstances. Furthermore, EBSD analysis has revealed that garnets porphyroblasts may often (perhaps >20% of the time) include more than one primary nucleation site and, thus, more than one fundamental crystal lattice orientation. These early forming crystal clusters may ultimately coalesce, separated by high-angle grain boundaries, to form a macroscopically visible porphyroblast (e.g., Daniel and Spear 1998; Spiess et al. 2001; Whitney et al. 2008; Whitney and Seaton 2010).

Garnet as a pressure and temperature sensor

One of the most important, and familiar, aspects of the 'petro-' in petrochronology involves deciphering metamorphic pressure and temperature to infer rocks' journeys through the crust and mantle. Garnet has arguably been the single most useful mineral for the estimation of evolving metamorphic *P–T* conditions for over forty years[1]. It is especially useful because of 1) its occurrence in diverse lithologies and *P–T* conditions, and 2) its relatively simple and well understood chemistry, which is dominated by divalent Fe, Mg, Ca, Mn, and trivalent Al, Fe cations (e.g., Grew et al. 2013) but is also sensitive to certain trace elements like Y. Because garnet is a major rock-forming mineral, its growth history is directly linked to broader rock wide petrologic evolution; so we must also develop the use of broader descriptions of the entire mineral assemblage and provide context for the growth of garnet and its changing chemistry. Here we review some of the techniques that have been developed to utilize garnet's chemical and mechanical properties to constrain *P–T*.

Compositional thermometry—Major elements. The advent of the electron microprobe in the 1950s sparked a revolution in metamorphic petrology as systematic characterization revealed that the compositions of co-existing mineral phases are often strongly correlated with metamorphic grade (e.g., Ramberg 1952; Kretz 1959). Garnet composition almost immediately became a focus, leading to the discovery that crystals commonly exhibit zoning from core to rim (Atherton and Edmunds 1965; Evans 1966; Evans and Guidotti 1966; Harte and Henley 1966; Hollister 1966; Atherton 1968) and in complex patterns around inclusions and upon contact with specific matrix phases (Tracy et al. 1976; Thompson et al. 1977; Tracy 1982; Figures 1 and 3). Relationships between mineral composition and metamorphic temperature suggested a geothermometer based upon the partitioning of Fe and Mg between garnet and biotite (e.g., Frost 1962; Kretz 1964; Saxena 1968, 1969; Thompson 1976b; Goldman and Albee 1977). This results primarily from garnet's large distorted cubic site favoring Fe rather than Mg at low temperature, under which conditions biotite's octahedral sites prefer Mg. Indeed, garnet typically contains far lower Mg content than most coexisting phases, with the ratio $Mg/Mg+Fe(X_{Mg})$ decreasing in the order cordierite > chlorite > biotite > chloritoid > staurolite > garnet (Albee 1965, 1972; Hensen 1971). The preference of each phase for Mg or Fe is reduced upon heating, thus imparting a temperature dependence of Fe–Mg partitioning between most co-existing phases (the volumetric effect of Mg–Fe exchange is comparatively minor). Garnet plays a particularly important role here because its low Mg content at low temperature establishes a much larger ΔX_{Mg} between it and a second equilibrated mineral (e.g., orthopyroxene or biotite) than a pairing between most other phase combinations would permit, explaining why garnet often occurs as a key mineral in exchange thermometer calibrations. The garnet side of these equilibria is shown in Figure 4, which demonstrates the relatively extensive Mg and Fe variation expected under possible crustal conditions, assuming a fixed bulk rock composition. After the classic experimental calibration by Ferry and Spear (1978), numerous refinements to the garnet–biotite exchange thermometer (Perchuk and Lavrent'eva 1983; Ganguly and Saxena 1984; Indares and Martignole 1985; Kleeman and Reinhardt 1994; Berman and Aranovich 1996; Gessmann et al. 1997; Holdaway et al. 1997; Mukhopadhyay et al. 1997; Holdaway 2000) have made this one of the most often used geothermometers.

Temperature dependent Fe–Mg equilibria between garnet and many other phases have also been calibrated as thermometers, all based on similar principles to the garnet–biotite example outlined above. It is beyond the scope of this review to discuss all of these in detail, but the reader is directed to Essene (1982, 1989) and Spear (1993) for more information.

[1] For example, Spear (1993) lists 37 geothermobarometers on page 517–519 of his book; 25 of these include garnet, far more than any other mineral.

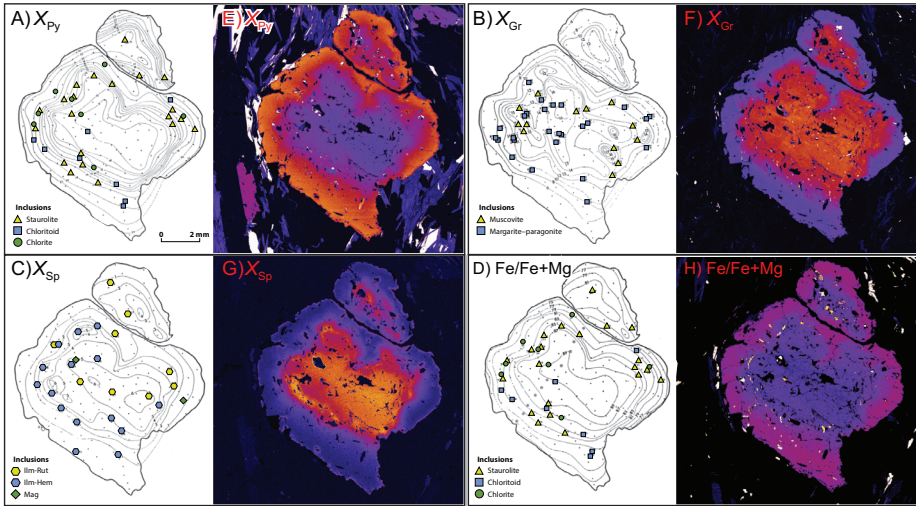

Figure 3. Garnet zoning, then and now. Panels A-D are some of the first 2-D garnet element zoning maps, hand-contoured from point analyses by R.J. Tracy as part of his graduate studies and published as Thompson et al (1977). These images of a crystal from the Gassetts Schist, Vermont, first hinted at the complexity of zoning in natural garnet crystals and were used to advance a model of progressive crystal growth during evolving *P* and *T*. The very first 2-D images had appeared a year earlier (Tracy et al 1976). Panels E-H are element maps of the same crystal, collected ~ 35 years later by the same R.J. Tracy in a ~12 hour run with an automated electron microprobe (Tracy et al 2012). The general zoning patterns were extremely well documented by the previous work, but modern techniques yield a far more detailed picture, particularly highlighting fine-scale zoning in the crystal core of the Ca map that is still difficult to construct a satisfactory growth model for. Computerized automation has revolutionized many aspects of metamorphic petrology, paving the way for the petrochronology discussed in this volume.

Compositional barometry. While low ΔV exchange equilibria were developed into mineral thermometers, high ΔV equilibria were explored as potential barometers, again with an early emphasis on garnet-bearing assemblages. Observation of and experimentation on the garnet–plagioclase system (Kretz 1959; Ghent 1976; Goldsmith 1980; Newton and Haselton 1981) led to calibration of a mineral barometer that uses the end member 'GASP' (garnet–aluminosilicate–silicate–plagioclase) reference reaction:

$$Ca_3Al_2Si_3O_{12} + 2\,Al_2SiO_5 + SiO_2 = 3\,CaAl_2Si_2O_8$$

This is pressure sensitive because of the large molar volume difference of reactants and products, and has been calibrated and recalibrated multiple times as new experimental data and activity–composition (*a–X*) models for garnet and plagioclase have become available (e.g., Ghent 1976, 1977; Newton and Haselton 1981; Koziol and Newton 1988; McKenna and Hodges 1988; Berman 1990; Holdaway 2001; Caddick and Thompson 2008). The relative performance of most of these calibrations was compared by Wu and Cheng (2006), but taken as a group the GASP calibrations have become probably the most widely used chemical geobarometer for metamorphic rocks, due in part to the large range of *P–T* conditions over which garnet and plagioclase can both co-exist with a suitable buffering assemblage. Uncertainties on temperature of equilibration, end-member thermodynamic properties (particularly enthalpy and entropy), mineral solution behavior, and measurements of garnet and plagioclase composition, likely combine to yield GASP uncertainties reaching or exceeding ±2 kbars in many cases (see discussions by, Hodges and McKenna (1987), McKenna and Hodges (1988), Kohn and Spear (1991) and Holdaway (2001) for more information).

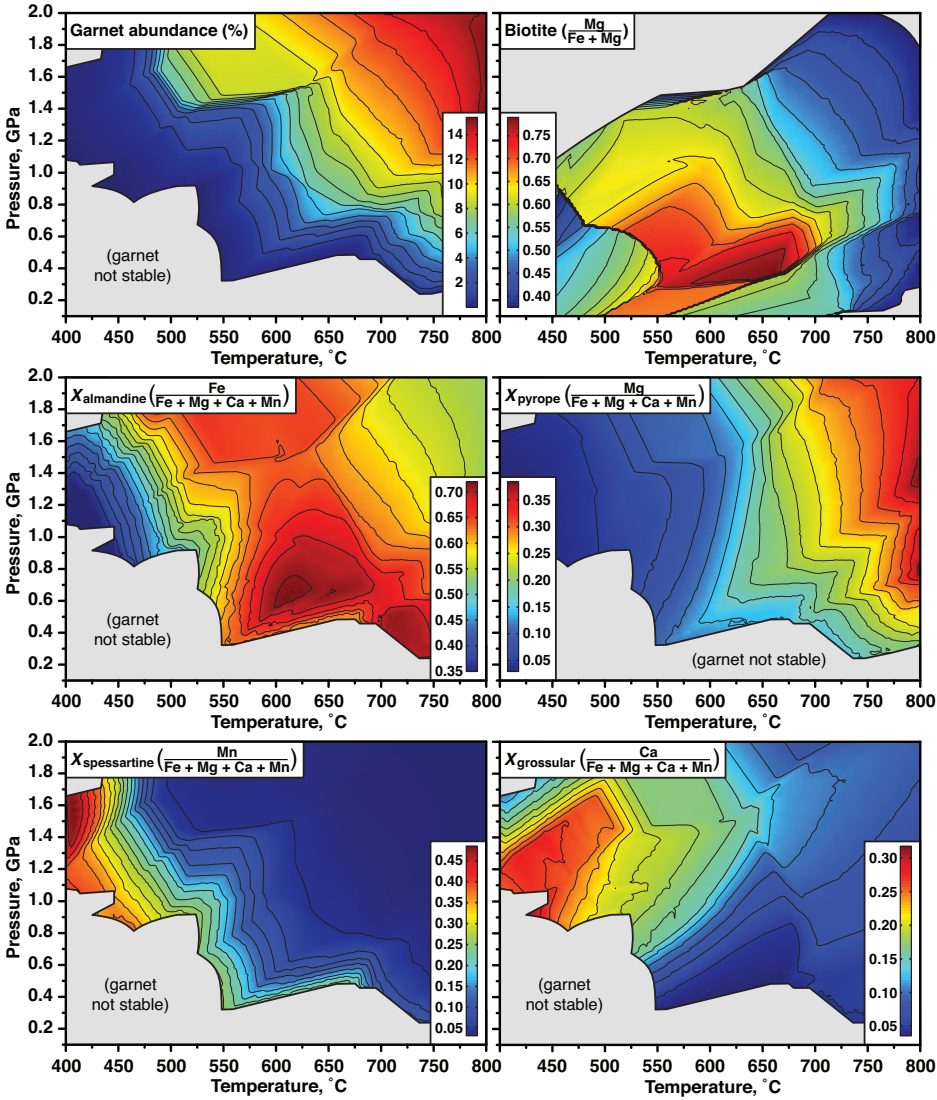

Figure 4. Mineral abundances and compositions in a pelitic rock at crustal conditions as a function of *P* and *T* for the 'average pelitic bulk-rock' composition from Caddick and Thompson (2008). Calculated using Perple_X (Connolly 2005) with the THERMOCALC ds5.5 dataset (updated from Holland and Powell 1998), and activity models described in Caddick and Thompson (2008), except for garnet (White et al 2005), amphibole and omphacite (both Diener and Powell 2012). The underlying calculation from which contours were extracted considers many additional phases that are not shown, with biotite and garnet in most regions of the diagrams co-existing with 5 or 6 additional phases (see annotated pseudosection for this rock, which appeared as Figure 1 in Caddick and Thompson (2008), noting that that diagram was calculated with earlier thermodynamic data and is thus not identical).

Many additional mineral systems have been suggested and calibrated for inferring pressure and temperature, with a significant proportion of these relying partly on the properties of garnet, e.g., garnet–plagioclase–biotite–muscovite, garnet–muscovite–plagioclase–quartz, garnet–biotite–plagioclase–quartz, garnet–ilmenite–rutile–kyanite–quartz, garnet–ilmenite–rutile–

plagioclase–quartz, garnet–clinopyroxene–plagioclase–quartz, garnet–orthopyroxene, garnet–clinopyroxene–phengite (Bohlen and Essene 1980; Ghent and Stout 1981; Bohlen et al. 1983; Hodges and Crowley 1985; Bohlen and Liotta 1986; Moecher et al. 1988; Hoisch 1990, 1991; Waters and Martin 1993; Pattison et al. 2003; Wu et al. 2004; Wu and Zhao 2006). Again, more details about many of these were provided by Essene (1989) and by Spear (1993).

Compositional thermometry—Trace elements. While the distribution of various trace elements in garnet can be used to determine reaction sequence, the applicability of geochronometers, and fluid/melt history (see discussions below), trace element (particularly yttrium) concentrations of coexisting accessory phases and garnet have also been utilized as thermometers in pelitic lithologies.

Pyle and Spear (2000) developed an empirical trace element thermometer for the temperature range of 450–550 ºC, by study of regional metamorphic rocks from New England. This method utilizes the yttrium content of garnet in xenotime-bearing pelites, assuming that the presence of xenotime buffers the rock in Y. Temperature and pressure estimates for calibration purposes, along with *P–T* paths, were determined by traditional thermobarometry and differential thermodynamics, respectively. Pyle et al. (2001) expanded this approach to the assessment of equilibrium partitioning of coexisting monazite–xenotime–garnet, developing a garnet–monazite thermometer. Critical in employing this thermometer is 1) accurate compositional information about all phases involved in the reaction (Foster et al. 2004; Hallett and Spear 2015) and 2) that monazite was a stable phase during garnet growth, i.e., that garnet and monazite were in equilibrium. Inclusion of homogeneous monazite in homogeneous or continuously zoned garnet may be considered a good candidate for such equilibration, though zoning in that monazite and the chances of its isolation from the reactive part of the rock warrant particular care, as further discussed by Lanari and Engi (2017, this volume). Uncertainties in the other parameters for calculation likely amount to a combined uncertainty of approximately ±25 ºC (Pyle et al. 2001). Pyle et al. (2001) note that garnet and monazite maintain compositional equilibrium even as garnet fractionation dramatically changes the Y budget in the reactive bulk composition, allowing for a consistent element partitioning during the rock's prograde history.

Thermobarometry of zoned garnet. If mineral composition is to be used to infer pressure and temperature but natural phases such as garnet are commonly chemically zoned (e.g., Figs. 1 and 3), where should one make a microprobe analysis, where should analyses of coexisting phases be made, and how can results be put into the context of an evolving *P–T* history? These questions have been addressed in detail (e.g., Essene 1989; Kohn and Spear 2000), and extreme caution should be taken before averaging data whose variability may be geologically meaningful. For example, the apparent repeatability of garnet zoning patterns suggests that this zoning records changes in pressure and temperature during crystal growth, leading to early models of garnet zoning due to sequential mineral reactions (e.g., Hollister 1966; Loomis 1975; Thompson 1976a; Tracy et al. 1976; Tracy 1982), which in turn led to direct use of garnet zoning to infer *P–T* paths during prograde metamorphism. Development of a differential thermodynamic approach, commonly referred to as the Gibbs method, allowed derivation of *P–T* paths for rocks, based upon garnet crystal zoning that is assumed to have been established during growth and an estimate of the *P–T* point at which garnet first began to grow (Spear and Selverstone 1983; Spear et al. 1984). Zoned garnet porphyroblasts containing complex suites of mineral inclusions present an additional opportunity, with thermobarometry on the hosts and their inclusions yielding complex information that may be interpreted as a simple *P–T* progression within a single orogenic event (e.g St-Onge 1987) or as overprinted conditions associated with multiple events or tectonic processes (e.g., Dorfler et al. 2014). As such, the most appropriate course for thermobarometry generally begins with careful consideration of mineral texture and mineral zoning (e.g., Essene 1989; Kohn and Spear 2000) with garnet often at the heart of this endeavor.

Forward models of phase equilibria. A powerful use of equilibrium thermodynamics in the understanding of metamorphic processes involves the calculation and interpretation of phase equilibria, and much modern petrochronology involves the coupling of geochronological methods with phase equilibria constraints. Prediction of the proportion and composition of each major phase in a rock, and how these would change as functions of pressure, temperature and system composition (in so-called 'pseudosections', 'isochemical phase diagrams' or 'mineral assemblage diagrams' such as Fig. 4) has had enormous influence on the petrologic community. This has been reviewed recently by Spear et al. (2016) and in this volume by Yakymchuk et al. (2017, this volume), and here we focus on the primary value from a garnet petrochronology standpoint: revealing how garnet growth or dissolution would be expected along any *P–T* path, how this might modify the residual rock composition (discussed also in detail by Lanari and Engi 2017, this volume), how garnet chemistry would evolve during growth, and how this is associated with changes in the co-existing assemblage, including the production or consumption of other minerals, fluids, or melt.

Most studies of garnet in crustal metamorphism are concerned with pelitic, greywacke, basaltic or carbonate lithologies, in which case reasonable approximations can be made by considering a thermodynamic system comprised of Na_2O, K_2O, CaO, FeO, MgO, Al_2O_3, SiO_2, H_2O, ±MnO, ±TiO_2, ±Fe_2O_3, ±CO_2. Incorporation of all or most of these components permits description of garnet as $(Fe^{2+},Mg,Ca,Mn)_3(Al,Fe^{3+})_2Si_3O_{12}$ and calculation of phase equilibria involving most *major* phases that this garnet is likely to co-exist with. The thermodynamics of MnO-bearing mineral end-members are generally less well-constrained than others, but MnO plays such a significant role in stabilizing garnet at low *P–T* conditions and on the modal proportion of garnet at higher *P–T* conditions (Symmes and Ferry 1991; Mahar et al. 1997; Tinkham et al. 2001; Caddick and Thompson 2008; White et al. 2014b) that its inclusion is often warranted. A plethora of relevant mineral, fluid and melt models have been described, with most recent contributions associated with various updates of the 'THERMOCALC' end-member dataset (Holland and Powell 1985, 1990, 1998, 2011). Even models for compositionally well-constrained minerals such as garnet have been reassessed numerous times (inlcuding but not limited to Wood and Banno 1973; Engi and Wersin 1987; Powell and Holland 1988; Hackler and Wood 1989; Koziol and Newton 1989; Berman 1990; Ganguly et al. 1996; Mukhopadhyay et al. 1997; White et al. 2000, 2005, 2014a,b; Stixrude and Lithgow-Bertelloni 2005; Malaspina et al. 2009). Seemingly minor updates to solid solution models can lead to significant changes in calculated phase equilibria unless end-member thermodynamic properties are modified accordingly (see discussion in White et al. 2014a). Furthermore, the relative stabilities and coexisting compositions of complex mineral solutions may respond inappropriately if applied beyond the limits (in composition, pressure or temperature) of their original calibration, though it can often be difficult to ascertain whether this is the case. It is thus informative to make direct comparison between $K_{Mg-Fe}^{Gar-Bio}$ derived from the mineral compositions predicted by phase equilibria calculations and $K_{Mg-Fe}^{Gar-Bio}$ derived from experimental calibrations such as Ferry and Spear (1978) across a range of *P–T* conditions and for a range of bulk-rock compositions (and thus additional buffering minerals in the calculated equilibria). Such comparisons, (e.g., Figure 6 of Caddick and Thompson 2008) highlight that, although experimentally determined partitioning is well recovered at many *P–T* conditions, it is poorly fit elsewhere, and reveal some unexpected consequences of utilizing complex activity-compositions models for numerous phases.

Comparison between calculated and natural garnet composition is one of the primary constraints on segments of *P–T* paths inferred from pseudosection calculations (Konrad-Schmolke et al. 2006; Gaidies et al. 2008a; Chambers et al. 2009; Cutts et al. 2010; Vorhies and Ague 2011; Hallett and Spear 2014a; Mottram et al. 2015). Many factors can lead to calculated compositions that fail to intersect at *P–T* conditions consistent with other observations,

including inappropriate assumptions of bulk composition or short length-scale compositional heterogeneity (e.g., Tinkham and Ghent 2005; Kelsey and Hand 2015; Guevara and Caddick 2016; Palin et al. 2016; Lanari and Engi 2017, this volume), the potential for crystal nucleation and growth at conditions removed from sample-wide thermodynamic equilibrium (e.g., Kretz 1973; Waters and Lovegrove 2002; Gaidies et al. 2011; Pattison et al. 2011; Kelly et al. 2013a,b, b; Carlson et al. 2015b) and the possibility of diffusive modification of crystal composition following growth (discussed in more detail below). Several recent approaches have focused more explicitly on garnet, developing computer codes that compare measured natural crystal zoning with thermodynamic predictions to automatically search for the most appropriate *P–T* path experienced, generally also considering modification of the bulk-rock composition upon garnet growth (e.g., Moynihan and Pattison 2013; Vrijmoed and Hacker 2014; Lanari et al. 2017). To some extent these are natural successors to the pioneering Gibbs method (Spear and Selverstone 1983; Spear et al. 1991; Menard and Spear 1993) and to calculations that forward model the chemical zoning established along prescribed *P–T* paths (e.g., Florence and Spear 1991; Gaidies et al. 2008a,b; Konrad-Schmolke et al. 2008; Caddick et al. 2010).

Given the relative ease of calculating phase equilibria, what is their value? As emphasized recently (e.g., Pattison 2015; Spear et al. 2015, 2016), the ability to calculate diagrams may have exceeded our capability to assess their predictions. For example, if a pseudosection predicts a 5 ºC, 0.5 kbar window within which a garnetiferous assemblage is stable in a relatively dry lithology, it may be unlikely that this assemblage will actually be found at these *P–T* conditions in nature due to (i) uncertainties in the thermodynamic data, and (ii) possible kinetic effects that may hinder sample-scale equilibration on the timescale that the rock passes through the *P–T* conditions of the field (Carlson et al. 2015b). This can be closely associated with the concept that the volume of any rock in mutual thermodynamic equilibrium (i.e., the equilibrium length-scale) probably changes throughout metamorphism as a function of *P*, *T* and fluid availability (e.g., Stüwe 1997; Guiraud et al. 2001; Carlson 2002). In fact, the equilibrium length-scale may be different for each element depending on the relative diffusive transport rate (in turn a function of elemental partitioning/solubility into the intergranular transporting medium; Baxter and DePaolo 2002b; Carlson 2002). The choice of appropriate bulk composition for a pseudosection calculation is thus often not trivial and this composition may have to change as subsequently refractory phases such as garnet (e.g., Spear et al. 1991; Marmo et al. 2002; Tinkham and Ghent 2005; Caddick et al. 2007; Konrad-Schmolke et al. 2008), hydrous fluid (e.g., Guiraud et al. 2001) or melt (e.g., Tajčmanová et al. 2007; Yakymchuk and Brown 2014; Guevara and Caddick 2016) are produced and fractionated from the reactive system. Lanari and Engi (2017, this volume) review bulk composition in more detail, demonstrating that use of an XRF-based rock composition to retrieve *P–T* conditions of zoned garnet growth, without modification of that composition to account for components sequestered by garnet, can produce significantly erroneous estimates if more than ~2 vol% garnet has been produced. Eventually the length-scales of equilibration may become small enough to establish domainal textures such as coronae, in which substantial chemical potential (μ) gradients are preserved over geological timescales and can best be interpreted through μ–μ equilibria (e.g., White et al. 2008; Štípská et al. 2010; Baldwin et al. 2015). The retention of chemical zoning in garnet is one obvious indicator that μ gradients are commonly maintained in metamorphic rocks.

Despite these various complications and limitations, equilibrium thermodynamic models are of immense importance to garnet petrochronology and to metamorphic petrology more broadly, as testified by the fact that the combined citations of the main papers describing the THERMOCALC, THERIAK-DOMINO and Perple_X programs (e.g., de Capitani and Brown 1987; Powell and Holland 1988; Connolly 1990; Powell et al. 1998; Connolly 2005, 2009; de Capitani and Petrakakis 2010) and the THERMOCALC dataset (e.g., Holland and Powell 1990, 1998, 2011) significantly exceed 10,000 at the time of writing. Recent successes with respect

to application within garnet petrochronology are given at the end of this chapter, but we would like here to highlight that the potential power of pseudosections in garnet petrochronology (albeit without the title) was elegantly demonstrated ~25 years ago when Vance and Holland (1993) coupled garnet compositions from the Gassetts Schist rocks that had previously been element mapped by Thompson et al. (1977; e.g., Fig. 3) with pseudosection constraints on the *P–T* path of garnet growth and isotopic dating of that garnet. This early adoption of garnet petrochronology led to estimations of heating and decompression rate, and to inferences about tectonic and thermal mechanisms for this metamorphism.

The loss of information. Compositional thermobarometry and comparison of pseudosections with natural mineral assemblages rely on the fundamental assumption that rocks faithfully record information associated with equilibration at a set of *P–T* conditions, often assumed to be peak *T*. However, a substantial body of empirical (e.g., Anderson and Olimpio 1977; Woodsworth 1977; Yardley 1977), experimental (e.g., Elphick et al. 1981; Loomis et al. 1985; Chakraborty and Ganguly 1991; Ganguly et al. 1998a; Vielzeuf and Saúl 2011) and modeled (e.g., Carlson 2006; Chu and Ague 2015) evidence suggests that major element zoning in garnet will relax at high temperature through volume diffusion. Furthermore, detailed observations indicate that exchange and net-transfer reactions can operate on the rims of garnet crystals after peak metamorphic conditions and that these can substantially modify the apparent *P–T* conditions recovered from mineral thermometry (e.g., Tracy 1982; Spear and Florence 1992; Kohn and Spear 2000; Pattison et al. 2003; Spear 2004). An illustrative example comes from a transect through the western Himalaya, where oxygen isotope thermometry and phase equilibria constraints (Vannay et al. 1999) reveal far higher temperatures than previously inferred for the same samples through major element garnet-based thermobarometry (Vannay and Grasemann 1998). The implication is that garnet–biotite compositions were reset by Mg–Fe exchange during cooling from peak temperatures of ~750 ºC to ~600 ºC, where exchange and diffusion became sufficiently sluggish to inhibit further substantial modification (effectively representing a closure temperature).

Diffusional resetting of metamorphic systems is covered in depth in this volume (Kohn and Penniston-Dorland 2017, this volume) and later in this chapter we discuss how diffusional *partial* resetting can be used to constrain heating and cooling timescales (i.e., geospeedometry). But here, we must consider the conditions at which compositional information in garnet is altered due to volume diffusion, thus compromising geothermobarometry. This is particularly pertinent to petrochronology because garnet is such an important constituent of many thermobarometers and major element diffusion within the garnet lattice is typically considered to be slower than in many other major silicate minerals in metamorphic rocks (Brady and Cherniak 2010). Numerous studies have thus sought to quantify the extent to which garnet zoning established during prograde growth will be modified at subsequent stages of metamorphism, with several trying to generalize results for a range of conditions (Florence and Spear 1991; Gaidies et al. 2008a; Caddick et al. 2010). Figure 5 is an example that shows the extent to which garnet prograde zoning will be preserved as a pelitic rock heats and is buried along the indicated *P–T* path, exploring a wide range T_{max}, heating rate and eventual crystal sizes. It indicates, for example, that if a crystal nucleates at thermodynamically-constrained 'garnet-in' and grows spherically to 1 mm diameter during ca. 6 Ma of heating to T_{Max} of 580 ºC (e.g., by following path '*b*' in Fig. 5, equating to ~25 ºC/Ma), its core will effectively preserve initial X_{Gar}^{Mg} and X_{Gar}^{Ca} contents but X_{Gar}^{Fe} (not shown) and X_{Gar}^{Mn} (not shown) will have been modified by more than 1 mole fraction unit due to volume diffusion subsequent to growth. Crystals achieving a 5 mm diameter along the same prograde path will retain their initial compositions at T_{max}. If heating continues at the same rate to 750 ºC, the core composition of crystals exceeding 1 cm diameter will have been partially modified and crystals smaller than 500 µm may preserve little or no major element zoning. Slower heating rates increase the crystal sizes for which crystal core compositions are lost (e.g., paths '*c*' and '*f*' in Fig. 5), while fast heating tend to preserve growth information (e.g., path '*a*').

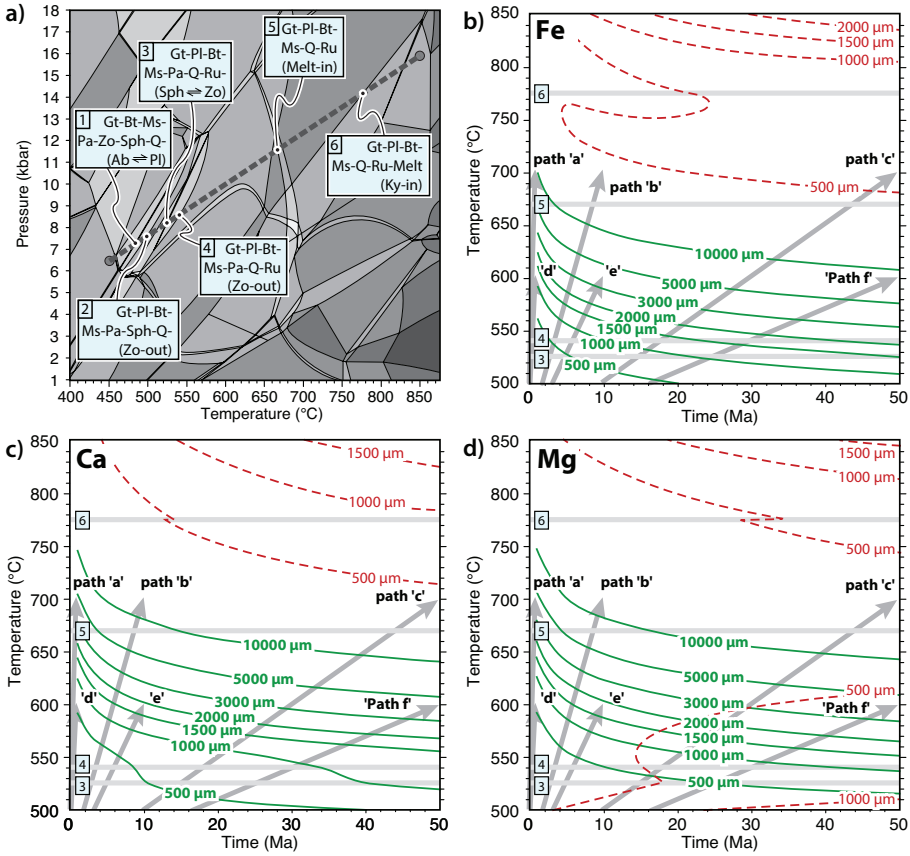

Figure 5. Garnet opening to resetting upon heating, modified from Caddick et al (2010). Phase stabilities in a pelitic rock were calculated along the burial and heating path shown in panel A, which also highlights significant equilibria encountered. Equilibrium garnet compositions at successive points along that path were used to establish growth zoning, and diffusional relaxation of this zoning was calculated between each successive point. Along this *P–T* path, a rock encounters reactions in the same order regardless of heating rate, which only controls the time available for diffusion at each temperature step. This crystal growth and diffusion model was run for ~ 13,000 variations of heating rate, maximum temperature and crystal size at that T_{Max}. Panels B-D summarize results of these calculations, contoured to show the T_{Max}–heating-duration–crystal-diameter relations for which garnet crystals first 'open' sufficiently for diffusion to noticeably modify the crystal core composition. Note that results concern prograde metamorphism only, simply showing which combination of parameters will retain initial garnet crystal core growth compositions upon reaching T_{Max} and which will be modified by diffusion (solid curves, labeled for crystal diameter). Horizontal gray lines numbered 3-6 indicate the assemblage phase boundaries traversed in the model *P–T* path shown in A. Dashed curves show the conditions for which diffusion becomes sufficiently effective to completely eradicate zoning in garnet. See Caddick et al (2010) for additional details.

A consequence is that crystals may appear to preserve prograde zoning *patterns*, such as bell-shaped Mn profiles, up to granulite-facies conditions but the absolute composition at all interior points within the crystal may have been substantially modified from their initial growth composition, rendering thermobarometry misleading. These resetting estimates are somewhat faster than previous estimates (e.g., Florence and Spear 1991), partly because of the use of different diffusivity data. Discretization of garnet porphyroblasts into sub-grains that may not be obvious optically will further reduce timescales of diffusional homogenization,

sometimes substantially so (e.g., Konrad-Schmolke et al. 2007). This loss of compositional information remains both a challenge and an opportunity for garnet petrochronology, reducing the sensitivity of *P–T* estimates but providing additional methods for inferring duration, as summarized in the geospeedometry section, below.

***The strength of garnet: Geo-ba-Raman-try*[2].** Previously discussed methods of thermobarometry rely on phase compositions that are generally assumed to have equilibrated near metamorphic peak temperature and/or pressure and to have experienced limited subsequent modification. These assumptions can be difficult to assess in natural samples, so alternative methods that make fewer (or at least different) assumptions are valuable. One of the most promising of these relies on a very different property of garnet: its resistance to elastic deformation.

Minerals trapped as inclusions during metamorphic growth of porphyroblasts generally experience approximately lithostatic pressure at the time of entrapment. Rocks expand (decompress) upon exhumation and undergo phase transformations accordingly, but mineral inclusions can retain a substantial proportion of the pressure at which they were trapped if the host phase can resist the deformation required to permit expansion of the inclusion, and if pressure is not 'lost' through development of cracks in the host. Identification of deformation around inclusions in high pressure diamond (Sorby and Butler 1869; Sutton 1921) first led to the concept of thermobarometry by study of stress in minerals hosting inclusions (Rosenfeld and Chase 1961). Focus turned to garnet porphyroblasts (Rosenfeld and Chase 1961; Rosenfeld 1969) because phases with low thermal expansivity and high bulk and shear moduli make good natural pressure vessels: their inclusions, which would naturally expand upon exhumation, are likely to retain a substantial fraction of their entrapment pressure (Zhang 1998; Izraeli et al. 1999; Guiraud and Powell 2006). A classic example comes from preservation of coesite and palisade quartz inclusions in garnet porphyroblasts, which led to the first identification of continental rocks that had been subducted to >90 km (Chopin 1984) based on the inference that coesite once existed as the stable SiO_2 polymorph but was pervasively inverted to quartz upon exhumation unless trapped as inclusions within garnet.

Substantial literature suggests that residual pressure should also be maintained in rocks lacking the obvious palisades inclusion textures, leading to studies that recovered ultra-high pressure conditions by measuring pressure-sensitive laser Raman peak positions of coesite and olivine inclusions in diamond and garnet (Izraeli et al. 1999; Parkinson and Katayama 1999; Sobolev et al. 2000). Correlations between pressure and the laser Raman spectra of several phases have been developed, due partly to the need for calibrants in high-pressure experiments (e.g., Hemley 1987; Schmidt and Ziemann 2000; Schmidt et al. 2013). Residual pressure (i.e., current pressure felt by a mineral inclusion, which may be substantially different to the pressure felt by crystals in other textural settings) can thus now be determined for these phases *in situ* with Raman techniques. However, a mineral inclusion with pressure sensitive Raman characteristics only makes an effective thermo-barometer in natural samples if its elastic properties contrast sufficiently with its hosting phase (otherwise the initial pressure felt by the inclusion may be lost as it deforms its host). A detailed survey of candidate mineral pairs (Kohn 2014) revealed several promising combinations, with quartz-in-garnet among the most sensitive barometers because of the relative compressibility of quartz and rigidity of garnet. Additionally, zircon inclusions in garnet might make a very sensitive thermometer (Kohn 2014), with uncertainties of quartz-in-garnet and zircon-in-garnet thermobarometry potentially as small as several hundreds of bars and tens of degrees, respectively.

The quartz-in-garnet laser Raman barometer was applied to quartz–eclogite, epidote–amphibolite and amphibolite facies metamorphic samples by Enami et al. (2007), who used a simple numerical model (Van der Molen 1981) to infer original metamorphic pressure from

[2] Kudos to editor Kohn for coining the term Thermoba-Raman-try (Kohn 2014).

measured residual pressure and reveal the high pressure history of samples that otherwise preserve little evidence of eclogite-facies equilibration. The need for more sophisticated modeling approaches has since been identified (Angel et al. 2014; Ashley et al. 2014a; Kohn 2014; Kouketsu et al. 2014) and available software now offers automated calculation with several choices of elastic model and simple correction of elastic properties for garnet composition (Ashley et al. 2014b). In an important validation of this methodology, application to experimentally derived quartz inclusions in garnet yielded "an entrapment pressure at 800 ºC of 19.880 kbar—essentially identical to the experimental pressure of 20 kbar" (Spear et al. 2014).

Application of Raman barometry (or ba-Raman-try) to high pressure lithologies has retrieved pressures of quartz or coesite trapping (e.g., Korsakov et al. 2010; Zhukov and Korsakov 2015), analysis of more complex suites of inclusions has revealed *P–T* paths of subduction zone garnet growth (Ashley et al. 2014a), and comparison with thermodynamic modeling has indicated the likely extent of overstepping the garnet isograd in subduction zone and Barrovian-sequence samples (Spear et al. 2014; Castro and Spear 2016). However, application to high temperature metamorphic rocks remains challenging, with Sato et al. (2009) describing Raman shifts which imply that the interface between quartz inclusion and garnet host can be subjected to tensile stress upon cooling and that the quartz inclusions thus preserve negative residual pressure, as discussed further by Kouketsu et al. (2014). Ashley et al. (2015) detailed an extreme case in which this effective under-pressuring led to polymorphic transformation of quartz inclusions to cristobalite. A further challenge for high temperature metamorphic rocks is that modeling currently relies on an assumption that only elastic deformation acted on the host and inclusion, raising substantial problems for rocks that may have experienced significant plastic deformation. Indeed, given that chemical diffusion in garnet could either establish pressure gradients after crystal growth (Baumgartner et al. 2010) or could act as a mechanism to reduce pressure variations, garnet crystals experiencing substantial intra-crystalline diffusion after inclusion of quartz probably make unreliable pressure vessels without additional consideration and modeling. However, for the many cases in which diffusive re-equilibration is minimal, thermoba-Raman-try is an exciting, and complementary, method of inferring pressure–temperature evolution during garnet growth.

An exciting future development involves the combined application of multiple systems. In particular, given that quartz-in-garnet and zircon-in-garnet respectively act a barometer and a thermometer (Kohn 2014), we note that their combined use would be compelling. This would raise the possibility of extremely detailed petrochronology in samples containing garnet (whose *P–T* and duration of growth can be determined chemically and with zoned isotope geochronology) with inclusions of both zircon (providing additional *P–T* information with Raman and trace element thermometry and additional time constraints with U–Pb geochronology) and quartz (providing sensitive constraint on evolution of *P* during garnet porphyroblast growth). This represents a very powerful suite of techniques for deciphering rates of change of pressure and temperature in the mid crust, and is clearly an important potential avenue for further development.

Garnet as a tracer of reaction pathways and fluid–rock interaction

Thus far, we have focused on the use of garnet as a monitor of the *P–T* evolution of the systems wherein it grows. In the following section we move from the '*P–T*' to the '*X*'—or composition—of the system during garnet growth. As system chemistry changes, often reflecting the role of fluids or the local production or consumption of key phases, garnet crystals can record aspects of that change especially in their trace element and isotopic zonation.

Stable Isotopes in Garnet. Oxygen is the most abundant element in the Earth's crust and a main component of the fluids that transport heat and mass during crustal metamorphism. Oxygen isotopes in whole rocks and minerals have been used to characterize the composition, relative

timing, and sources of these metamorphic fluids (e.g., Bickle and Baker 1990; Baumgartner and Valley 2001). In cases where the fluid history is complex, distinct garnet growth zones may be associated with evolving fluid compositions and sources. Additionally, the oxygen isotopic values of co-existing mineral pairs have been utilized as a thermometer due to the measurable and temperature-dependent fractionation between different minerals (e.g., Chacko et al. 2001; Valley 2001; Valley et al. 2003). In this section, we review the use of oxygen isotopes in garnet as a marker of open system fluid flow, local reaction history, and as a crustal thermometer.

Historically, a principal objective of stable oxygen isotope studies was to determine peak temperatures by utilizing the temperature-dependent fractionation of oxygen isotopes between coexisting mineral pairs, determined either experimentally or empirically (Taylor and Sheppard 1986; Richter et al. 1988; Clayton et al. 1989; Zheng 1991, 1993; Kohn and Valley 1998; Chacko et al. 2001; Valley et al. 2003). The principles of equilibrium fractionation factors (Chacko et al., 2001) and stable isotope thermometry (Valley 2001) have been reviewed in great detail in a previous volume of this series, so only more recent contributions, specifically in relation to its application with garnet ($\Delta^{18}O$ mineral–garnet thermometry), will be discussed briefly here. Quartz–garnet oxygen isotope pairs have been used most often to constrain metamorphic temperatures (Rumble and Yui 1998; Peck and Valley 2004; Moscati and Johnson 2014). Peck and Valley (2004) utilize garnet–quartz pairs for thermometry of quartzites from the southern Adirondacks, NY. Conceptually, if most of the oxygen in the quartzites is in the quartz, any effect of oxygen isotope exchange will be recorded in the $\delta^{18}O$ of the minor phase, in this case garnet. Refractory accessory minerals like garnet are closed to oxygen diffusion during growth (Valley 2001), and as quartz in a quartzite acts as an infinite reservoir for oxygen diffusion, this mineral pair can be retentive of the peak temperature isotope fractionation, even if the rock is slowly cooled (Kohn and Valley 1998). Metamorphic temperatures of ~700–800°C were calculated from the quartzites from the southern Adirondacks, with no grain size dependence, suggestive of slow oxygen diffusion in garnet and closure temperatures of at least 730 °C (Peck and Valley 2004).

The analysis of oxygen isotopes in garnet continues to benefit from increased accuracy and precision related to the improvement of *in-situ* analytical techniques (Vielzeuf et al. 2005; Kita et al. 2009; Page et al. 2010), and also from texturally constrained samples (see Electronic Appendix for a discussion on the historical challenges related to analysis of $\delta^{18}O$ in garnet). When quartz is fully armored by a mineral with slow diffusion of oxygen, such as garnet, then any diffusive exchange of oxygen between quartz and host during cooling is minimal. Hence, garnet–quartz mineral pairs as determined by *in-situ* techniques can offer a detailed temperature and fluid ($\delta^{18}O$) history (Strickland et al. 2011). As Russell et al. (2013) note, if combined with constraints on the timing (via garnet geochronology) and *P–T* conditions (via phase equilibria modeling, or even Raman barometry of quartz in garnet) of garnet growth, then a robust *P–T–t–f* metamorphic history is attainable.

Without metasomatism at elevated pressures and temperatures, metamorphic rocks will tend to inherit the bulk rock oxygen isotopic composition of the protolith (Fig. 6). This can be recorded in the $\delta^{18}O$ of the individual minerals, though an accurate knowledge of the equilibrium isotope fractionation factors among coexisting phases is required in order to properly interpret these measured isotope compositions. Garnet has one of the lowest $\delta^{18}O$ of all minerals, lower than that of bulk rock $\delta^{18}O$, and thus increases with increasing temperature (Kohn 1993) . In some lithologies (e.g., metabasites), garnet $\delta^{18}O$ is close to the whole rock and can encode the $\delta^{18}O$ of the whole rock (Putlitz et al. 2000). Any deviation in garnet $\delta^{18}O$ from initial values can be produced by processes including a) change in temperature inducing changing equilibration fractionation factors (see above), b) changing mineral assemblages and modal proportions during progressive metamorphism (Kohn 1993; Young and Rumble 1993), and c) open system change in the reactive $\delta^{18}O$ composition of the bulk rock from the

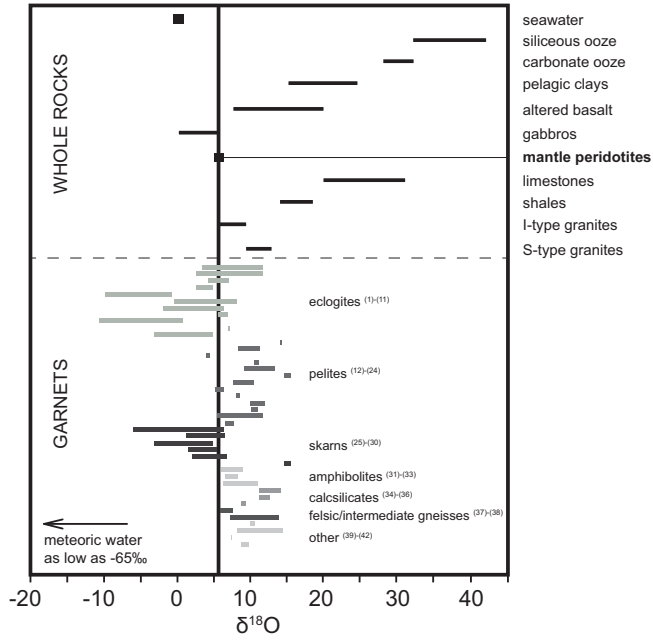

Figure 6. Compilation of $\delta^{18}O$ data of whole rock and garnet analyses. Whole rock analyses and average mantle value ($\delta^{18}O = 5.80‰$) from Eiler (2001). References to garnet data include: (1)(31)Errico et al (2013), (2)Martin et al (2014), (3)(33)Page et al (2014), (4)Rubatto and Angiboust (2015), (5)Rumble and Yui (1998), (6)Russell et al (2013), (7)Zheng et al (1998), (8)Burton et al (1995), (9)Chen et al (2014), (10)(12)Gordon et al (2012), (11)(24)Masago et al (2003), (13)Kohn and Valley (1994), (14)Kohn et al (1993), (15)Kohn et al (1997), (16)Lancaster et al (2009), (17)(32)(34)Martin et al (2006), (18)Martin et al (2011), (19)Raimondo et al (2012), (20) Skelton et al (2002), (21)van Haren et al (1996), (22)Young and Rumble (1993), (23)(30)(36)(39)Ferry et al (2014), (25)Crowe et al (2001), (26)Clechenko and Valley (2003), (27)D'Errico et al (2012), (28)Jamtveit and Hervig (1994), (29)Page et al (2010), (35)Sobolev et al (2011), (37)Gauthiez-Putallaz et al (2016), (38)Vielzeuf et al (2005), (39)Peck and Valley (2004), (41)Moscati and Johnson (2014), (42)Abart (1995).

interaction of externally-derived fluids (Kohn and Valley 1994). Because oxygen diffusion in garnet at crustal conditions is sluggish (Coghlan 1990; Burton et al. 1995; Vielzeuf et al. 2005), any change in garnet $\delta^{18}O$ during its growth can be preserved in its concentric zonation (Kohn et al. 1993; Skelton et al. 2002), in one case even after a regional granulite facies overprint (Clechenko and Valley 2003). These effects on garnet $\delta^{18}O$ are further discussed below.

Kohn (1993) developed a model showing the effect of net transfer reactions during prograde heating for systems that are closed to externally-derived fluids. It was predicted that the fractional crystallization of (low $\delta^{18}O$) garnet during metamorphism would result in an increase in the $\delta^{18}O$ of garnet from core to rim. However, this effect was calculated to be minor (~1‰ or less over 150°C of heating) and independent of bulk composition (Kohn 1993). This was further tested in natural samples from regionally metamorphosed rocks from Chile (Kohn et al. 1993), where the difference between garnet cores and rims from metapelites and amphibolites was 0.5‰ and < 0.1‰, respectively. These observations suggest that garnet growth occurred in a system closed to infiltration of fluids out of $\delta^{18}O$ equilibrium with the bulk rock, and are similar to observations from regionally metamorphosed amphibolites and schists from Vermont (Kohn and Valley 1994) and New Hampshire, U.S.A (Kohn et al. 1997). Comparably, the fractionation of $\delta^{18}O$ due to (internally-derived) devolatilization of a meta-basalt was shown to be small, with garnet rims having a $\delta^{18}O$ less than 1‰ compared to garnet cores (Valley 1986; Kohn et al. 1993).

The mechanism most likely to result in large changes in garnet $\delta^{18}O$ from core to rim is open system fluid infiltration. A large amount of work on $\delta^{18}O$ in garnet has focused on its ability to elucidate the source of externally derived fluids in various metamorphic settings. The infiltration of these fluids, often over substantial thermal and chemical gradients, can cause significant zoning of $\delta^{18}O$ in garnet, offering a relative time marker for fluid flow (Skelton et al. 2002), especially when the protolith composition differs significantly from mantle-like compositions (~5–6‰; Fig. 6), or when the fluids are derived from devolatilization of high $\delta^{18}O$ sediments (Errico et al. 2013), interaction with low $\delta^{18}O$ meteoric water (Russell et al. 2013; Fig. 6), or rehydration in a mid-crustal shear zone (Raimondo et al. 2012).

Russell et al. (2013) examined the $\delta^{18}O$ record of garnets from a series of orogenic eclogites and found that these crystals can display a range of $\delta^{18}O$ that falls well outside that expected for mantle-derived protoliths. While the intracrystalline variation of $\delta^{18}O$ in these garnets is small (increase of ~1–2‰ between core and rim), the absolute $\delta^{18}O$ values record the origin of these eclogites, distinguishing between those derived from altered, oceanic upper crust (Trescolmen, Alps; 7.7 to 8.3‰) and high-temperature infiltration of meteoric water into mafic intrusions buried *in-situ* with subaerial, continental crust (Western Gneiss Region, Norway; −1.2 to −0.2‰). Indeed, extremely negative $\delta^{18}O$ values in eclogitic garnet from the Dabie (−10‰; Zheng et al. 2006) and Kokchetav (−3.9‰; Masago et al. 2003) terranes have been interpreted as evidence of extreme infiltration of meteoric water, possibly derived from a rift environment involving low $\delta^{18}O$ glacial melt water. Rumble and Yui (1998) analyzed eclogitic garnets from the Qinglongshan ridge in the Sulu terrane, and found bulk garnet $\delta^{18}O$ values as low as −11.1‰ (Fig. 6), also attributing such negative values as reflecting alteration of the protolith by meteoric waters at high paleo-latitudes and/or –altitudes prior to subduction. Other low garnet $\delta^{18}O$ values are observed in several studies from hydrothermal skarns where variable fluid sources in open systems are recorded in zoned garnet (Jamtveit and Hervig 1994; Crowe et al. 2001; Clechenko and Valley 2003; D'Errico et al. 2012). D'Errico et al. (2012) observed a large range in intragrain $\delta^{18}O$ values (–4 to 4‰) from a hydrothermal system in the Sierra Nevada batholith, attributing early, low $\delta^{18}O$ values to meteoric water input, with higher values resulting from variable mixing of magmatic and metamorphic fluids.

Some examples offer instances where garnet $\delta^{18}O$ records changing fluid compositions (e.g., Kohn and Valley 1994; Martin et al. 2011; Errico et al. 2013; Page et al. 2014; Rubatto and Angiboust 2015). Many of these cases of strongly zoned garnet $\delta^{18}O$ are recorded in eclogites. Rubatto and Angiboust (2015) observed eclogitic garnet cores from the Monviso ophiolite in the Western Alps with $\delta^{18}O$ values of 0.2–2.0‰, recording ocean floor metasomatism of the basaltic protolith. High-pressure metasomatism is recorded in the garnet rims, with $\delta^{18}O$ values of 3.5–6.0‰. While these rocks are found in a shear zone adjacent to down-going lithospheric mantle, Monviso serpentinites ($\delta^{18}O$ of 3.0–3.6‰) were not found to be the source of the metasomatizing fluid; high $\delta^{18}O$ fluids from dehydrating metasediments were instead suggested to be the primary source for fluid influx at depth.

A final example of garnet $\delta^{18}O$ recording multiple metasomatic events comes from two separate findings from the well-studied Franciscan Complex (Errico et al. 2013; Page et al. 2014). Garnet crystals from eclogite and amphibolite blocks record contrasting fluid flow histories (Errico et al. 2013). Amphibolites, which are inferred to record an early subduction initiation history (Anczkiewicz et al. 2004), are metasomatized by an early influx of sediment-derived fluids, recorded in their garnet rims (~8‰; Errico et al. 2013; see Fig. 6). Eclogitic blocks have high $\delta^{18}O$ garnet cores (~6–11‰), interpreted to record extreme ocean floor alteration of the protolith, with fluid-mediated exchange with the overlying mantle wedge at depth recorded in low $\delta^{18}O$ garnet rims (3–5‰; Errico et al. 2013). Page et al. (2014) suggest that their observed shifts in garnet $\delta^{18}O$ (2–3‰) are evidence of limited fluid flow during burial where garnet rims are formed during metasomatism at high fluid/rock ratios during exhumation/re-burial, with possible interaction with highly oxidized fluids.

In all of the cases shown above, analysis of garnet $\delta^{18}O$ has elucidated the source and relative timing of fluid–rock interaction in a variety of tectonic settings. Garnet $\delta^{18}O$, combined with a detailed *P–T* and temporal record, has great potential to provide an important marker for metamorphic fluid flow, especially in hydrothermal and subduction zone systems where the role of exotic external fluids is most observable. Combining $\delta^{18}O$ with studies of fluid inclusions in garnet (where preserved) can provide an even more detailed fluid history of burial/prograde (primary fluid inclusions) and exhumation/retrogression (secondary fluid inclusions), coupling these techniques to elucidate the source and composition of fluids.

Increasingly, stable isotopes other than oxygen are utilized in metamorphic systems to study the nature and scale of fluid flow, particularly in subduction zone systems, and relying (mainly) on the interpretation of whole rock isotopic analyses. Stable isotopes of lithium, calcium, and magnesium are ideal for studying the effects of diffusion due to their large relative mass differences, and are likely to be particularly useful in natural systems where strong chemical potential gradients exist. If garnet growth occurs in an environment with high fluid flux or large chemical gradients, then large diffusion-driven mass fractionation may be recorded in growing porphyroblasts, and *in-situ* or microsampled stable isotope analyses of garnet can produce a detailed record of such fluid and mass transfer. The subduction interface, where the overlying mantle wedge comes into contact with subducting metasediments and metabasaltic rocks, is an ideal locale for such studies, given the strong chemical contrasts in several chemical components between these lithologies. Studies that have focused on the length-scales and timescales of subduction zone fluid flow have utilized isotope systems including calcium (John et al. 2012), lithium (Zack et al. 2003; Penniston-Dorland et al. 2010) and magnesium (Pogge von Strandmann et al. 2015). Bulk isotopic analyses on garnet separates have been limited to just a few studies (e.g., on magnesium; Pogge von Strandmann et al. 2015). Notably also, Bebout et al. (2015) developed a technique to measure the variation in $\delta^{7}Li$ in garnet using SIMS, in order to determine whether the lithium isotopic record could help elucidate the nature of fluid flow during subduction zone metamorphism of metasediments from Lago Di Cignana, Western Alps. Finally, Cr (Wang et al. 2016) and Fe (Williams et al. 2009) isotopes have been utilized for studying evolving redox conditions (using Cr and Fe) and the effects of partial melting processes (using Fe).

As these isotopes are primarily limited to measurement by solution ICP-MS or TIMS, bulk analyses of garnet have been the primary focus of earlier studies. A promising new direction may involve the use of SIMS for *in-situ* analysis, where applicable. However, detailed microdrilling from texturally or compositionally constrained garnet growth zones, in tandem with various stable isotope analyses (oxygen and otherwise), has the potential to link these geochemical tracers to *P–T-t* constraints for various metamorphic (and igneous) processes, thus expanding the incorporation of various stable isotope systems to the garnet petrochronologist's toolbox.

Trace elements in garnet. Garnet is often zoned in trace elements, with cores that are enriched in Y and HREE (Hickmott et al. 1987; Chernoff and Carlson 1999; Pyle and Spear 1999; Otamendi et al. 2002). These highly compatible elements tend to resist re-equilibration at elevated temperatures owing to their low inter- and intragranular diffusivities (Lanzirotti 1995; Spear and Kohn 1996; Otamendi et al. 2002; Carlson 2012; Bloch et al. 2015). Thus, trace element zoning can be preserved at upper amphibolite and even granulite facies, in which major element zoning is often erased (Fig. 5), providing a useful tool for deciphering high-temperature metamorphic processes (Spear and Kohn 1996; Hermann and Rubatto 2003). Early garnet trace element studies required secondary ion mass spectrometry (Hickmott et al. 1987) or synchrotron (Lanzirotti 1995) techniques. However, LA-ICPMS is increasingly now used for trace element analyses at adequate spatial resolution and sensitivity for many applications.

The analyzed distribution of trace elements, specifically REEs, can be utilized for interpretation of garnet geochronology (e.g., zonation of radioactive parent elements; see later section), changes in garnet growth rate, and changes in reaction history, specifically with relation to accessory phases. Often, trace element zonation is sensitive to different specific mineral reactions or matrix processes than the major elements, thus offering complementary information. Insofar as trace element zonation relates to dateable accessory phases, trace elements in garnet represent an often crucial correlative part of accessory phase petrochronology. Garnet can be vividly zoned in REE's (see expanded discussion below), as well as elements such as Zr (Anczkiewicz et al. 2007), Cr (Spear and Kohn 1996); Yang and Rivers (2001); (Martin 2009; Angiboust et al. 2014), P (Spear and Kohn 1996; Chernoff and Carlson 1999; Kawakami and Hokada 2010; Hallett and Spear 2015; Jedlicka et al. 2015; Ague and Axler 2016), and As (Jamtveit et al. 1993). Here, we present a summary of the controlling mechanisms for partitioning of trace elements in garnet.

Hickmott et al. (1987), Hickmott and Spear (1992), and Hickmott and Shimizu (1990) were among the earliest contributions to interpret remnant trace element zoning in garnet (in metapelites from the Tauern Window and Massachusetts), finding controls on trace element concentrations related to elemental fractionation during progressive metamorphism, fluid–rock interaction, and the breakdown of trace element-rich minerals. Numerous contributions have built upon these earlier studies in attempting to decipher metamorphic processes and rock reaction histories from garnet trace element zoning, with additional examples cited below.

Carlson (2012), Moore et al. (2013), Cahalan et al. (2014) and Carlson et al. (2014) have sought to determine how various trace elements are structurally incorporated into natural garnet, and to calibrate the rates and mechanism of diffusion of these elements in garnet, utilizing samples collected from the aureole of the Makhavinekh Lake Pluton, Labrador. Using lattice dynamic calculations, Carlson et al. (2014) found that the incorporation of trace elements into garnet is likely dominated by menzerite- (for REE) and alkali-type (for Li and Na) coupled substitutions at a low energetic cost. This energetic cost will (i) decrease as the host garnet unit-cell increases, (ii) decrease as temperature increases or pressure decreases, and (iii) decrease substantially with contraction of the ionic radius across the lanthanide series. These observations, as well as diffusivities calculated through the use of stranded diffusion profiles in the Labrador garnets (Carlson 2012) have been shown to have profound implications for the interpretation of Lu–Hf garnet ages (Kelly et al. 2011; see also later sections), the preservation of matrix trace element distributions during porphyroblast crystallization (or overprint zoning; see examples below), element mobility, and intergranular solubility (Carlson et al. 2015a). Finally, Cahalan et al. (2014) found that the diffusion of Li in garnet is strongly governed by coupled substitution with slowly diffusing REE, and thus Li zoning may be retained during metamorphism (even at elevated temperatures) and utilized as a monitor of fluid– (and/or melt–) rock interaction.

Simple Rayleigh fractionation between a growing garnet crystal and the rock matrix would result in the incorporation of Y + HREE into garnet cores, with smoothly decreasing 'bell-shaped' profiles of these elements towards garnet crystal rims due to their relatively high garnet/matrix partition coefficients (e.g., Hollister 1966; Otamendi et al. 2002; Lapen et al. 2003; Anczkiewicz et al. 2007; Kohn 2009; Fig. 7). In contrast, MREE and LREE generally display a slight increase in abundance towards garnet crystal rims, or show no zonation at all. Garnet REE profiles can, however, deviate from these simple profiles, as observed in a number of settings. This may be due to a number of factors including 1) diffusion-limited REE uptake during prograde metamorphism, 2) resorption (or recrystallization), 3) syn-growth breakdown of a REE-bearing accessory phase, 4) breakdown of REE-bearing major phases, 5) change in the kinetics of garnet growth, 6) overprint zoning, and 7) infiltration of trace element-rich fluid. Let us treat these each in turn.

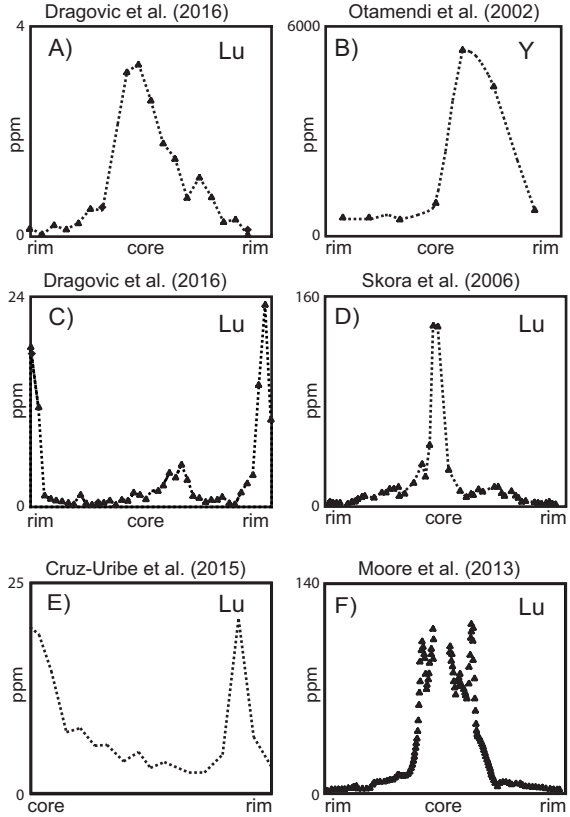

Figure 7. Garnet trace element zonation from various studies. A. Example of Rayleigh fractionation; modified from Dragovic et al (2016). B. Rayleigh fractionation example; modified from Otamendi et al (2002). C. Lu enriched in garnet rim, possibly from breakdown of accessory phases; modified from Dragovic et al (2016). D. Diffusion-limited REE uptake example; modified from Skora et al (2006). E. Core to rim profile showing Lu annulus from breakdown of accessory phase; modified from Cruz-Uribe et al (2015). F. Example showing intermediate peaks in Lu, possibly from change in local garnet-forming reaction; modified from Moore et al (2013).

Diffusion-limited REE uptake. Diffusion of trace elements to a growing garnet crystal can be relatively slow compared to the crystal's growth rate (Skora et al. 2006; Moore et al. 2013). An early nucleating garnet crystal will sequester highly compatible elements ($K_D > 1$), forming a high concentration central peak in zoning profiles (Fig. 7). As a result of the slow intergranular diffusion, a steep chemical potential 'depletion halo' will form around the early-growing crystal (supply is slower than uptake). Increased temperature during progressive metamorphism will increase intergranular mobility, relaxing the chemical potential gradient of REE around the growing garnet crystal and possibly permitting a secondary REE peak in the growing garnet. REE abundance in the crystal core is dependent on the K_D (relative to garnet precursor phases) and matrix concentration of each element, with HREE exhibiting the strongest fractionation into garnet. The location and magnitude of the secondary peak will depend on the intergranular diffusivity of the element and its dependence on temperature, with MREE exhibiting a rimward secondary peak compared to the HREE, owing to their lower intergranular diffusion rate (and higher ionic radii). For LREE, this will manifest itself as a low abundance in crystal cores, potentially increasing at the crystal rim.

Resorption (/recrystallization). Annular maxima in trace element abundances may result from the partial consumption of garnet during an orogenic cycle (i.e., during prograde heating/burial or retrograde dissolution). At elevated temperatures, Y + HREE would be liberated from the resorbed garnet rim. Elements that have a strong affinity for garnet will preferentially re-partition into the remnant crystal rim, and subsequently diffuse inward at a rate controlled partly by temperature (Lanzirotti 1995; Pyle and Spear 1999). Kelly et al. (2011), utilized Lu–Hf garnet data from Makhavinekh Lake Pluton, Labrador, to suggest that the strong preferential reincorporation of Lu relative to Hf results in false apparent Lu–Hf garnet ages. Using their model, higher degrees of garnet resorption and Lu retention would result in younger apparent ages and stranded diffusion profiles of Lu at remnant crystal rims. Gatewood et al. (2015) make a similar observation based on Sm-enriched rims likely formed during resorption and leading to young apparent Sm–Nd rim ages.

Interface-coupled dissolution–reprecipitation (ICDR) can also result in unique trace element zoning. Ague and Axler (2016) present garnet Na, P, and Ti distribution maps from a high-pressure felsic granulite from the Saxon Granulite Massif, showing sharply defined cross-cutting chemical domains that likely record ICDR during retrograde fluid–rock interaction. While major element zonation is absent at such temperatures (>900 °C) due to intracrystalline diffusion, retention of zonation of these trace elements highlights their far lower diffusivities at these conditions (Ague and Axler 2016).

Breakdown of an accessory phase. The presence of accessory phases can buffer trace element activities, thereby exerting strong controls on their partitioning into garnet. Several studies have linked REE zoning in garnet with the growth and breakdown of phases such as monazite, allanite, epidote, apatite, or xenotime (Hickmott and Shimizu 1990; Hickmott and Spear 1992; Chernoff and Carlson 1999; Pyle and Spear 1999; Yang and Rivers 2002; Corrie and Kohn 2008; Stowell et al. 2010; Gieré et al. 2011; Cruz-Uribe et al. 2015; Dragovic et al. 2016; Engi 2017, this volume; Fig. 7). Pyle and Spear (1999) showed that in xenotime-bearing, garnet-zone assemblages, the early presence of xenotime would buffer Y and result in high-Y garnet cores. Continued growth of garnet would deplete the matrix in Y, eventually resulting in loss of xenotime and a subsequent decrease in Y towards garnet rims. Yang and Rivers (2002) also suggested that enrichment of certain REE in garnet can be associated with the breakdown of particular minerals: enrichment in LREE associated with the breakdown of allanite, in MREE with epidote, and in HREE with xenotime or zircon. Using trace element zoning patterns in both garnet and tourmaline, Gieré et al. (2011) modeled the metamorphic evolution of rocks from the Central Alps, relating this evolution to the growth and breakdown of accessory and major phases. The presence of subhedral annuli enriched in Ca, Sr, Y, and HREE was associated with the breakdown of allanite, while internal zones of these annuli were associated with garnet growth coincident with the breakdown of detrital monazite. Hallett and Spear (2014a) suggest that P zoning in garnets from the Humboldt Range, NV, results from breakdown of a phosphate phase such as apatite, or melting reactions involving the breakdown of plagioclase. Finally, the discontinuous breakdown of Y-rich mineral phases such as epidote and allanite was invoked to explain Y annuli in garnets from metapelitic rocks of the Black Hills, South Dakota (Yang and Pattison 2006).

Breakdown of major rock-forming phases. Konrad-Schmolke et al. (2008) used a path dependent thermodynamic forward model and published trace element partition coefficients to model major and trace element distribution in garnet, comparing modeled elemental distributions to those observed in UHP garnets from the Western Gneiss Region, Norway. The modeled trace element distributions result from a sequence of garnet-producing mineral breakdown reactions (specifically the breakdown of chlorite, epidote, and amphibole) during subduction, combined with progressive fractional modification of the effective bulk composition upon garnet growth. Along an inferred subduction *P–T* path, changes in the calculated

abundance of major phases and in trace element partitioning between those phases and garnet generated synthetic distributions of major and trace elements in garnet. HREE zoning patterns are largely predicted by fractionation into the garnet core by a Rayleigh-type process, with possible perturbations towards the garnet rim for some effective bulk compositions resulting from breakdown of epidote and amphibole. The liberation of MREE and LREE into garnet results from epidote- and amphibole-consuming reactions, and is expressed as intermediate peaks in a growing garnet crystal. These peaks are shown to form progressively further from the crystal core for decreasing atomic numbers (or garnet/matrix partition coefficient), as is also described in Zermatt-Saas Fee garnets (Skora et al. 2006).

Konrad-Schmolke et al. (2008) also relate trace element distributions in garnet to possible interpretations of garnet geochronological methods. Strong partitioning of radioactive parent elements such as Lu and Sm into a growing garnet crystal will have significant effects on the interpretation of a garnet age (see below). The models from Konrad-Schmolke et al. (2008) show that most of the Lu partitioned into garnet during early growth comes from the breakdown of chlorite. Therefore, Lu–Hf in garnet from a subducting lithology could date chlorite breakdown reactions, with the Sm–Nd system possibly tracking the growth of garnet via the breakdown of epidote or amphibole and thus the amphibolite/blueschist to eclogite facies transition.

Changes in the kinetics of garnet growth. For elements that strongly partition into a growing garnet crystal (i.e., Y + HREE), a decrease in the garnet growth rate can lead to an increase in the concentration of that particular element in the garnet's outermost surface (Hickmott and Spear 1992). The combined presence of these elemental annuli in a zone of relatively inclusion-free garnet has been partly attributed to such decreases in garnet growth rate (Lanzirotti 1995; Yang and Rivers 2001; Yang and Pattison 2006).

Overprint zoning. Pre-existing matrix heterogeneities or former accessory phases can be retained as overprint zoning in the chemistry of garnet that grows in these locations (Menard and Spear 1996; Spear and Kohn 1996; Yang and Rivers 2001, 2002; Kohn 2004; Vielzeuf et al. 2005; Martin 2009; Carlson et al. 2015a). Martin (2009) shows sub-millimeter scale Y and Cr zoning in garnet from central Nepal that defines an internal foliation, spiraling from the rim to the core of crystals, similar to patterns often portrayed by inclusion trails. These garnets lack well-defined inclusion patterns, so only the trace element zoning in garnet offers a diagnostic tool for determining the relative timing of deformation, possibly even helping to determine the sense of rotation of a porphyroblast relative to the matrix foliation.

Infiltration of trace element-rich fluid. Infiltration of an externally-derived fluid whose trace element concentrations are out of equilibrium with the mineral assemblage may result in distinct trace element zoning patterns (Jamtveit and Hervig 1994; Stowell et al. 1996; Moore et al. 2013; Angiboust et al. 2014; Hallett and Spear 2014b). Invoking the 'exotic fluid' interpretation has often proved challenging because examples of patchy or oscillatory zoning can often be equally well explained by pre-existing heterogeneities (see above). This is especially true with respect to REE zoning in garnet, as corroborating evidence from fluid inclusions or coincident zoning in major elements is usually missing. Moore et al. (2013) explain REE zoning in rims of Franciscan blueschist garnets as related to fluid infiltration, because zoning in these elements is also coincident with annuli in Ca and Mn, presumably also enriched in the metasomatizing fluid. Moore et al. (2013) note that such zonation can act as a time marker because rock-wide infiltration would result in similar trace element zoning for all garnet crystals growing during the interval influenced by the fluid flow event.

A vivid example of garnet trace element zonation involving the infiltration of exotic fluids comes from the fossil subduction zone of the Western Alps, where Angiboust et al. (2014) observe patchy and oscillatory Cr zoning in garnets from shear zone eclogites (Fig. 8). The complex Cr zoning, coupled with both enrichments of Mg, Ni, Cr, and LILEs and with boron

isotopic signatures in metasomatic minerals, was interpreted to reflect the large-scale episodic infiltration of serpentinite-derived fluids (via antigorite breakdown) at ca. 80 km depth at the slab–mantle interface (Angiboust et al. 2014). While this appears to contrast with garnet oxygen isotope interpretations presented earlier (sediment-derived fluid source), Monviso eclogites experienced multiple phases of metasomatism, and as the Tethyan seafloor (slow-spreading ridge) dominantly comprised serpentinized mantle and pelites, mafic blocks were likely to have interacted with multiple sources of fluid (Angiboust, pers. comm.).

Ultimately, linking the concentrations and zoning of trace elements in garnet to the evolution of the mineral assemblage and the timing of garnet growth can be a powerful petrochronologic tool, especially when comparing the competing roles of fluid infiltration, intergranular element mobility, and crystal growth rate.

Concluding this review of the ways in which garnet can record petrologic or tectonic processes and conditions, we turn now to the topic of direct garnet chronology. As we shift gears, we encourage the reader to keep in mind the "petro-" of garnet, and realize that direct garnet chronology allows the petrochronologist to date any of these conditions and processes, and in the best case, constrain their rate or duration (e.g., Fig. 2). The "petro-" of garnet provides the motivation for garnet petrochronology; otherwise we would just be dating a mineral.

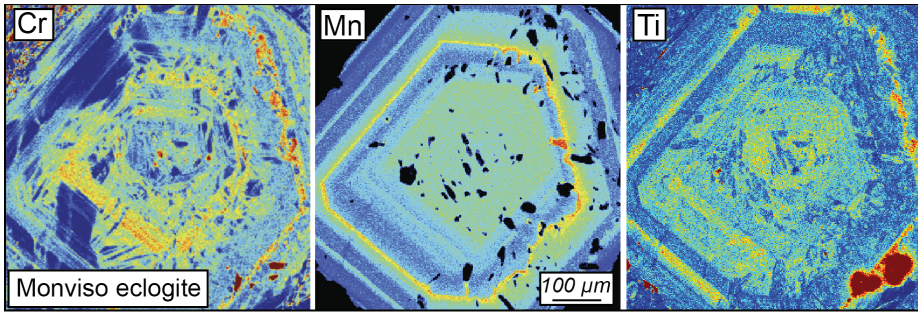

Figure 8. Cr, Mn, and Ti zoning from a garnet from the Monviso ophiolite of the Western Alps, modified from Angiboust et al (2014). Note patchy zoning in the core and oscillatory-zoned rims. Trace element annuli attributed to influx of externally derived fluid from antigorite breakdown of associated mantle wedge serpentinites.

CHRONO- OF GARNET

Even today, many in the geoscience community are unaware, or unconvinced, that the growth of garnet can be dated directly, precisely, and accurately with the Sm–Nd or Lu–Hf isotope systems. Much of that skepticism stems from the early history of garnet geochronology in the 1980's and 1990's before certain modern methods were developed. Since then, direct garnet geochronology has evolved to approach the hopes of would-be petrochronologists of decades past. At the same time, garnets have also become one of most often utilized minerals for 'geospeedometry' (Lasaga 1983; e.g., Chakraborty and Ganguly 1991) whereby the durations of tectonic and metamorphic events (generally events related to heating and cooling) can be accurately reconstructed by modeling stranded diffusion profiles within garnet. Valuable advances have also been made in linking the growth (and chronology) of accessory phases such as monazite and zircon to the growth or breakdown of garnet via textural and chemical means (e.g., Engi 2017, this volume; Lanari and Engi 2017, this volume; Rubatto 2017, this volume; Williams et al. 2017, this volume); we view the integration of accessory phase petrochronology with true garnet petrochronology as one

of the more exciting future applications which may be inspired by this full RiMG volume. Indeed, the decision to approach time-consuming garnet geochronology might be established and motivated by preliminary accessory phase petrochronology, thermodynamic modeling, and thin section petrography. While we leave it to other authors to describe advances in linking accessory phase dating to garnet, in this section, we will review the past, present, and future of direct garnet geochronology and garnet geospeedometry. Together, these two methods provide the 'chrono' in garnet petrochronology including absolute ages, absolute durations, and relative rates of thermal processes at conditions wherein garnets exist.

Garnet geochronology

van Breemen and Hawkesworth (1980) and Griffin and Brueckner (1980) first recognized that garnet's relatively high Sm/Nd ratio (as compared to most other common minerals) could be exploited for geochronology. Garnet growth is dated with the isochron method by pairing it with the hosting 'whole rock' and/or other mineral separates with which it grew (and subsequently evolved isotopically) in an isochron diagram (for a review of garnet isochron basics, see Baxter and Scherer 2013). Further exploration of Sm–Nd garnet geochronology continued in a few labs through the 1980's until 1989 when the first attempts to date garnet via U–Pb (Mezger et al. 1989) and Rb–Sr (Christensen et al. 1989) were published. Despite the novelty of these studies, concerns surrounding the problem of contaminating mineral inclusions in garnet, matrix heterogeneity, and open system mobility of daughter isotopes in the rock system pushed garnet geochronology via U–Pb and Rb–Sr out of favor (for example, see Zhou and Hensen 1995; DeWolf et al. 1996; Romer and Xiao 2005; Sousa et al. 2013). In a positive twist, it was in part the recognition that such U–Pb analyses of 'garnet' were dominated by accessory mineral inclusions that led to the advancement of accessory phase petrochronology with textural and chemical links to garnet growth (e.g., Hermann and Rubatto 2003; Pyle and Spear 2003; Wing et al. 2003; Foster et al. 2004). Sm–Nd garnet geochronology survived this period, but not without lingering skepticism stunting its further development, especially given the time and analytical effort required to overcome the challenges of contaminating inclusions and low Nd concentrations. In 1997, the first Lu–Hf garnet geochronology was published by Duchene et al. (1997). Since that time, significant advances have been made for both Lu–Hf and Sm–Nd garnet geochronology, both in terms of sample preparation, isotopic analysis, and data interpretation. With modern methods, garnet geochronology via Lu–Hf and Sm–Nd can yield accurate and precise ages of garnet directly from the garnet itself. In this section of the chapter, we will review some of the key advances, and remaining caveats, of which any user or interpreter of garnet geochronology should be aware.

Garnet isochron age precision. The precision of an isochron age (Fig. 9) depends on how well the slope of the isochron is constrained. Age precision (i.e., slope precision) depends on three main factors: 1) the analytical precision of the isotopic datapoints, 2) the spread in parent/daughter between lowest and highest points in the isochron, and 3) the scatter in the isochron. In general, the slope of the isochron is constrained most precisely when the analytical precision of each point is best, the spread in parent/daughter ratio is largest, and the scatter is smallest. Let us first address the importance of analytical precision and isochron spread in theoretical two-point isochrons. Then in the next section, we will explore the effect of adding additional points to an isochron and their scatter therefrom.

Modern mass spectrometry (TIMS or MC-ICP-MS for Sm–Nd, MC-ICP-MS for Lu–Hf) permits <10 ppm 2RSD analytical precision for $^{143}Nd/^{144}Nd$ and $^{176}Hf/^{177}Hf$ when sample size is unlimited (~100 ng of Hf or Nd). TIMS is the optimal tool for Nd analysis given higher net ion efficiency (especially as sample size decreases), whereas MC-ICP-MS is the optimal tool for Hf for the converse reason. Oftentimes, especially in applications requiring smaller amounts of garnet to be extracted and analyzed (such as zoned garnet chronology,

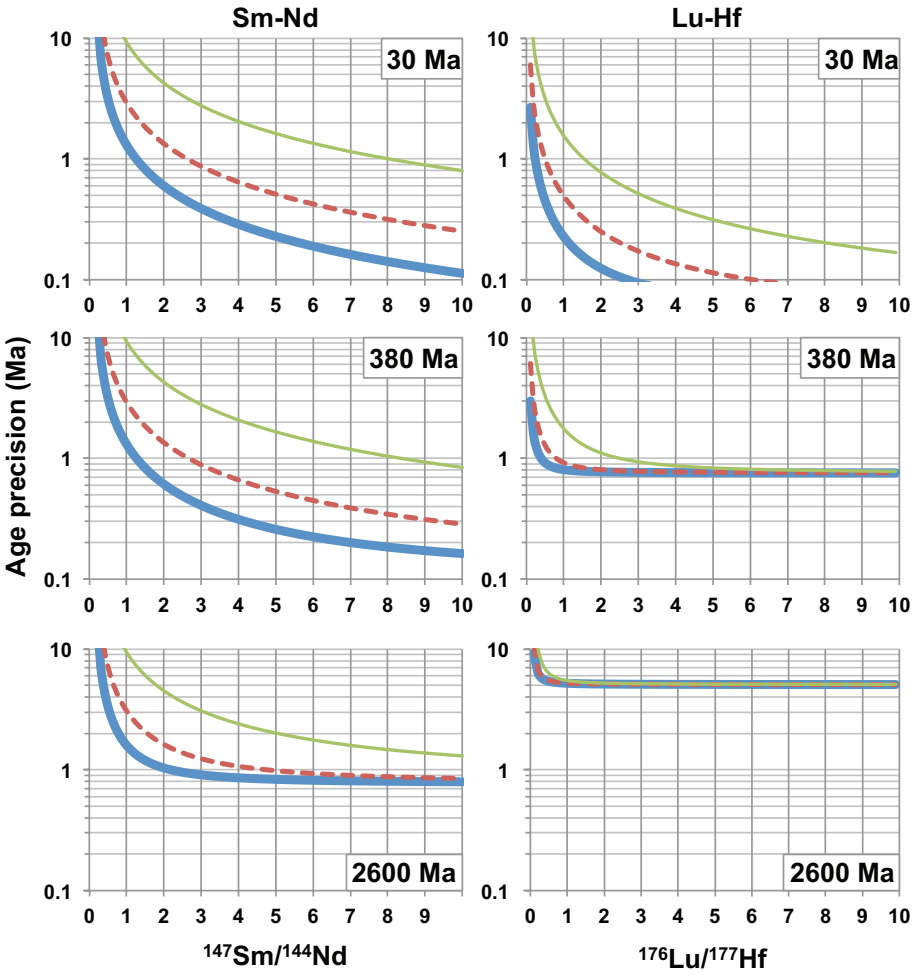

Figure 9. Garnet–matrix two-point isochron age precision as a function of parent/daughter isotope ratio for garnets of three different ages: Alpine (30 Ma), Acadian (380 Ma), Archean (2.6 Ga). In all plots, the bold lower line is for 10ppm (2σ) analytical precision on the garnet daughter isotope analysis, the dashed middle line is for 30ppm, and the thin upper line is for 100ppm. 10ppm analytical precision is achievable for $^{176}Hf/^{177}Hf$ when load size is unlimited (10s to 100s of ng Hf run on MC-ICPMS) and for $^{143}Nd/^{144}Nd$ (run as NdO^+ on TIMS) when load size is >4ng. As sample size decreases, as is usually the case for small amounts of clean garnet with low Hf and Nd concentration, analytical precision worsens (see text for discussion). $^{147}Sm/^{144}Nd$ analytical precision is 0.03% and $^{176}Lu/^{177}Hf$ is 0.2% indicative of optimal performance on TIMS and MC-ICPMS, respectively. Matrix $^{147}Sm/^{144}Nd$ is 0.15 whereas matrix $^{176}Lu/^{177}Hf$ is 0.02, each typical values for crustal rocks. If additional points are included in the isochron, the age precision can change depending on the MSWD (see text for discussion).

see below), the amount of Nd and Hf is much less than desired for optimal analysis. This sample size limitation has been one of the major factors limiting garnet geochronology. Figure 10 shows a compilation of garnet data, cleaned as well as possible with modern methods (see discussion below). Daughter element concentrations in clean garnet are generally less than 0.5 ppm and often below 0.1 ppm for Nd and Hf, meaning that tens of

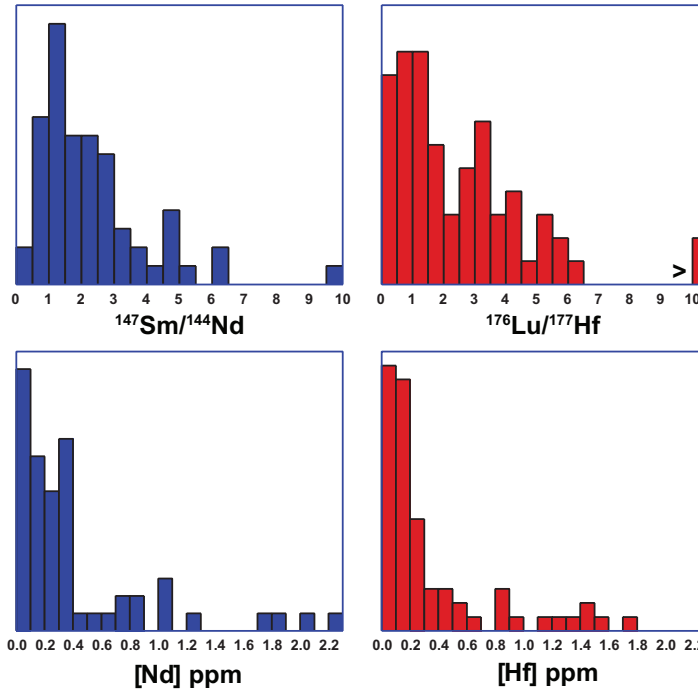

Figure 10. Histograms of reported garnet Sm–Nd and Lu–Hf data after cleansing efforts to remove inclusions using the methods of Pollington and Baxter (2011) for Sm–Nd and Lagos et al (2007) for Lu–Hf. $^{147}Sm/^{144}Nd$ and $^{176}Lu/^{177}Hf$ data are taken from Baxter and Scherer (2013), [Nd ppm] and [Lu ppm] concentration data correspond to the parent/daughter data and are compiled from the Baxter Lab and Scherer Lab (Erik Scherer, pers. comm.). Some $^{176}Lu/^{177}Hf$ data are off scale reaching as high as 50. Most well cleansed garnet has $^{147}Sm/^{144}Nd$ and $^{176}Lu/^{177}Hf > 1.0$, and [Nd ppm] and [Hf ppm] < 0.4.

milligrams of clean garnet may still only provide a few nanograms of Nd or Hf for analysis. Note that in estimating required sample size, one must consider the sample loss that occurs during mineral separation and garnet cleansing (see below) which can often exceed 80% of the raw garnet mass (e.g., Pollington and Baxter 2011). As analytical methods continue to improve, we can push to smaller and smaller garnet sample sizes and higher resolution petrochronology. Fortunately, recent and continuing advances in mass spectrometry permit improved analytical precision even as sample size decreases (Harvey and Baxter 2009; Schoene and Baxter 2017, this volume; Baxter and Scherer 2013; see Bast et al. 2015). For example, sub-nanogram loads of pure Nd standard solution analyzed as NdO^+ via TIMS can still yield external precision < 30 ppm 2RSD, though experience shows that sub-nanogram samples run through column chemistry typically return internal precisions 2–5 times worse (Schoene and Baxter 2017, this volume). Small sample analysis of Hf via MC-ICP-MS remains a limitation in most labs, though use of a desolvating nebulizer (Aridus), refined cone geometry, and 10^{12} ohm resistors, permits sub-nanogram loads of Hf from dissolved samples run through column chemistry and analyzed via MC-ICP-MS to yield 50–180 ppm 2RSE internal precision (Bast et al. 2015). Daughter isotope precision plays a larger role in controlling age precision for Paleozoic and younger samples and when parent/daughter ratio is lower, whereas parent/daughter isotope precision plays a larger role for Proterozoic and older samples and when parent/daughter ratio is higher (see Baxter and Scherer 2013). In general, $^{147}Sm/^{144}Nd$ ratios measured by isotope dilution (ID)TIMS can yield external

precision (i.e., by assessing reproducibility of mixed standard solutions, or homogeneous dissolved natural rock samples) better than 0.1% with modern methods. $^{176}Lu/^{177}Hf$ analysis via ID-MC-ICPMS is less precise—more typically 0.1 to 1.0%—because making precise mass bias corrections and spike subtraction is more challenging given that there are only two isotopes of Lu (though MC-ICP-MS permits addition of a secondary element, such as Erbium, for purposes of mass bias correction; e.g., Bast et al. 2015).

Most clean garnet yields parent/daughter greater than 1.0 for both isotopic systems (Fig. 10), perhaps slightly more often for $^{147}Sm/^{144}Nd$ than for $^{176}Lu/^{177}Hf$. It is also interesting to note that the very highest parent/daughter ratios (as high as 50; Lagos et al. 2007) are from $^{176}Lu/^{177}Hf$. These observations are an indication that $^{176}Lu/^{177}Hf$ tends to be much more strongly zoned from core (highest Lu/Hf) to rim (lowest Lu/Hf) owing to strong Rayleigh fractionation of parent Lu (over daughter Hf) into garnet, than $^{147}Sm/^{144}Nd$ which tends to have more uniform zonation (for example, see Fig. 7, or modeling of Kohn (2009), or LA-ICP-MS data from Anczkiewicz et al. (2007) and Anczkiewicz et al. (2012). Overall, as shown in Figure 9, theoretical two-point isochrons between clean garnet with parent/daughter >1.0 and a whole rock or matrix as the lower second point on the isochron can generally yield age precision between ±1.0 and ±0.1 million years (Baxter and Scherer 2013) assuming optimal analytical precision. If the garnet has parent/daughter «1.0, age precision (and sometimes accuracy, see below) degrades quickly. As sample size decreases and analytical precision predictably worsens, poorer age precision also results, though ±1–5 million years age precision is often still achievable in most cases.

Multi-point isochrons and the MSWD. If more than two points populate an isochron (which is always desirable), a statistical opportunity exists to evaluate that scatter and include it in the uncertainty of the isochron's slope, and the age. The most geochronologically relevant statistical measure of this scatter is the 'mean square of weighted deviates' or MSWD (e.g., Wendt and Carl 1991). It compares the scatter expected given the reported analytical uncertainty to the actual scatter of data from an isochron. When the observed scatter matches the statistically predicted scatter given analytical uncertainty, the MSWD is near 1.0; in this case additional points to the isochron can lead to better precision than that shown in Figure 9. Much higher MSWD will in turn lead to poorer (higher) age uncertainty and means that there is real geologic scatter from a single isochron; that is, some of the points populating the isochron fail one of the fundamental isochron assumptions. High MSWD isn't necessarily bad news though. If the high MSWD is due to multiple garnet analyses that scatter off the isochron, this may be an indication of resolvable age variation in the garnets being analyzed. Since it has been shown that garnet from the same rock (e.g., Skora et al. 2008; Herwartz et al. 2011) or the same crystal (e.g., Pollington and Baxter 2010; Dragovic et al. 2015) can span growth ages of many millions of years or even tens to hundreds of millions of years, such scatter and high MSWD is a useful and expected indicator of resolvable age zonation (also see Kohn 2009) that might encourage further textural or zoned garnet geochronologic analysis. In this regard, a range of individual two-point garnet–matrix ages is of greater meaning than a lumped average growth age produced by a multi-point isochron with high MSWD (e.g., Pollington and Baxter 2010; and see Fig. 16 discussed in the section on Zoned Garnet Geochronlogy below). If high MSWD is due to scatter from multiple whole rock, matrix, or mineral analyses (including poorly cleansed garnet) on the low side of the isochron, that could mean that one or more of those points doesn't belong and should be removed (this is discussed in a later section). Or, it may reflect real heterogeneity in the local rock matrix that, unfortunately, must be included in the age and its uncertainty (also discussed in a later section). MSWD less than 1.0 generally means that analytical uncertainties have been overestimated. Overestimation—sometimes referred to as 'conservative' estimation—of analytical uncertainty can also change a dataset that would yield a very high MSWD into

a dataset that yields a lower MSWD, unintentionally masking what may in fact be important geological scatter. The savvy geochronologist, or interpreter of geochronologic data, will be careful to look for such high 'conservative' estimates of analytical uncertainty in reported isochron data. It is therefore crucial that estimates of analytical uncertainty are accurate, not 'conservative', as both over and underestimates can have deleterious effects on age interpretation masking what could be important information about the system.

The garnet point on the isochron and the problem of inclusion contamination. Garnet geochronology with Lu–Hf or Sm–Nd works because garnet uniquely fractionates parent from daughter creating an unusually high parent/daughter ratio. The garnet always represents the high point (or points, if one makes multiple measurements of the garnet) on the isochron. However, essentially all garnets contain micro-inclusions of other minerals that may be older (if inherited) or younger (if accessed by cracks) than the crystallization age of the garnet itself. The problem of inclusions continues to be the greatest challenge for successful garnet geochronology; if inclusions in garnet are not sufficiently removed, resulting 'garnet' ages can be imprecise, and worse, grossly inaccurate. Unfortunately, the published literature is full of such examples and the reader is invited to critically evaluate the literature themselves in light of the perspective and data we offer in this section. At the same time, the notion that we cannot overcome the challenge of inclusions remains the greatest misconception that continues to limit the credibility and broader use of garnet geochronology. In fact, numerous methodologies have been developed that provide solutions to the inclusion problem in almost all cases, leading to clean garnet and robust, precise, and accurate garnet ages.

Why inclusions are a problem. The problem of contaminating inclusions was recognized in the very first paper on garnet geochronology in 1980 (van Breemen and Hawkesworth 1980). Micro-inclusions can be inherited from significantly older episodes, and some inclusions can be reset or precipitated after garnet growth during retrograde cracking and fluid influx. Therefore, in the worst case, a 'garnet' analysis that still contains abundant inclusions can lead to grossly *inaccurate* apparent ages that can be younger or older than the true garnet age (e.g., Fig. 11). In general, inherited (i.e., older) inclusions that have a parent/daughter isotope ratio lower than the host rock (or younger inclusions that have a parent/daughter ratio greater than the host rock) will pull the contaminated garnet down off the true isochron to create falsely young ages. The converse is also true. Of course, the more contaminated the 'garnet' analysis is, the lower its apparent parent/daughter, the greater the potential inaccuracy (Fig. 12). Even if included phases are in age equilibrium with the garnet (i.e., they lie perfectly on the garnet–matrix isochron) their presence in the 'garnet' analysis will pull the 'garnet' point down along the isochron, reducing the spread along the isochron, thus worsening the age precision (Fig. 12). The reader is referred to a great number of published studies that define and describe the problem of inclusion contamination for garnet geochronology (e.g., Zhou and Hensen 1995; Scherer et al. 2000; Prince et al. 2001; Thoni 2002; Baxter and Scherer 2013).

How to solve the problem of inclusions. In the past 20 years numerous methods have been developed to eliminate most inclusions from most garnets thereby solving the inclusion problem. Any attempt to clean a garnet separate begins and ends with careful handpicking of finely crushed separates. However, good handpicking alone is usually inadequate to fully alleviate the inclusion problem (e.g., Thoni 2002). Micro-inclusions that may not be visible to the naked eye can escape even the most diligent handpicking. So, the most successful methods to cleanse garnets of their micro-inclusions all involve a 'leaching' or 'partial dissolution' procedure in various strong acids either to dissolve away problem inclusions in discarded solution leaving pure garnet for analysis, or, to dissolve away pure garnet in the analyzed solution leaving problem inclusions behind in a solid residue. The former has been successfully employed for Sm–Nd geochronology (e.g., Zhou and Hensen 1995; DeWolf et

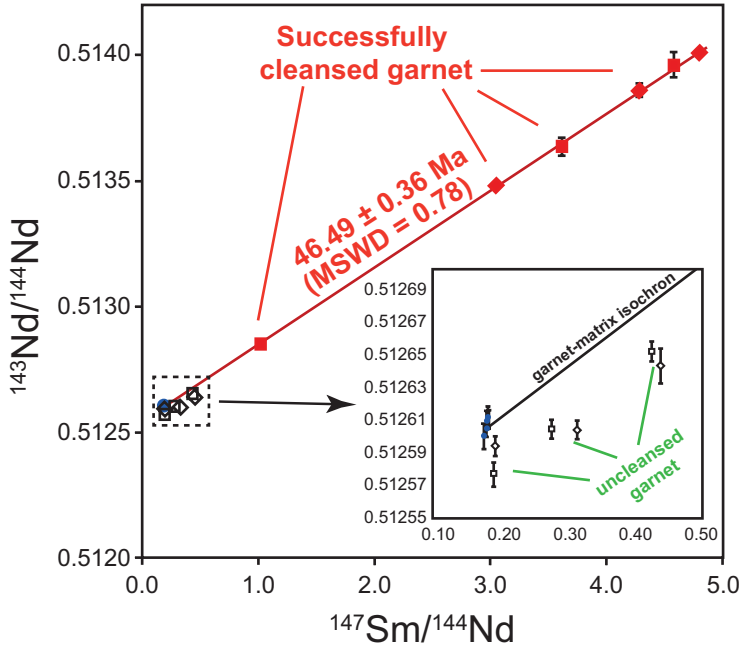

Figure 11. The problem of inclusions, and the success of partial dissolution to solve it. Sm–Nd isochron data are from a mafic blueschist (modified from Dragovic et al 2012). The lower inset shows uncleansed garnet (open symbols) dominated by inclusions prior to partial dissolution. Any attempt to create an age by pairing an uncleansed garnet with the matrix (filled circles) would lead to falsely young—even negative—ages. Main figure shows the same garnets after proper partial dissolution cleansing (filled diamonds and squares) and resultant accurate and precise isochron age.

al. 1996; Amato et al. 1999; Scherer et al. 2000; Baxter et al. 2002; Thoni 2002; Anczkiewicz and Thirlwall 2003; Pollington and Baxter 2011) where the most insidious inclusions are REE-rich minerals like monazite or clinozoisite which will dissolve in acid more readily than their garnet host. The latter has been successfully employed for Lu–Hf geochronology (e.g., Scherer et al. 2000; Lagos et al. 2007) where the most insidious inclusion is Hf-rich zircon, which is extremely resistant even to hydrofluoric acid at typical hotplate temperatures. This dichotomy does mean it is difficult to design a single cleansing method optimized for both Lu–Hf and Sm–Nd geochronology on the same sample aliquot. This, along with the analytical differences described earlier, in turn explains the dearth of studies where both Lu–Hf and Sm–Nd geochronology on the same samples yield optimal quality results from both systems. Some of the variables to consider when testing a partial dissolution method on a given garnet sample include: 1) acids used (e.g., Anczkiewicz et al. (2004) use sulfuric acid which attacks phosphates well, but does little to silicate inclusions like epidote if they are a factor, whereas HF partial dissolution of Amato et al. (1999) removes silicates well, but dissolves much of the garnet too requiring a delicate balance), 2) duration (anywhere from 15 to 180 min in HF have proven useful in different cases; e.g., Baxter and Scherer (2013)), 3) grain size (anywhere between 250 and 100 mesh size is recommended; finer grain size may lead to problems with garnet reactive surface area being too high; Pollington and Baxter 2011).

The term ‘partial dissolution’ cleansing is preferred over ‘leaching’ as the latter syntax could be interpreted to mean that something is actually leaching out of the garnet lattice itself. This leads to questions about whether the ‘leaching’ procedure is preferentially ‘leaching’ out

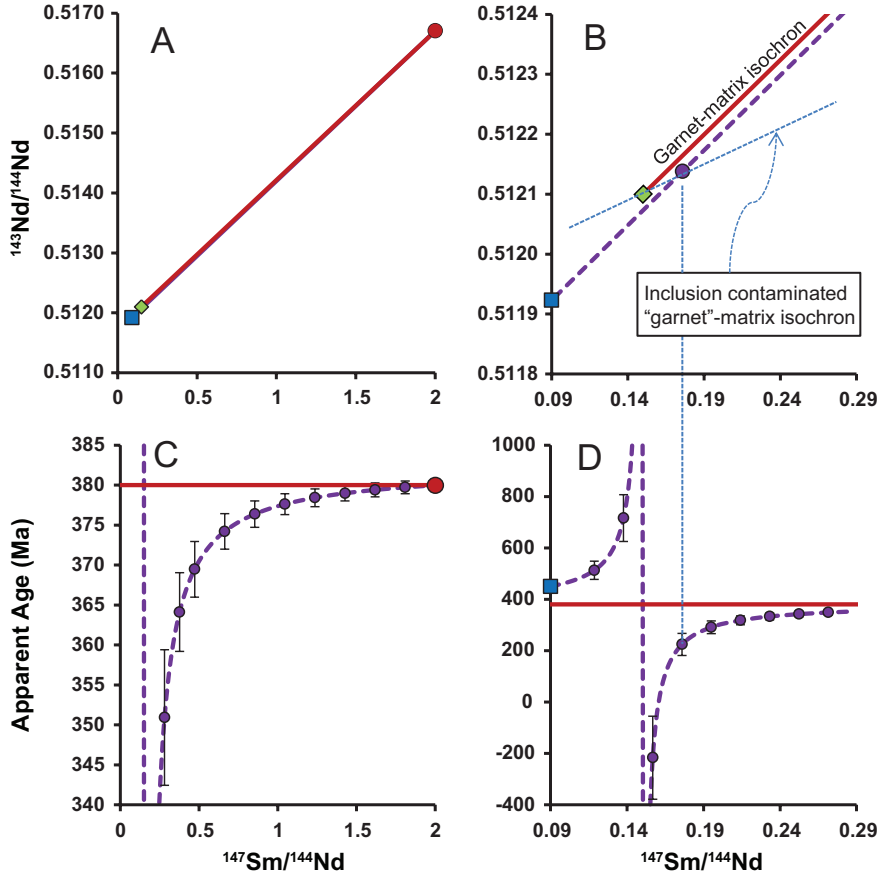

Figure 12. Effects of contamination by inclusions. These theoretical diagrams shown are for the Sm–Nd system but also qualitatively apply to the Lu–Hf system. Clean garnet (circle) has high $^{147}Sm/^{144}Nd$ ratio. Diamond is the matrix. Square is a low $^{147}Sm/^{144}Nd$ inherited inclusion (e.g., monazite for Sm–Nd or zircon for Lu–Hf) yielding an age of 450 Ma when paired with the host matrix. A and B show the true garnet–matrix isochron (solid line, with an age of 380 Ma) and a garnet–inclusion mixing array (bold dashed line). C and D show the apparent "garnet"-matrix age for "garnet" data points (circles) with varying amounts of inclusion contamination along the garnet–inclusion mixing line. Note that heavily contaminated "garnet" plotting near the matrix $^{147}Sm/^{144}Nd$ can yield imprecise and grossly inaccurate ages that are older or younger than the true garnet–matrix age, including even negative ages. B and D show a single example of a heavily contaminated "garnet" data point paired with the matrix to create a falsely young apparent isochron age with shallower slope (fine dashed) than the true garnet–matrix age. Two-point isochron age error bars shown are determined assuming the analytical parameters outlined in Figure 9.

parent vs. daughter (or vice versa). Here, it is important to note that none of the aforementioned studies have shown any evidence that the partial dissolution methods being employed create any fractionation or change of the garnet chemistry itself. When garnets are well cleaned they give remarkably consistent age results that would be impossible if some fractionation via 'leaching' was occurring (see Fig. 11). Differential 'leaching' of parent and daughter is also extremely unlikely because the mechanism for 'leaching' would be solid state diffusion through the garnet lattice; diffusivities at hot-plate temperatures (~100–200°C) are too slow to allow for any significant diffusion of REE and even slower Hf. Alpha-decay induced lattice damage that may enhance diffusive loss in U/Th-rich minerals like metamict zircon is not

an issue in garnet given the orders of magnitude smaller alpha flux in garnet due to lower concentrations of the alpha producing elements (e.g., Sm), the much slower decay rate of Sm, and single alpha decay for ^{147}Sm to stable ^{143}Nd. Should any fractionation effects be found (and no evidence yet exists to suggest there should be) it would be more likely to affect the Lu–Hf rather than the Sm–Nd system given the stronger chemical difference between the REE Lu and the HFSE Hf (as opposed to the REE's Sm and Nd). In summary, there is no evidence to suggest that partial dissolution cleansing of inclusions is affecting the remaining *clean* garnet's Sm–Nd and Lu–Hf chemistry at all.

How to know the garnet is clean (or clean enough). Because contaminating inclusions have much lower parent/daughter ratios, and much higher daughter element concentrations than their garnet hosts, well-cleaned garnet generally will exhibit high parent/daughter ratio and low daughter element concentration. Figures 10 and 13 provide two different compilations of 'garnet' parent/daughter ratio and daughter element concentration data to illustrate this. Figure 13 depicts the full range of published garnet data from a partial compilation of the literature. No screening was used in this compilation except to include only data reported as 'garnet' by the authors. Note the remarkable range in the data spanning many orders of magnitude, and the conspicuous negative relationship between parent/daughter ratio and daughter element concentration. In general, higher ^{147}Sm/^{144}Nd and lower Nd concentration indicates a cleaner garnet. But where do we draw the line between clean, clean enough, and dirty garnet? Rather than single out specific studies as good or bad, we present in Figure 10 similar compilations of published and unpublished Sm–Nd and Lu–Hf garnet data from over 100 different garnet-bearing rocks analyzed in the Boston University Lab (data from Ethan Baxter) and the Muenster Lab (personal communication from Erik Scherer) as they represent a subset of data prepared in a consistent manner, reflecting modern practices for Sm–Nd (by Baxter and colleagues using partial dissolution methods described by Pollington and Baxter 2011) and Lu–Hf (by Scherer and colleagues using partial dissolution methods described by Lagos et al. 2007). By no means does this mean that every sample in these plots is a perfectly cleansed garnet (that is surely not the case). But it does give an indication of the range of measured garnet compositions that typically results from best practices in these two particular labs that is instructive for sake of comparison. For Sm–Nd, 90% of the data indicate ^{147}Sm/^{144}Nd > 1.0 and [Nd] ppm < 0.4. For Lu–Hf, 90% of the data indicate ^{176}Lu/^{177}Hf > 0.5 and [Hf] ppm < 0.4. If the garnet doesn't exceed these cutoffs after the first attempt to cleanse it, we suggest additional attempts. Baxter and Scherer (2013) recommend that garnet is clean enough to avoid significant effects of inclusion contamination when it has parent/daughter ratio > 1.0, generally coinciding with daughter element concentration < 1.0. These of course are arbitrary cutoffs but are meant to provide some guidance in establishing the confidence (i.e., accuracy) of a given garnet age. Figure 12 also shows an example of the progressively diminished effect of inclusion contamination as a garnet is cleansed.

A good way to evaluate whether a garnet separate is clean is by comparison to in situ LA-ICP-MS or SIMS analysis (e.g., Prince et al. 2001; Anczkiewicz et al. 2007; Stowell et al. 2010; Stowell et al. 2014; Gatewood et al. 2015; Dragovic et al. 2016). Ideally, any garnet would first be lasered *in situ* to establish a baseline for clean parent/daughter and daughter element concentration in the garnet. Careful screening of laser data (considering multiple elements) is crucial to eliminate even slightly contaminated spots from the data (i.e., contamination by non-garnet mineral inclusions), because garnet Nd and Hf concentrations in clean garnet are so low (< 1 ppm, sometimes < 0.1 ppm). Still, LA-ICP-MS analysis can provide a valuable comparison to full garnet analysis of cleansed samples to see if partial dissolution was successful. Figure 14 shows an example from large garnets from Townshend Dam, Vermont from Gatewood et al. (2015). Note first the raw dataset for [Nd] ppm showing abundant spikes of high Nd (over 100 ppm!) within the garnet vividly depicting the significant presence of inclusions. After screening away most of the inclusion-contaminated points,

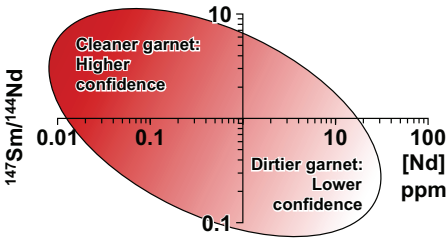

Figure 13. $^{147}Sm/^{144}Nd$ vs. [Nd] ppm for "garnet" data. The oval outlines a compilation of hundreds of published "garnet" data in the literature, a great many of which had not been properly cleansed of inclusions. Compare to the data from cleansed and uncleansed garnet shown in Figures 10, 11. Garnets with $^{147}Sm/^{144}Nd$ >1 and [Nd] <1 ppm is more likely to be clean and will return an accurate garnet age (darker shading). Garnets with very low $^{147}Sm/^{144}Nd$ and/or very high [Nd] ppm (lighter shading) constitute a large amount of the published data, these are almost certainly contaminated by inclusions; use of such analyses for a garnet isochron age will lead to less precise and possibly inaccurate results (see Figure 12).

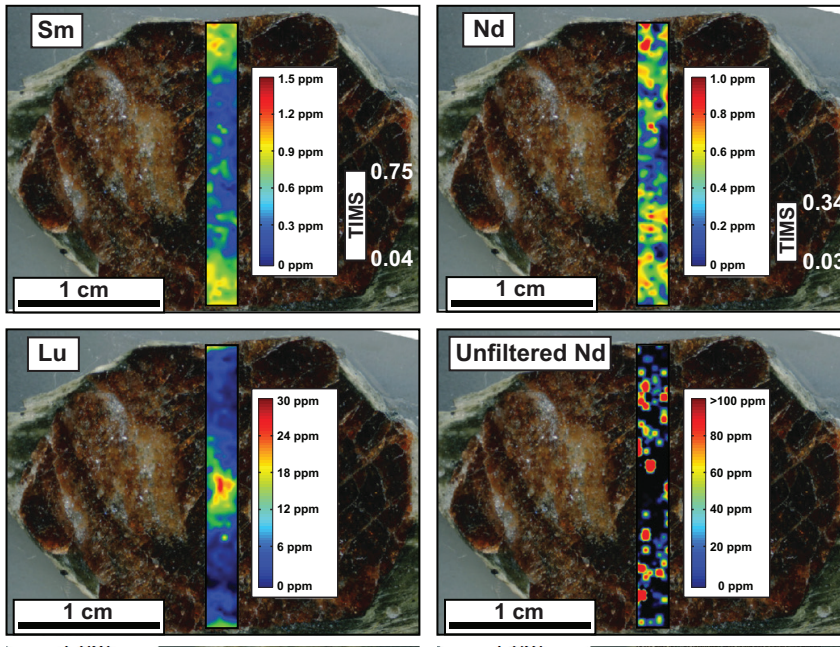

Figure 14. LA-ICPMS maps of Sm, Nd, Lu [ppm] in garnet from Townshend Dam, Vermont (modified from Gatewood et al 2015). Note Sm is slightly zoned with enrichments at the rim, whereas Lu is more strongly zoned with enrichments at the core. Nd is unzoned, except for numerous high spots reflecting Nd-rich inclusions. Bottom right panel shows raw unfiltered Nd data where the highest analyses show [Nd] in excess of 100ppm. Top right panel shows [Nd] data after carefully filtering out the most egregious contamination, revealing the underlying mostly clean garnet with concentrations <1ppm. White bars and values show the range of ID-TIMS analyses of the same Vermont garnets after proper cleansing reported by Gatewood et al (2015), showing good agreement with the laser data.

the refined LA-ICP-MS data show low [Nd] from 0.03 ppm to 0.5 ppm. In this study, these values are a close match for the cleaned bulk garnet data analyzed via TIMS, indicating success in cleansing away these inclusions and recovering true clean garnet.

Another vivid example of the success of partial dissolution cleansing, and the great importance of doing so, is shown in Figure 11 from Dragovic et al. (2012). Here, note where the 'garnet' data plot when they were intentionally analyzed without partial dissolution cleansing.

These data yield low $^{147}Sm/^{144}Nd < 0.45$ and high [Nd] ppm between 0.9 and 2.8 ppm along a crude mixing trend with an inherited inclusion population with low $^{147}Sm/^{144}Nd$ (akin to the theoretical example shown in Fig. 12b). Any of these 'garnets', when paired with the matrix, would give falsely young ages; a few would even give negative ages. But consider these very same garnet samples after experiencing a proper partial dissolution. Now, these data give high $^{147}Sm/^{144}Nd$ between 1 and 5 with [Nd] between 0.03 ppm and 0.07 ppm and plot together on a remarkably tight isochron indicating the time of garnet growth in this mafic blueschist.

The second point on the isochron. It takes a slope to calculate an age, a line to calculate a slope, and two points to make a line. Three, four, or five points lend further statistical credence to a linear isochron relationship but without at least a second point, isochron geochronology is a non-starter. In this regard, the second point on the isochron is just as important and powerful as the garnet point on the isochron in determining age precision and accuracy. The second point on the isochron must be an accurate and precise measurement of the rock matrix reservoir with which the garnet initially grew in isotopic equilibrium (e.g., $^{143}Nd/^{144}Nd$ or $^{176}Hf/^{177}Hf$). In the very simplest scenario (rarely achieved in real systems), an isotopically homogeneous parent rock or melt simultaneously crystallizes all its minerals, including garnet, such that the entire rock is in initial isotopic equilibrium and all minerals remain closed systems from that point until the present day. In this case, one could measure anything else in the rock—the entire whole rock itself, just the matrix, or any subset of the various other minerals in the rock—as a representation of that initial rock reservoir and pair it with the pure garnet to form a two point isochron. Additional garnets (with high Sm/Nd or Lu/Hf) or additional whole rock, matrix, or mineral analyses (with low Sm/Nd of Lu/Hf) would further populate the isochron and a happy multi-point isochron with a perfect MSWD of 1.0 would result. In reality, many rocks (or protoliths) are not perfectly isotopically homogeneous at the onset of garnet growth, the whole rock and matrix may differ due to parent/daughter Rayleigh fractionation during garnet growth, the matrix may experience open system change of parent/daughter or daughter isotope composition after/during garnet growth, and different mineral phases may grow or close to isotopic exchange with the rock reservoir at different times than the garnet. Any of these factors can conspire to create an inaccurate or imprecise garnet isochron age if such data that don't belong are included on an isochron. Stated differently, more points on an isochron are only a good idea if those points belong on the isochron. The good news is that most of these effects are very minor to negligible most of the time. Let us explore these each in turn.

Initial matrix heterogeneity. If the rock reservoir is initially heterogeneous for whatever reason, how can we know what the garnet actually grew in equilibrium with? Igneous protoliths are probably least susceptible to this issue given that they are fairly homogenous when they first form. However, ancient layered sedimentary protoliths where each layer may include inherited minerals of varying provenance can present problems in this regard. For isotopic systems like U–Pb or Rb/Sr where the range of parent/daughter ratio among phases can be several orders of magnitude, this can create enormous heterogeneities (via differential radiogenic ingrowth) the effects of which can be severely problematic for garnet (or any) isochron geochronology in those systems (e.g., Romer and Xiao 2005). Fortunately, with the exception of garnet, most common minerals (and rocks) have a limited range of Lu/Hf and Sm/Nd ratios such that the magnitude of matrix heterogeneities is much smaller. Still, matrix heterogeneity can be significant given the high precision and accuracy often desired (and achievable) with modern methods.

Let us consider a layered sedimentary protolith. The layers have varying $^{147}Sm/^{144}Nd$ (or $^{176}Lu/^{177}Hf$) which has led to varying $^{143}Nd/^{144}Nd$ (or $^{176}Hf/^{177}Hf$). Let us now permit garnet to grow instantaneously and with uniform distribution in that layered rock. [In reality, the different layers may have different enough major element chemistry so as to preferentially crystallize garnet more on certain layers than in others, but let us ignore that for the present

discussion]. At any given location in the layered rock system, the new garnet crystallizes with an average composition reflective of the equilibrium lengthscale (*Le*) for that element in the system (see Baxter and DePaolo (2002a,b), and DePaolo and Getty (1996) for further discussion). The equilibrium lengthscale for a given element, *Le*, is dependent on the effective diffusivity (D^*) of the element within the intergranular transporting medium (ITM; Baxter and DePaolo 2002b), and the local reaction/exchange rate (R) for that element between the matrix minerals and the ITM: $Le = (D^*/R)^{1/2}$. The effective diffusivity (D^*) includes both the diffusivity in the ITM, and the partitioning of that element between the solid minerals and the ITM. Elements (like Sr) that are strongly partitioned (i.e., soluble) into the fluid filled ITM have high D^* and smear out and average $^{87}Sr/^{86}Sr$ over a large equilibrium lengthscale. Elements like Nd and Hf are very weakly partitioned (i.e., insoluble) into the fluid filled ITM of most crustal fluids and thus have relatively low D^*; thus $^{143}Nd/^{144}Nd$ and $^{176}Hf/^{177}Hf$ of the ITM (and any garnet crystallizing from it) will closely match the local bulk matrix solid. In practice, this means you wouldn't want to pair a garnet from one layer with bulk matrix from another layer. But, if you crushed up the entire rock and sampled a representative average garnet separate and matrix from the entire volume, the heterogeneities average out and the problem goes away. However, now consider the growth of a very large garnet porphyroblast large enough to grow over several compositional layers. A single crystal like this would be attractive for high-resolution microsampling and zoned geochronology. In this scenario, each concentric growth ring, or even different portions of the same growth ring, of the garnet may inherit a different starting $^{143}Nd/^{144}Nd$ (or $^{176}Hf/^{177}Hf$) depending on the layer(s) it is in. When focusing on a single crystal, or portions thereof, it is no longer advisable to use a large averaged whole rock to anchor the isochron in a heterogeneous protolith. Instead, one must carefully analyze and evaluate the extent of porphyroblast scale matrix heterogeneity via multiple measurements and include them all on an isochron. This is an important statistical acknowledgement of the uncertainty about the second point on the isochron that will result in larger age errors and larger MSWD. Gatewood et al. (2015) shows a vivid example of the effects of such cm scale matrix heterogeneity on zoned garnet geochronology from a layered meta-sedimentary rock. On the contrary, Pollington and Baxter (2010) saw no such effect when conducting zoned garnet chronology in a homogeneous rock matrix, most likely inherited from an igneous protolith. Overall, it is always advisable to evaluate the extent of matrix heterogeneity of any rock, try to avoid major heterogeneities and lithologic contacts if possible, and match multiple garnets (or bulk garnet separates) and average matrix from the same rock volume to average out heterogeneities.

Whole rock vs. matrix. We define a 'whole rock' as the entire rock volume including the garnet itself. We define the 'matrix' as the entire rock volume excepting the garnet. As a garnet with much higher Sm/Nd and Lu/Hf than the original whole rock grows, it will alter the Sm/Nd and Lu/Hf of the remaining matrix via simple Raleigh fractionation. Strictly speaking, the core of the garnet (the initial fraction of garnet to grow) should be paired with the 'whole rock', whereas the outermost rim of the garnet (the final bit to grow) should be paired with the matrix. In general it is advisable to measure both matrix and whole rock from the same rock averaged volume to establish the significance of that difference for your particular rock. For Sm–Nd, the general finding is that matrix and whole rock are very rarely different enough to make a significant difference to the age. This is largely due to the fact that the concentration of Nd and Sm in clean garnet is usually one or more orders of magnitude smaller than the concentration in the matrix. It would require a lot of garnet to create a significant difference in parent/daughter. The Lu–Hf system is more susceptible to this process as Lu concentrations in garnet can be much higher (up to an order of magnitude or more) than the whole rock especially at the onset of garnet growth, whereas Hf concentrations are very low. This could lead to more significant Rayleigh fractionation

effects leaving the residual matrix with even lower Lu/Hf after garnet growth. Fortunately, for either system, if the time duration between growth of core and growth of rim is short, negligible radiogenic daughter in-growth (and rotation of the isochron beyond horizontal) will have occurred. In this case, shifting Sm/Nd or Lu/Hf of the matrix to different values along a near horizontal line near the time of garnet growth will have negligible effect on the final isochron age determination. Finally, because most garnets also include (and effectively sequester) other minerals the net change to the host rock composition is offset and minimized. Rocks with low Nd or Hf concentrations (< 10 ppm) and a large timespan between growth of garnet core and rim are therefore more susceptible to this easily accounted for effect.

Open system change of matrix. If the matrix experienced any kind of open system exchange, or loss, or gain of Sm, Nd or Lu, Hf there is potential to skew the garnet–matrix isochron age relationship. Mechanisms may include partial melting where a melt is lost from the system, the injection of a melt into the system, or the passage of fluids through the system. Most common crustal fluids have low solubilities of REE and Hf so only in extreme cases of focused fluid flow should we observe major Sm/Nd or Lu/Hf loss or gains. Important examples of such open system mobility of REE have been found in crustal fluids (Zack and John 2007; Ague 2011). Loss of an internally derived partial melt would leave the solid residue with a higher Sm/Nd or Lu/Hf ratio. But as long as the internally derived melt would be in Nd and Hf isotopic equilibrium with the bulk solid there would be no isotopic fractionation in the melt depleted residue. This should generally be the case, unless incongruent melting of a very old protolith (where significant mineral scale Nd or Hf isotopic differences had already evolved) created a melt with different isotopic composition (e.g., Zeng et al. 2005) and that melt was extracted quickly, before isotopic equilibrium could be restored via diffusion; in this case the resulting effect on age should be evaluated. Fortunately for the Sm–Nd and Lu–Hf systems (as opposed to U–Pb or Rb–Sr), such radiogenic differences are relatively small given the narrow range of Sm/Nd and Lu/Hf that exist among most common minerals (e.g., Romer and Xiao 2005). Introduction of an external melt or fluid into the system has the potential to be much more problematic, regardless of when the metasomatic event occurred with respect to garnet growth. External melts or fluids could bring completely different Nd or Hf isotopic chemistry that could mix with the original rock matrix pulling it vertically up or down well off the garnet–matrix isochron. Changes in Sm/Nd or Lu/Hf may also occur which could add to the effect if the metasomatic event happened a long time after garnet growth (when the isochron had already rotated well past horizontal). In general, the garnet geochronologist should avoid samples bearing evidence of open system metasomatism: in a vein, next to pegmatite, near a lithologic contact. Or, great care should be taken to evaluate the isotopic extent of that metasomatism to try and recreate the original rock matrix as well as possible. In some cases, the garnet inclusions may serve as a guide towards reconstructing the original rock matrix, but as we have seen, these minerals inclusions (if they are inherited from earlier events) do not always accurately reflect the garnet's original isotopic growth environment.

Non-garnet mineral growth and/or closure. The very first garnet geochronology papers chose minerals (like clinopyroxene in an eclogite, for example; Griffin and Brueckner 1980) rather than a whole rock to pair with the garnet in two-point isochrons. Some papers continue to add other minerals along with a whole rock or matrix to anchor the garnet isochron. Most of the time, these mineral data plot very near the whole rock or matrix (i.e., with similarly low parent/daughter) and have little effect on the age. But sometimes these individual minerals plot slightly off the isochron, leading to higher MSWD if included, or different absolute ages if employed instead of the whole rock. Which point is a better representation of the rock reservoir with which the garnet grew in isotopic equilibrium? On the one hand, the clinopyroxene and garnet in an eclogite both reflect growth at eclogite facies conditions (whereas the whole rock may have other phases that grew before or since eclogite facies) and thus one could argue they are a

good match if the goal is to date eclogite facies conditions. However, it is almost certainly the case that clinopyroxene has a different effective 'closure' time (due to processes like diffusion or matrix recrystallization) than the garnet, so if the clinopyroxene has a different $^{147}Sm/^{144}Nd$ than the matrix it will evolve off the garnet–matrix isochron and should not be included. The magnitude of this effect depends on the difference in closure/growth age of clinopyroxene vs. garnet, and on the difference in $^{147}Sm/^{144}Nd$ between clinopyroxene and the matrix. But, if the matrix itself is made up of all these minerals, how then can we argue that the matrix is any better a choice? The reason is that the matrix itself has remained a closed system and represents an appropriate rock-averaged Sm–Nd and Lu–Hf composition from which the garnet first grew. Resistant accessory phases (like monazite or zircon) are the exception in that they can retain their inherited isotopic signatures and generally do not participate as reactants in garnet growth.

The second point(s) on the isochron cannot be overlooked. At a minimum, it is worth measuring a representative whole rock and matrix. Pure non-garnet mineral separates may not be good choices for the isochron, especially when their parent/daughter ratio differs greatly from the matrix and/or their growth or closure time differs greatly from that of garnet. Avoid rocks with evidence for open system exchange, of significant layering or heterogeneity. If heterogeneity exists, it must be evaluated and included in the isochron to acknowledge that uncertainty (e.g., Gatewood et al. 2015). While many of these issues have the potential to completely ruin U–Pb or Rb–Sr garnet geochronology, they are rarely a major problem for Sm–Nd and Lu–Hf geochronology if reasonable care is taken to evaluate them.

Why Do Lu–Hf and Sm–Nd Ages Differ? The Complementarity of Lu–Hf and Sm–Nd Garnet Geochronology. One of the powerful opportunities of garnet geochronology is the theoretical ability to date the same garnet (or garnet-bearing rock) with both Lu–Hf and Sm–Nd. As discussed above, this hasn't been done as often as we would like given the different instruments required for optimal analysis (i.e., TIMS for Sm–Nd and MC-ICPMS for Lu–Hf) and because the most popular methods employed for removing inclusions are opposite for Lu–Hf and Sm–Nd. Thus, most labs are optimally equipped for one or the other, but rarely for both. Still, a growing number of labs have attempted to date the same garnet-bearing rocks with both methods (e.g., Lapen et al. 2003; Kylander-Clark et al. 2007; Cheng et al. 2008, 2016; Skora et al. 2009; Anczkiewicz et al. 2012; Smit et al. 2013) leading to interesting observations that, when fully understood can lead to valuable insights about the rock's history. Both systems are well suited for garnet geochronology, though their different pros and cons may make one more suitable for a given sample suite or application, and thus powerfully complementary when used in concert.

A notable observation made in many (though not all) of such combined studies is that Lu–Hf garnet ages tend to be older than Sm–Nd ages from the same rock. Why is this the case? The possible answers can be grouped into three categories, one (or more) of which may apply in any given situation:

1. Different parent isotope zonation for Lu–Hf and Sm–Nd (e.g., Skora et al. 2009)
2. Different 'closure temperature' for Lu–Hf and Sm–Nd (e.g., Yakymchuk et al. 2015)
3. Something is wrong with the Sm–Nd age or the Lu–Hf age

Let us address each scenario in turn as each provides an opportunity to further explore some of the important differences and complementarity of Lu–Hf and Sm–Nd garnet geochronology.

Different parent isotope zonation for Lu–Hf and Sm–Nd. As discussed in the section on trace elements above, Lu is very strongly partitioned into garnet during its growth as compared to other common matrix minerals. On the contrary, Sm, Nd, and Hf are all weakly partitioned

into garnet as compared to other matrix minerals (though Sm not as weakly as Nd, hence the reason that garnet can still have high Sm/Nd *ratios* despite relatively low Sm and very low Nd *concentrations*). Thus, garnets tend to be strongly zoned in Lu (with highest Lu concentrations in the early grown core as much as ~100 times higher than rims with low Lu; Figs. 7 and 14) whereas Sm, Nd, and Hf tend to be unzoned or with slight enrichments toward the rim (e.g., Lapen et al. 2003; Cheng et al. 2008; Skora et al. 2008; Peterman et al. 2009; Anczkiewicz et al. 2012; Smit et al. 2013; Gatewood et al. 2015; Fig. 15). Because the age information contained within a garnet crystal is based on the concentration of the parent element (Lu or Sm) this chemical zonation means that Lu–Hf ages will generally be skewed towards the age of core growth (where more of the Lu resides) whereas Sm–Nd ages will be skewed towards the age of rim growth (where more of the Sm resides). It is also important to note that while these general trends for Lu and Sm zonation are common, more complex zonation in Lu and/or Sm can exist in certain garnets ((see trace element section, above). This underscores the value of analyzing the core-to-rim Lu and Sm zonation of the actual samples in question as they have implications for interpreting the different 'bulk' Lu–Hf and Sm–Nd garnet ages. Lapen et al. (2003), Skora et al. (2009), and Kohn (2009) show examples of how measured Lu and Sm zonation can be used to model bulk ages by identifying where/when during garnet growth the parent element and mass averaged age would plot (e.g., Fig. 15). Such modeling requires certain assumptions including growth symmetry (e.g., perfect spherical shells), growth rate (constant vs. episodic), but are generally very useful in explaining age differences and, in the best case, placing constraints on total growth duration (e.g., Skora et al. 2009). For garnets that never experience temperatures above ~650 °C (above which diffusive mobilization may become significant; see below) the difference in Lu vs. Sm zonation is the dominant reason why Lu–Hf ages are different (generally older) than Sm–Nd ages. Both systems date primary growth, but they reflect different stages of that prolonged growth duration.

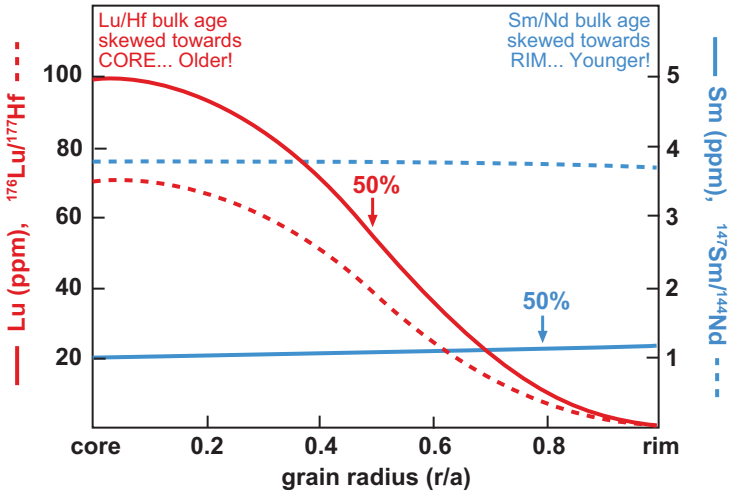

Figure 15. Conceptual zonation diagram of Lu, Hf, Sm, Nd resulting from simple Rayleigh fractionation during growth (modified from Kohn 2009). "*r/a*" on the *x*-axis indicates relative radial location from garnet core to rim of radius "*a*". "50%" shows the radial location where exactly half of the parent isotope is in core-ward and rim-ward garnet portions. Lu is strongly zoned, varying by two orders of magnitude from core to rim, whereas Sm is only slightly zoned. Note spherical symmetry involved in this model. This zonation is the primary reason that Lu–Hf bulk grain ages tend to be older than Sm–Nd bulk grain ages. Because $^{147}Sm/^{144}Nd$ is nearly unzoned, the Sm–Nd system offers a better chance at precise zoned garnet chronology from core-to-rim, whereas Lu–Hf offers a better chance to precisely date the earliest growth of garnet core.

Different 'closure temperature' for Lu–Hf and Sm–Nd. Because most garnets grow below their 'closure temperature' for Sm–Nd and Lu–Hf, and never experience higher temperatures, diffusive 'closure' is generally *not* at play when interpreting garnet geochronologic data, including the difference between Sm–Nd and Lu–Hf ages. However, for garnets that did experience temperatures in excess of ~650 ºC during or after their growth, the issue of diffusive 'closure' (i.e., Dodson 1973) or perhaps more appropriately diffusive 're-opening' (i.e., Caddick et al. 2010; Watson and Cherniak 2013) may come into play. Numerous papers have attempted to place constraints on the 'closure temperature' of garnet for both systems but, as pointed out and modeled by Ganguly and Tirone (1999) the classic Dodson formalism for closure is rarely appropriate for garnet because it is rarely completely reset before dropping through a closure temperature interval. As Watson and Cherniak (2013) describe, the matter is more often one of diffusive 'opening' whereby a garnet is heated for some period of time to temperatures high enough that diffusive resetting may begin. For example, Baxter et al. (2002) used the diffusion data of Ganguly et al. (1998b) to show that only the outermost few 10s of microns of a garnet crystal would be affected by age resetting during heating up to ~660 ºC (over a span of 12 million years), resulting in a negligible degree of bulk age resetting (depending on the grain size of course). Since then, numerous studies—both experimental and empirical—have sought to constrain the diffusivity of the REE (i.e., Sm, Nd, Lu: e.g., Carlson (2012), Tirone et al. (2005), Van Orman et al. (2002) and Hf: Bloch et al. (2015)). While all REE (including Sm, Nd, and Lu) appear to diffuse at the same rate within existing uncertainties, some overall discrepancy exists amongst existing studies of REE diffusion. Ganguly et al. (1998b) and Tirone et al. (2005) return diffusivities for the REE about an order of magnitude higher than those of Van Orman et al. (2002), Carlson (2012), and Bloch et al. (2015). Bloch et al. (2015) suggest that the difference may reflect a concentration dependence on REE diffusivity (i.e., lower concentrations diffuse via a faster diffusion mechanism) such that the faster Tirone et al. (2005) data are more appropriate for geochronologic applications. In any case, the data of Tirone et al. (2005) represent the fastest and thus provide a lower constraint on the temperatures at which REE in garnet become mobile for garnets, which of course itself is also dependent on grain size and cooling rate. Rather than quote blanket 'closure temperatures', interpreters of garnet geochronologic data should explore the partial diffusive resetting of ages by means of simple analytical or numerical modeling for the grain size and specific heating/cooling history that may have existed in the given system. Ganguly and Tirone (2001) and Watson and Cherniak (2013) provide useful analytical formalisms that may be used in general cases. Baxter et al. (2002), Korhonen et al. (2012), and Dragovic et al. (2016) are examples where simple case specific modeling was employed to constrain the likely extent of resetting. Baxter and Scherer (2013) model the range of temperatures required to reset a bulk garnet age just 5% (i.e., just beginning to 're-open') and 95% (i.e., essentially completely reset) for given grain size, temperature, and dwell time at that temperature. The reader is encouraged to consult these papers and model the diffusive resetting of Nd or Hf age information in their specific case.

The recent experimental data of Bloch et al. (2015) confirmed previous empirical inferences (e.g., Scherer et al. 2000; Kohn 2009; Anczkiewicz et al. 2012; Smit et al. 2013) that the diffusivity of Hf is considerably lower (by an order of magnitude, or more) than that of all the REE, including Lu. Without question, Hf diffusivity is much slower than Nd diffusivity; thus the Sm–Nd system is more susceptible to thermal diffusive resetting than the Lu–Hf system. That is, the 'closure temperature' of Hf is significantly higher than that of Nd. Bloch and Ganguly (2015) present diffusion modeling to show that the time required to fully reset Hf isotopic composition of garnet is 10–1000 times longer (at a given temperature) than the time required to fully reset Nd isotopes. Thus, for garnets experiencing temperatures above ~650 °C, the difference in Hf vs. Nd diffusivity should result in generally younger Sm–Nd ages (which have been partially reset) vs. Lu–Hf ages. Yakymchuk et al. (2015) shows a good example of this in a high temperature (~850 ºC) migmatite where other possibilities (Lu vs. Sm zonation) can be ruled out.

Something wrong with the Lu–Hf or the Sm–Nd Age? As discussed above, there are numerous other reasons why a given Sm–Nd or Lu–Hf age might simply be flawed, in which case comparisons to good Lu–Hf or Sm–Nd data are misguided. Perhaps most notorious is the effect of inclusions, especially as most samples are not cleaned with methods optimized for both Sm–Nd and Lu–Hf (see above). While this chapter prefers not to enter the business of identifying 'bad' published data, we will point out that both good and bad certainly do exist in the literature. As previously discussed, Sm–Nd or Lu–Hf garnet data where the parent/daughter ratio is <1.0 and/or the daughter element concentration is >0.5 ppm should be scrutinized carefully as these are the hallmarks of inclusion contamination that can create significant age inaccuracies (see Figs. 12, 13, 14). While high Nd or Hf concentration and low $^{147}Sm/^{144}Nd$ or $^{176}Lu/^{177}Hf$ do not necessarily prove age-distorting contamination, experience shows that such data usually indicate an inclusion problem that should be addressed or evaluated in some way (Smit et al. 2013) before the resulting age is accepted.

An additional factor unique to the Lu–Hf system is the possibility of diffusive decoupling of parent Lu from daughter Hf. Because Lu (and all REEs) diffusive at a much faster rate than Hf (see above discussion and Bloch et al. 2015), it is theoretically possible that Lu zonation may smooth out within a garnet, or that Lu may diffuse into or out of a garnet as *P–T* changes (only if garnet–matrix Lu partitioning changes) subsequent to garnet growth, all while the Hf isotopic composition remains locked in. While the effects of such Lu mobility on resulting age can vary depending on the situation, most often this would result in a counterclockwise rotation of the garnet–matrix isochron and falsely old ages. As with all closure-related arguments for garnet geochronology, it is important to note again that this process is only possible when garnet is heated above the 'closure temperature' for Lu (> ~650°C) for a significant period of time, and most enhanced for smaller garnets, and the highest temperatures. This argument rarely applies to the majority of greenschist and amphibolite facies garnets that never experience such high temperatures. When this process is at play, Lu–Hf ages can be compromised, thus rendering meaningful comparisons to good Sm–Nd data impossible. Papers by Kohn (2009), Anczkiewicz et al. (2012), Bloch et al. (2015), Bloch and Ganguly (2015), and (Kohn and Penniston-Dorland 2017, this volume) discuss and develop this potentially confounding problem for Lu–Hf geochronology while Anczkiewicz et al. (2012) shows compelling evidence for its occurrence in a natural setting.

Zoned garnet geochronology. The vast majority of published garnet geochronology, and the entire discussion in this chapter up to this point, involves what we call 'bulk garnet' geochronology. As long as no unintended fractionation of the garnet occurs (for example, due to magnetic separation which may select against garnet portions with differing amount of magnetic inclusions; e.g., Lapen et al. 2003), a 'bulk age' simply represents the parent isotope weighted (based on parent element zonation) average age of the garnet (Fig. 15). For a garnet that grew very rapidly (i.e., whose growth duration is within the age precision), such a bulk age is a valuable and precise measure of the growth event. However, if the garnet growth duration exceeds the attainable age precision (as may often be the case) the 'bulk age' is of limited petrochronologic utility, representing only an average age within an unresolved timespan of garnet growth. Insofar as multi-point bulk garnet isochrons might display scatter amongst clean garnet data with high parent/daughter, the bulk age precision (poorer) and MSWD (higher) represent a valuable indication that the garnet may have resolvable age zoning. Consider for example, the dataset in Figure 16 from Pollington and Baxter (2010). All of these garnet data are from the same rock. All of these garnet data are clean, passing any test of inclusion contamination. Matched with the matrix data, we can calculate a multi-point age of 25.5 Ma with a disappointing precision of ±5.3 Ma and eyebrow-raising MSWD of 270. Here is a reminder that poor MSWD, especially when caused by scatter of clean garnet at high parent/daughter, is not necessarily (nor even often) an indication that something has gone wrong. Rather it is a statistical invitation to explore the hypothesis of resolvable age zonation through means of zoned garnet geochronology.

In fact, the data shown in Figure 16 are from different zones of the same single garnet crystal, sampled as concentric rings from core to rim. With this context, the dataset suddenly makes sense. Instead of a single ill-advised multi-point isochron, what we really have are twelve individual two-point isochrons that reveal a 7.5 million year growth duration (Pollington and Baxter 2010). With the textural context of each garnet growth zone, we find that multiple two-point isochrons are better, and more appropriate, than a single multi-point isochron.

Zoned garnet geochronology is not new. In fact, the first attempts to extract and date different garnet growth zones spanned work between 1988–1999 (Cohen et al. 1988; Christensen et al. 1989, 1994; Vance and Onions 1990, 1992; Burton and Onions 1991; Mezger et al. 1992; Getty et al. 1993; Vance and Harris 1999). These papers used Rb–Sr and/or Sm–Nd to date two or three concentric growth zones in single 1–5 cm garnet crystals, separated via some combination of sawing, crushing, and plucking. Stowell et al. (2001) pioneered a core-drilling procedure to extract different garnet zones for Sm–Nd geochronology in a number of settings including contact metamorphism in Alaska, granulite facies migmatites in Fiordland, New Zealand, and granulites from the Cascades of Washington USA. Solva et al. (2003) separately analyzed core and rim of magmatic pegmatite garnet constraining Permian magmatism in the Alps. Ducea et al. (2003) were the first to employ a microdrilling apparatus (the MicroMill™) to extract garnet from three concentric growth zones from high temperature garnets in two Western North American sites. They modeled their data to constrain cooling rates from peak magmatic arc temperatures. In their study, the MicroMill™ was used to directly extract garnet in powdered form from individual drilled pits in core and rim. Pollington and Baxter (2010) used the MicroMill™ for chemically contoured sampling of concentric zones in a large 6 cm garnet from the Austrian Alps (Fig. 16). The spatial and age resolution of the Pollington and Baxter (2010) study permitted not just a constraint on total growth duration, but also the recognition of two significant pulses in the rate of garnet growth, correlated with chemical and textural features indicative of evolving thermodynamic and tectonic conditions, that would have otherwise have been missed. Pollington and Baxter (2010, 2011) used the Micromill™ to drill out concentric trenches, between which solid garnet annuli were left for collection, crushing, partial dissolution cleansing, and Sm–Nd TIMS analysis. They found that garnet powders derived from the drill trenches could not be cleaned of inclusions due to the extremely fine grain size; thus, the material from drilled trenches was discarded. Since then, three other studies (Dragovic et al. 2012, 2015; Gatewood et al. 2015) have employed the microdrilling methodology outlined in Pollington and Baxter (2011) extracting between 3 and 10 annuli per garnet crystal in blueschist facies rocks from Sifnos, Greece (Dragovic et al. 2012, 2015) and regional metamorphic schists from Townshend Dam, Vermont (Gatewood et al. 2015; the same rocks first dated by Christensen et al. 1989). Most of the studies cited in this paragraph show that < 1.0 Myr Sm–Nd age precision is achievable even as sample size decreases with more highly resolved sampling and smaller sample sizes.

Until recently, Lu–Hf zoned geochronology had not been attempted, in large part due to sample size limitations given that most labs still require 10's–100's ng Hf for MC-ICPMS analysis, but this is changing. Herwartz et al. (2011) separated cores and rims of strongly color zoned garnet from the Alps by crushing and handpicking, which were subsequently dated via Lu–Hf. This first study of garnet age zonation with Lu–Hf revealed an old inherited Variscan (~333 Ma) core surrounded by much younger Alpine (~38 Ma) rims, which these authors interpreted as evidence of two distinct cycles of subduction to mantle depths separated by three hundred million years. Nesheim et al. (2012) separated and grouped cores and rims of multiple garnet crystals in a single Mesoproterozoic sample from Idaho, USA, revealing mixed garnet ages bracketed by two major garnet growth events at ~1330 and ~1080 Ma. Anczkiewicz et al. (2014) extracted and dated three growth zones, based on textural and chemical patterns, from a large 3 cm garnet crystal from the Himalaya (see further discussion below). Schmidt et al. (2015) used saw cuts to sample up to 4–6 solid growth zones in four different 3–5 cm garnets for Lu–Hf geochronology. Rather than the surrounding matrix (which could not be sampled in this study), Schmidt et al. (2015) anchored each interior garnet analysis with the Lu-depleted

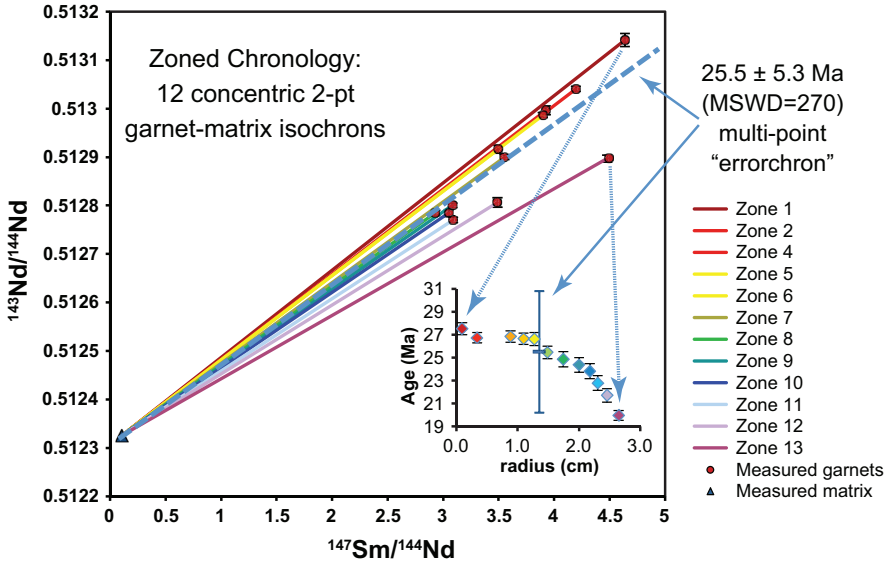

Figure 16. Zoned garnet geochronology for a single porphyroblast from Stillup Tal, Austria (modified from Pollington and Baxter 2010). Each garnet "zone" represents a concentric growth zone from core (zone 1) to rim (zone 13). When each is paired with the matrix, a pattern of systematically younging two-point isochron ages is seen from core to rim, spanning about 7.5 million years as shown (inset). Bold dashed line is the ill-advised multi-point 'errorchron' resulting from combining all garnet data and the matrix.

outermost rim in two-point 'garnet only' isochrons. The resulting age data suggest a total span of garnet growth of at least 12 million years. Cheng et al. (2016) presented Lu–Hf analysis of 12 micro-sawed garnet zones (not concentric) within two single crystals from the Huwan shear zone, China. Resulting two-point isochrons display ages ranging from 400 to 264 Ma which are interpreted to reflect mixing of at least two distinct episodes of garnet growth spanning that time.

Zoned garnet geochronology, despite its first applications almost 30 years ago, remains in its infancy, but its potential is great. Methodologies have now been developed to extract well-defined chemically contoured growth zones of garnet from single crystals of ~5 mm of greater diameter, clean those garnet portions of inclusions, analyze their isotopic composition even as sample size diminishes, and extract accurate and precise Sm–Nd, or Lu–Hf ages on each zone. Pollington and Baxter (2011) review the potential and current limitations for zoned garnet geochronology by Sm–Nd. As analytical approaches continue to improve for Sm–Nd and Lu–Hf smaller, more highly resolved records will become increasingly feasible. This is the exciting future that awaits garnet petrochronology.

Geospeedometry with garnet

Given the time and expense required to obtain high precision zoned garnet geochronology data, additional methods of inferring approximate metamorphic duration are desirable, particularly for understanding events on timescales too short to resolve isotopically. Although diffusion was discussed previously as an obstacle to thermobarometry, chemical profiles that retain stranded and incompletely flattened chemical (or more precisely, chemical potential) gradients provide an opportunity to infer maximum metamorphic duration. This obstacle/opportunity duality often referred to as 'geospeedometry' (c.f. Lasaga 1983) is discussed in detail by Kohn and Penniston-Dorland (2017, this volume) and reviewed briefly here because garnet has proven to be a particularly useful phase for geospeedometric study of tectono-metamorphism (e.g., Chakraborty and Ganguly 1991; Perchuk et al. 1999; Dachs and Proyer

2002; Fernando et al. 2003; Faryad and Chakraborty 2005; Storm and Spear 2005; Ague and Baxter 2007; Galli et al. 2011; Hallett and Spear 2011; Viete et al. 2011; Spear 2014).

Fick's first and second laws relate flux, J, and chemical concentration, C, of component i to distance, x, and time, t:

$$J_i = -D_i \frac{\partial C_i}{\partial x}$$

$$\frac{\partial C_i}{\partial t} = D_i \frac{\partial^2 C_i}{\partial x^2}$$

where D_i is the diffusivity. Numerous experimental and modeling studies have ascertained Arrhenius relationships between D and T for various major (e.g., Elphick et al. 1981; Loomis et al. 1985; Chakraborty and Ganguly 1991; Ganguly et al. 1998a; Carlson 2006; Ganguly 2010; Vielzeuf and Saúl 2011; Chu and Ague 2015) and trace elements (e.g., Tirone et al. 2005; Carlson 2012; Bloch et al. 2015) in garnet. The primary fitting parameters in most cases are a pre-exponential constant and an activation energy term, although many formulations consider activation volume and oxygen-fugacity terms, and some (e.g., Carlson 2006; Chu and Ague 2015) explicitly account for changes in diffusion coefficient across the range of possible garnet compositional space (e.g., stating that Fe would diffuse at a different rate through a grossular-dominated crystal than through an almandine-dominated crystal).

Geospeedometry (Lasaga 1983) typically uses Ficks' second law cast into an appropriate geometry (e.g., Crank 1975) to model how an imposed initial chemical zoning profile would relax with time, with the aim of finding the duration that best-fits an analyzed profile (e.g., in a microprobe traverse through a garnet crystal). For diffusion of trace elements, D is essentially independent of chemical composition (though see Bloch et al. 2015 who posit a concentration dependence on REE diffusivity) and diffuses only in response to its own chemical potential gradients, so that calculation is straightforward with analytical (e.g., Crank 1975) or numerical techniques. Major element diffusion through the garnet lattice is less straightforward, with mass and charge balance constraints requiring neutrality at each point throughout the crystal and mandating coupling of diffusion. In essence one can think of this as follows: Fe cannot freely flow left through a 1-D model of a garnet crystal unless one or several other components are flowing right to compensate and maintain charge and volume. The four main divalent cations in garnet are thus often considered simultaneously, by generation of a 3×3 element diffusion matrix that couples tracer diffusivities of each component with their relative compositions. The fourth element is generally considered a dependent component (Lasaga 1979):

$$D_{ij} = D_i^* \delta_{ij} - \left[\frac{D_i^* z_i z_j C_i}{\sum_{k=1}^{n} z_k^2 C_k D_k^*} \right] \left[D_j^* - D_n^* \right]$$

where D^* is a tracer diffusivity, z is the charge of the component of interest, n is the dependent component, and δ_{ij} is the Kronecker delta. For the example of Ca as the dependent component, Ficks' second law thus expands to:

$$\begin{bmatrix} \frac{\partial c_{\mathrm{Fe}}}{\partial t} \\ \frac{\partial c_{\mathrm{Mg}}}{\partial t} \\ \frac{\partial c_{\mathrm{Mn}}}{\partial t} \end{bmatrix} = \begin{bmatrix} \frac{\partial D_{\mathrm{FeFe}}}{\partial x} & \frac{\partial D_{\mathrm{FeMg}}}{\partial x} & \frac{\partial D_{\mathrm{FeMn}}}{\partial x} \\ \frac{\partial D_{\mathrm{MgFe}}}{\partial x} & \frac{\partial D_{\mathrm{MgMg}}}{\partial x} & \frac{\partial D_{\mathrm{MgMn}}}{\partial x} \\ \frac{\partial D_{\mathrm{MnFe}}}{\partial x} & \frac{\partial D_{\mathrm{MnMg}}}{\partial x} & \frac{\partial D_{\mathrm{MnMn}}}{\partial x} \end{bmatrix} \begin{bmatrix} \frac{\partial c_{\mathrm{Fe}}}{\partial x} \\ \frac{\partial c_{\mathrm{Mg}}}{\partial x} \\ \frac{\partial c_{\mathrm{Mn}}}{\partial x} \end{bmatrix} + \begin{bmatrix} D_{\mathrm{FeFe}} & D_{\mathrm{FeMg}} & D_{\mathrm{FeMn}} \\ D_{\mathrm{MgFe}} & D_{\mathrm{MgMg}} & D_{\mathrm{MgMn}} \\ D_{\mathrm{MnFe}} & D_{\mathrm{MnMg}} & D_{\mathrm{MnMn}} \end{bmatrix} \begin{bmatrix} \frac{\partial^2 c_{\mathrm{Fe}}}{\partial x^2} \\ \frac{\partial^2 c_{\mathrm{Mg}}}{\partial x^2} \\ \frac{\partial^2 c_{\mathrm{Mn}}}{\partial x^2} \end{bmatrix}$$

which can be solved simply with a finite difference approach, as described in more detail in Spear's MSA monograph (1993) and in Ganguly's EMU Notes in Mineralogy (2002) and Reviews in Mineralogy and Geochemistry (2010) chapters.

Although the numerical solution is straightforward, constraining the initial, pre-diffusion profile is often difficult. Typically, initial profiles are either drawn subjectively, based upon the remnant preserved zoning and a petrologically and geometrically reasonable estimate of what the 'undiffused' profile must have looked like (e.g., Dachs and Proyer 2002; Ague and Baxter 2007), or are assumed to be insignificantly zoned at peak temperature and develop zoning on rims due to changing equilibrium conditions during exhumation and cooling (e.g., O'Brien and Vrána 1995; Ganguly et al. 2000; Storm and Spear 2005). Kohn and Penniston-Dorland (2017, this volume) review such retrograde resetting in detail. A final constraint on initial profile comes from incorporation of information from equilibrium thermodynamic calculations to generate model profiles that would form during growth along a given *P–T* path (e.g., Florence and Spear 1991, 1993; Gaidies et al. 2008b; Caddick et al. 2010; Galli et al. 2011).

In all cases, the timescales retrieved by diffusion speedometry are only as good as (i) the initial profile modeled, (ii) the diffusivity data applied, (iii) the appropriate boundary conditions being set on the model, (iv) knowledge of the *P–T* and f_{O_2} conditions that the sample experienced. Garnet-based speedometry is probably most useful for defining maximum timescales of metamorphic heating that are consistent with retention of observed chemical zoning, thus yielding minimum permissible rates. Most diffusion occurs at or near to T_{max} and a characteristic *T* of diffusion can be quantified for a complex *P–T* history accordingly (e.g., Chakraborty and Ganguly 1991). This means that speedometry is generally most sensitive to the duration spent near peak temperature, with more subtle information required to infer lower temperature metamorphic rates. Methodologies are also generally incapable of distinguishing single long 'events' from multiple, briefer pulses, typically only revealing the total integrated $D(T)\cdot t$ (e.g., Ague and Baxter 2007; Kohn and Penniston-Dorland 2017, this volume). Thus without additional textural or compositional (thermodynamic) constraints there can be significant non-uniqueness in results, with strong, negative correlation between apparent peak temperature and apparent metamorphic duration. An example of this (from Galli et al. 2011) is described in the following section, which draws together aspects of both the 'petro' and 'chrono' of garnet into true petrochronology.

EXAMPLES OF PETRO-CHRONOLOGY OF GARNET

Figure 2 of this chapter provided a list of techniques to extract the 'petro-' of garnet and a list of techniques to extract the 'chrono' of garnet. The first two sections of the chapter have detailed those methodologies. Now, the stage is set for their integration into true garnet petrochronology. Below, we have chosen five examples from the literature of the past decade that show the great potential of garnet petrochronology. Other good examples exist (most of them have already been cited elsewhere in this chapter) and many more are in progress. Our hope is that, through these examples and our template in Figure 2, the reader will appreciate how to conceive of a garnet petrologic application, appreciate the unique and complementary value of the information extracted therefrom, and independently decide that it is worthy of the time and effort required.

Petrochronology of garnet: High pressure crustal metamorphism

Cheng et al. (2013; 2016) and Cheng and Cao (2015) present an impressive garnet petrochronologic dataset from eclogite samples of the Huwan shear zone in the northwestern boundary of the Hong-an orogen (Western Dabie). This suite of papers represents an excellent example of the power of garnet petrochronology via: 1) combined Lu–Hf and Sm–Nd geochronology, 2) zoned garnet geochronology, 3) *P–T* constraints on garnet growth

via thermodynamic modeling, and 4) comparison to zircon ages from the same sample suites. Cheng et al. (2013) presented combined Lu–Hf and Sm–Nd geochronology from the same handpicked eclogite garnet aliquots. Multi-point isochrons (Fig. 17) show remarkable consistency yielding 260.4 ± 2.0 Ma (n = 10; MSWD = 1.4) for Sm–Nd and 260.0 ± 1.0 (n = 9; MSWD = 1.0) for Lu–Hf. The tight agreement of each isochron data point, and between Sm–Nd and Lu–Hf ages are indicative of successful geochronology. The agreement between Lu–Hf and Sm–Nd ages itself is noteworthy, contradicting the oft-cited generalization that Lu–Hf ages are older than Sm–Nd ages. Here, according to the authors, handpicking efforts appear to have preferentially removed the Lu-rich garnet cores (that would normally skew a bulk crystal Lu–Hf age toward the early stages of garnet growth); thus both Lu–Hf and Sm–Nd ages date the same rim portion of the garnet. Eclogite facies mineral inclusions and *P–T* estimates from garnet rim chemistry pin the 260 Ma age to peak eclogite facies conditions. However the story, and the innovative garnet petrochronology, does not end there. The 260 Ma age of eclogite facies metamorphism is not reflected in zircon age data from the same area, which instead cluster mostly around 310 Ma. Thus, the garnet records an entire eclogite facies event that is apparently missed by the zircons. Subsequent papers by Cheng and Cao (2015) and Cheng et al. (2016) presented zoned garnet chronology on other eclogites from the field area to test whether garnet cores might in fact record an age more consistent with the zircon data. In the 2015 paper, garnet cores yielded Lu–Hf ages of 296.7 ± 3.8 Ma and rims gave both Lu–Hf and Sm–Nd ages of ~255 Ma. The Lu–Hf core age likely represents a mix between ~310 Ma eclogitic garnet and ~255 Ma eclogitic garnet, reflecting 40 million years of prolonged subduction zone metamorphic conditions between 1.9 and 2.4 GPa at 500 °C to 575 °C, as constrained by intersecting core and rim isopleths in pseudosections. Finally, the 2016 paper revealed an even broader scatter of Lu–Hf data from multiple microsawed zones in a large garnet megacryst spanning 400 to 250 Ma; these ages matched age spectra of newly acquired zircon data. The data presented in this series of papers shows a range of ages because each garnet bearing sample, and each zone of individual garnet crystals, reflects and records a different stage in the complex evolution of this terrane. Only through direct garnet petrochronology were these authors able to recognize at least two distinct (ca. 400 Ma and ~310–255 Ma), and prolonged, episodes of subduction zone metamorphism, thus motivating further study on convergent margin geodynamics.

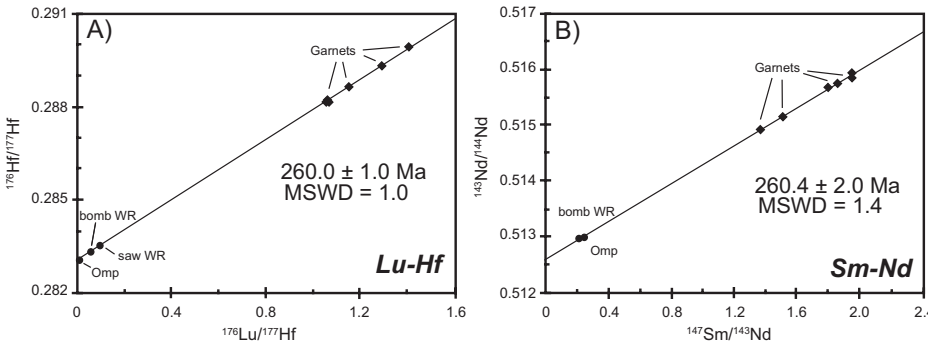

Figure 17. Lu–Hf and Sm–Nd multi-point garnet isochrons from the same garnet-bearing eclogite (modified from Cheng et al 2013). Note the perfect agreement of the two ages. When Lu–Hf and Sm–Nd are used to date the exact same age generation of garnet (in this case the rim) the two chronometers agree. Later work by Cheng et al (2016) found that garnet cores from other eclogites in this field area indeed contain an older generation of garnet. All garnet growth generations were linked to *P–T* conditions via thermodynamic modeling of garnet chemical isopleths, revealing multiple subduction episodes. "Bomb-WR" indicates sample in which the whole rock was fully dissolved in a Parr bomb.

Petrochronology of garnet: Geospeedometry and the timescales of granulite facies metamorphism

A primary motivation for deciphering metamorphic *P–T* paths is that knowledge of *P–T* evolution can help to reveal processes that control the evolution of plate margins and influence heating and cooling of Earth's crust. Garnet petrochronology helped to address this in the case of granulite facies rocks from the Gruf Complex, eastern Central Alps. Assemblages in these rocks have long been thought to record substantially higher temperatures than in many surrounding lithologies (e.g., Droop and Bucher-Nurminen 1984) and they do not correlate easily with simple tectonic models of Alpine evolution. In a study of Gruf granulites and charnockites, Galli et al. (2011) constrained reaction sequences through careful textural analysis before estimating *P–T* conditions by (i) combining experimental constraints to determine the position of key reactions, (ii) mineral thermobarometry, (iii) construction of appropriate pseudosections for peak metamorphic conditions, and (iv) multiphase mineral thermobarometry to constrain the equilibration *P–T* of late-stage coronae and symplectites. Results suggest peak temperatures in excess of 900 ºC at ~9 kbar, with subsequent symplectite formation at closer to 720–740 ºC and ~7 kbar (Fig. 18a). Intriguingly, garnet crystals retain remnant 'prograde' chemical zoning (dashed curves in Fig. 18d), raising the question of how such high temperatures were achieved, how briefly they must have been maintained for, and what tectonic mechanisms were responsible. Zircons from Gruf charnockites contain Permian (~290–260 Ma) cores overgrown with Tertiary (~34–29 Ma) rims, with orthopyroxene inclusions implying that core ages record or post-date granulite facies metamorphism (Galli et al. 2012). Galli et al. (2011) thus described a two stage model, with ~900 ºC Permian metamorphism overprinted by symplectite formation during Alpine orogenesis (Fig. 18b-c). A coupled garnet growth and diffusion model was constructed for an assumed *P–T* path that experiences both events, using an appropriate bulk-rock composition and thermodynamic constraints to establish growth zoning during prograde metamorphism. Results were inconsistent with observed garnet zoning unless the initial event was rapid, experiencing ultra-high temperature conditions for less than ~1 Myrs (Fig. 18d). Typical Alpine metamorphic timescales of several tens of millions of years result in complete loss of prograde zoning if peak *T* is ~900 ºC, though a rapid early 900 ºC event overprinted by tens of millions of years of Alpine metamorphism reaching more typical peak temperatures for the region (~ 720 ºC) yielded relatively good fits to measured garnet compositions. In this petrochronology study, Galli et al. (2011) thus concluded that granulite facies temperatures were only sustained for a very brief period and were probably unrelated to Alpine collisional tectonics. Rocks then resided in the mid crust for ~250 Myrs, before experiencing exhumation and a second phase of metamorphism at conditions and rates compatible with interpretations from elsewhere in the region, possibly due to mechanical interaction with melts that now form an adjacent pluton (Galli et al. 2013).

Petrochronology of garnet: Timescales of lower crustal melting

Stowell et al. (2010, 2014) provide excellent examples of the use of petrochronology in understanding the timescales and conditions of high-temperature metamorphism, partial melting, and the generation of high Sr/Y magmas in the lower arc crust of Fiordland, NZ. Stowell et al. (2010) combined Sm–Nd garnet geochronology on drilled cores and rims, trace element zoning in garnet, phase equilibria modeling and U–Pb zircon geochronology to provide an integrated history of a short duration, high-pressure melting event recorded by the Pembroke Granulite. Garnet core and rim ages were indistinguishable within each sample (e.g., core age of 123.5 ± 2.1 Ma; rim age of 122.5 ± 2.1 Ma for a dioritic gneiss), attesting to the short duration of garnet growth. The duration of garnet growth and subsequent partial melting event

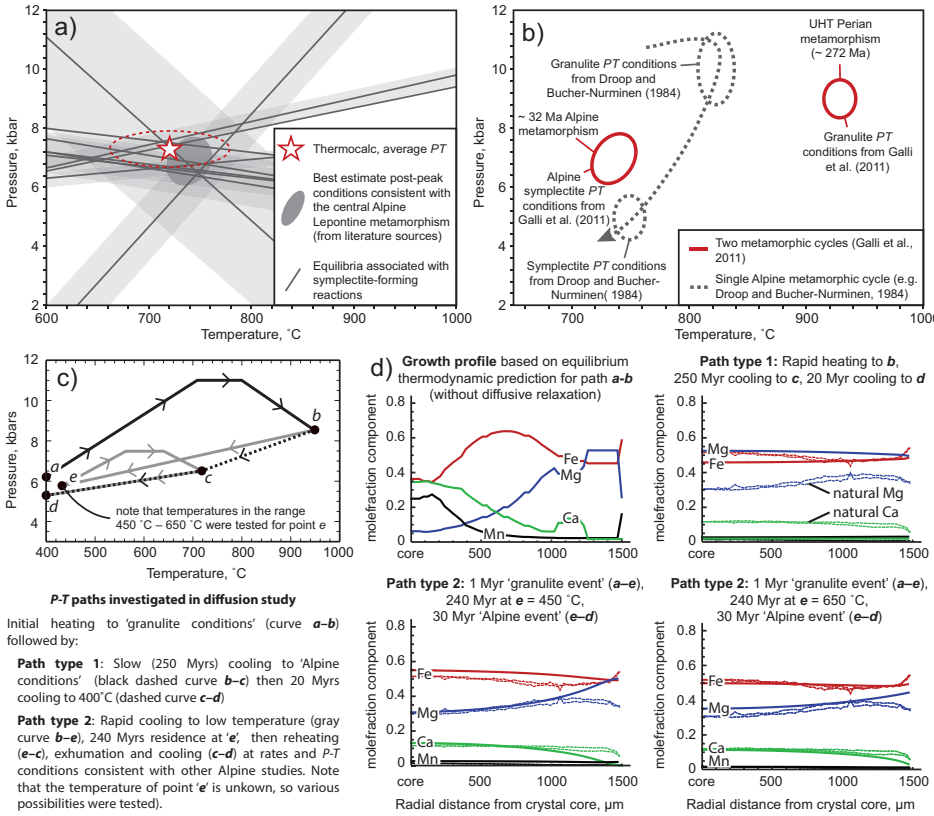

Figure 18. Evolution of the Gruf complex modified from Galli et al (2011). A. Calculated locations of observed reactions in coronae and symplectites. B. *P–T* estimate for corona formation in the context of the peak *P–T* experienced, with age constraints where available. C. *P–T* path types for which model results are shown in subsequent panels. E. Garnet growth and diffusion model results showing: core-to-rim zoning in the absence of intra-crystalline diffusion in garnet; 'type 1' path experiencing slow cooling from peak temperature; 'type 2' path experiencing rapid UHT conditions followed by a long duration at 450 ˚C, then a 30 Ma 'Alpine metamorphic event'; 'type 2 path' but with intermediate residence at 650 ˚C. In each case, the solid curves are model results and the dashed curves show natural crystal zoning. See Galli et al (2011) for more details.

is constrained by comparing bulk garnet and zircon ages from a gabbroic gneiss showing no evidence of melting (garnet age of 126.1 ± 2.0 Ma) to bulk garnet and zircon ages from a dioritic gneiss that shows melting evidence (a garnet reaction zone and leucosome; peritectic garnet age of 122.6 ± 2.0 Ma). Well-preserved HREE zoning in the dioritic gneiss was attributed to the continued consumption of accessory phases during garnet growth. Phase equilibria modeling of the gabbroic gneiss indicates peak metamorphic conditions at 1.1–1.4 GPa and 680–815 ºC, with garnet growth occurring during a > 0.5 GPa increase. Intrusion of the Western Fiordland Orthogneiss (125–115 Ma) is synchronous with the granulite-facies event, indicating that voluminous arc magmatism may have triggered garnet growth and partial melting.

The combined geochronologic and thermodynamic approach allowed for the interpretation that thickening of arc crust resulted in high-pressure metamorphism and that granulite-facies garnet growth lasted 3–7 Ma, with subsequent partial melting occurring shortly thereafter, perhaps as little as 3 Ma later.

Stowell et al. (2014) dated an additional nine granulite-facies rocks from around the Malaspina pluton using Sm–Nd garnet geochronology, and obtained ages ranging from 115.6 ± 2.6 Ma to 110.6 ± 2.0 Ma, roughly 10 Ma later than that from the Pembroke Granulite (at conditions of ~920 °C and 1.4–1.5 GPa), suggesting that high-pressure metamorphism and partial melting was diachronous over a > 3000 km^2 area of the mid- to lower crust. Stowell et al. (2014) suggest this may result from pulsed underplating of magma in the lower crust or 'drip-style' delamination of the lowermost crust. High-precision garnet geochronology allowed resolution of the diachronous nature of high-pressure metamorphism and partial melting, and when combined with constraints on the *P–T* conditions (and *P–T* path) during garnet growth, allows for interpretation of the regional tectonic framework upon loading, partial melting, and extensional collapse of the Fiordland arc crust.

Petrochronology of garnet: Subduction zone dehydration

Garnet growth typically results from the breakdown of hydrous phases during subduction zone metamorphism, and can thus be a powerful proxy for subduction zone devolatilization (Baxter and Caddick 2013). Dragovic et al. (2012, 2015) utilized zoned Sm–Nd garnet geochronology coupled with phase equilibria modeling in order to constrain the duration and rate of devolatilization during subduction of mafic and felsic lithologies, respectively, from the Cycladic Blueschist Unit of Sifnos, Greece. These papers combined some of the techniques described in previous sections (i.e., zoned geochronology and pseudosections), but also highlighted and resolved some of the challenges associated with Sm–Nd isotopic analyses of very small sample sizes. Dragovic et al. (2012) microdrilled three chemically distinct, concentric zones from each of two separate garnet crystals and dated them using Sm–Nd. All six garnet fractions could be placed onto a single isochron (see Fig. 11), indicating to a first order that garnet growth was very brief. When separated into three isochrons, the duration of garnet growth was calculated to be *0.04 Ma*, with a 2σ *maximum* duration of *~1 Ma*. Dragovic et al. (2015) took this *much* further, microdrilling and dating ten growth zones from each of two garnet crystal which revealed three distinct pulses of crystal growth, with the final pulse growing a majority of the garnet and occurring in < 0.8 Ma (Fig. 19a).

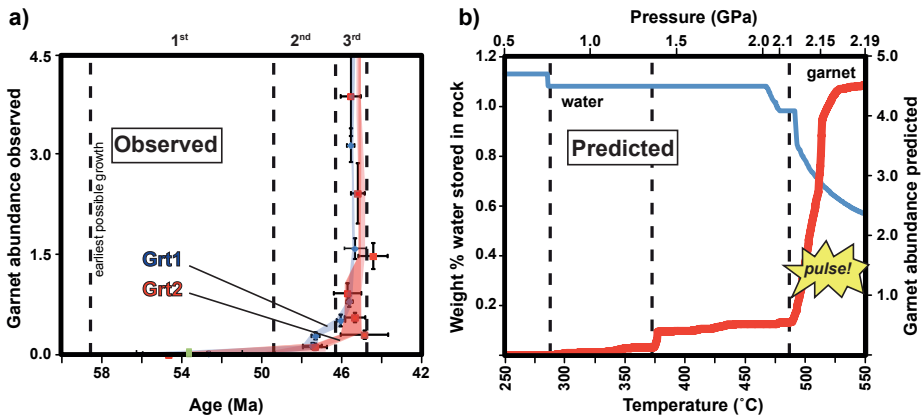

Figure 19. Devolatilization and garnet growth history recorded in zoned garnet porphyroblasts from Sifnos, Greece (modified from Dragovic et al. 2015). A. Volume abundance of garnet over time showing pulses of garnet growth in two garnet crystals from nineteen microdrilled growth zones. The final pulse lasted < 0.8 Ma. B. Associated fluid release as modeled using a path dependent thermodynamic forward model. The aforementioned final pulse released > 0.5 wt.% fluid from the bulk rock.

In Dragovic et al. (2012), the *P–T* conditions for the interval of garnet growth were calculated with separate pseudosections for whole rock (for initiation of growth) and 'garnet depleted rock' (for the termination of growth) bulk compositions. Results imply initiation of crystal core growth at ~2.0 GPa and ~460 ºC and termination of rim growth ~2.2 GPa and ~560 ºC. In Dragovic et al. (2015), a path dependent thermodynamic forward model was employed in which phase equilibria were calculated at 0.5 ºC intervals along a prescribed *P–T* path, with stable garnet and fluid fractionated from the effective bulk composition at every interval. In both contributions, the change in bulk rock water content during the < 1 Ma garnet growth interval was calculated at ~ 0.3–0.5 wt%. The path dependent thermodynamic model was especially useful here, simultaneously 1) discerning the likely subduction *P–T* path, 2) modeling observed growth pulses of garnet, and 3) predicting the evolution of fluid release (Fig. 19b).

Both studies thus suggested a pulse of fluid release and heating (~100 ºC/Ma) spanning just hundreds of thousands of years. The high spatial resolution attainable by zoned garnet geochronology, the ability to measure smaller samples sizes (thinner growth zones), and the coupling with thermodynamic constraints gave the ability to distinguish whether garnet growth, and thus metamorphic devolatilization, was temporally continuous or focused into pulses of mineral growth and fluid production.

Petrochronology of garnet: Collisional tectonics and inverted metamorphic gradients

An improved understanding of the evolution of the well-known Himalayan inverted metamorphic gradient has been a goal of tectonic studies for several decades. The Lesser Himalayan sequence in Sikkim exposes an unusually complete section through the inverted Barrovian sequence, and a remarkable group of studies have repeatedly analyzed a suite of samples with various techniques to build a detailed picture of the evolution of these rocks. For example, sample 24/99 is an aluminous garnet schist from the Lesser Himalaya, first described by Dasgupta et al. (2009) and representing the low temperature base of the inverted metamorphic sequence. Dasgupta et al. (2009) subjected 24/99 to element mapping and quantitative microprobe analysis, using garnet–biotite thermometry and two methods of multiphase thermobarometry to infer that it reached peak conditions of ~ 525 ºC, 5 kbar. Pseudosection constraints suggested a somewhat higher peak temperature but confirmed texturally-derived interpretations that garnet grew at the expense of chlorite and chloritoid.

Garnets from all of the Barrovian zones were dated with Lu–Hf at very high precision in order to constrain the temporal evolution of the sequence. For example, garnet in sample 24/99 was dated using Lu–Hf at 10.6 ± 0.2 Ma, suggesting that it experienced the youngest garnet growth in the sampled transect (Anczkiewicz et al. 2014). In the same study, zoned Lu–Hf geochronology on a kyanite grade sample implied garnet core growth at 13.7 ± 0.2 Ma and rim growth at 9.9 ± 3.8 Ma (Anczkiewicz et al. 2014). Taken together, data constrain the duration of prograde metamorphism (using first garnet growth as a marker) across the Lesser Himalayan sequence, showing that ages decrease towards structurally lower levels (and lower metamorphic grade) and suggesting that the garnet isograd swept through the entire sequence from garnet-grade to sillimanite-grade in ~6 Myrs.

The size, shape and distribution of every garnet crystal in a several cubic centimeter block of sample 24/99 was then mapped in 3-D (Gaidies et al. 2015). Analysis of results suggested clustering and no spatial ordering of garnet, providing little evidence for diffusion-controlled crystallization and suggesting that garnet nucleation and growth could have been controlled by crystal interface processes (Gaidies et al. 2015). Thin sections were cut through the geometric cores of the largest garnet crystals and were carefully characterized to define inclusion mineralogy and fabrics, and to quantify major element zoning profiles. Thermodynamic models helped to refine *P–T* paths, and garnet diffusion speedometry gave constraints on both the heating and cooling rates, though the extent of diffusion was limited in 24/99 because it did not reach a particularly high maximum temperature.

This entire remarkable dataset is shown to be consistent with models of a coherent Lesser Himalayan block being buried during collision (Anczkiewicz et al. 2014; Chakraborty et al. 2016). All rocks reached their respective peak metamorphic conditions simultaneously but with those samples that eventually reach highest grade passing through garnet-in reactions first and thus recording earliest garnet growth (Anczkiewicz et al. 2014). This truly represents an integrated garnet petrochronology application.

OUTLOOK

Both the 'petro' and the 'chrono' of garnet have evolved significantly over the past several decades, and that evolution will continue as analytical methodologies improve and as the creativity of the scientific applications grows. We have touched on many aspects of that evolution here, showcasing a few examples of the current state of the art garnet petrochronology. Once, we were barely able to see the 'tree rings' of garnet growth. If the concentric growth rings in a garnet crystal can be likened to the pages of a history book (as suggested in Baxter and Scherer 2013), while we first only got to read the title, and then progressed to reading the title of each chapter, we are now able to read the record with the resolution of several pages. New petrologic techniques (thermodynamic, isotopic, textural, mechanical) are like learning new vocabulary that allows us to extract greater meaning and context from every chapter and page of that garnet chronology. What will the future hold? How soon and with what new analytical breakthroughs will we be able to read every single word of that garnet tree ring history book? Garnet petrochronology is not a panacea; its limitations and challenges must also be understood to fully harness its potential and it is quite possible that we will never be fully satisfied with the resolution of the story preserved in metamorphic rocks, or our ability to read that story. But as Lu–Hf and Sm–Nd geochronology become increasingly precise and accessible, and our understanding of the processes that embed chemical and isotopic signatures in crystals improve, garnet will surely become an ever more important member of the cadre of modern petrochronometers discussed in this RiMG volume. So although we have dwelled mostly here on previous examples and current methods, above all we encourage the reader to consider the *potential* of garnet petrochronology in deciphering the evolution of crustal processes.

ACKNOWLEDGMENTS

EFB gratefully acknowledges NSF award 1250497/1561882. MJC gratefully acknowledges NSF awards EAR–1250470 and EAR–1447568 (to MJC and BD). We thank E.E. Scherer for providing data in Figure 10 as well as numerous discussions on garnet geochronology. We thank Robert Anczkiewicz, David Pattison, and Pierre Lanari for valuable reviews, Matthew Kohn for his feedback, and Martin Engi for his patient, detailed and constructive editorial handling. We thank R.J. Tracy for providing the materials for Figure 3, for patiently emphasizing the importance of 'chemo-petrography', and for guiding our collection and interpretation of countless 'chemo-petrographic' images. We thank John Rosenfeld for providing his 'favorite rotated garnet photo' from an original print for Figure 1c.

REFERENCES

Abart R (1995) Phase-equilibrium and stable-isotope constraints on the formation of metasomatic garnet–vesuvianite veins (SW Adamello, N Italy). Contrib Mineral Petrol 122:116–133

Aerden D, Bell TH, Puga E, Sayab M, Lozano JA, de Federico AD (2013) Multi-stage mountain building vs. relative plate motions in the Betic Cordillera deduced from integrated microstructural and petrological analysis of porphyroblast inclusion trails. Tectonophysics 587:188–206

Ague JJ (2011) Extreme channelization of fluid and the problem of element mobility during Barrovian metamorphism. Am Mineral 96:333–352

Ague JJ, Axler JA (2016) Interface coupled dissolution–reprecipitation in garnet from subducted granulites and ultrahigh-pressure rocks revealed by phosphorous, sodium, and titanium zonation. Am Mineral 101:1696–1699

Ague JJ, Baxter EF (2007) Brief thermal pulses during mountain building recorded by Sr diffusion in apatite and multicomponent diffusion in garnet. Earth Planet Sci Lett 261:500–516

Albee AL (1965) Phase equilibria in three assemblages of kyanite-zone pelitic schists, Lincoln Mountain Quadrangle, central Vermont. J Petrol 6:246–301

Albee AL (1972) Metamorphism of pelitic schists: reaction relations of chloritoid and staurolite. Geol Soc Am Bull 83:3249–3268

Amato JM, Johnson CM, Baumgartner LP, Beard BL (1999) Rapid exhumation of the Zermatt–Saas ophiolite deduced from high-precision Sm–Nd and Rb–Sr geochronology. Earth Planet Sci Lett 171:425–438

Anczkiewicz R, Thirlwall MF (2003) Improving precision of Sm–Nd garnet dating by H_2SO_4 leaching: a simple solution to the phosphate inclusion problem. Geol Soc London Spec Pub 220:83–91

Anczkiewicz R, Platt JP, Thirlwall MF, Wakabayashi J (2004) Franciscan subduction off to a slow start: evidence from high-precision Lu–Hf garnet ages on high grade-blocks. Earth Planet Sci Lett 225:147–161

Anczkiewicz R, Szczepanski J, Mazur S, Storey C, Crowley Q, Villa IM, Thirlwall ME, Jeffries TE (2007) Lu–Hf geochronology and trace element distribution in garnet: Implications for uplift and exhumation of ultra-high pressure granulites in the Sudetes, SW Poland. Lithos 95:363–380

Anczkiewicz R, Thirlwall M, Alard O, Rogers NW, Clark C (2012) Diffusional homogenization of light REE in garnet from the Day Nui Con Voi Massif in N-Vietnam: Implications for Sm–Nd geochronology and timing of metamorphism in the Red River shear zone. Chem Geol 318:16–30

Anczkiewicz R, Chakraborty S, Dasgupta S, Mukhopadhyay D, Kołtonik K (2014) Timing, duration and inversion of prograde Barrovian metamorphism constrained by high resolution Lu–Hf garnet dating: A case study from the Sikkim Himalaya, NE India. Earth Planet Sci Lett 407:70–81

Anderson DE, Olimpio JC (1977) Progressive homogenization of metamorphic garnets, south Molnar, Scotland: Evidence for volume diffusion. Can Mineral 15:205–216

Angel RJ, Mazzucchelli ML, Alvaro M, Nimis P, Nestola F (2014) Geobarometry from host–inclusion systems: The role of elastic relaxation. Am Mineral 99:2146–2149

Angiboust S, Agard P, Raimbourg H, Yamato P, Huet B (2011) Subduction interface processes recorded by eclogite-facies shear zones (Monviso, W. Alps). Lithos 127:222–238

Angiboust S, Pettke T, De Hoog JCM, Caron B, Oncken O (2014) Channelized fluid flow and eclogite-facies metasomatism along the subduction shear zone. J Petrol 55:883–916

Argles TW, Prince CI, Foster GL, Vance D (1999) New garnets for old? Cautionary tales from young mountain belts. Earth Planet Sci Lett 172:301–309

Ashley KT, Caddick MJ, Steele-MacInnis M, Bodnar RJ, Dragovic B (2014a) Geothermobarometric history of subduction recorded by quartz inclusions in garnet. Geochem Geophys Geosystem 15:350–360

Ashley KT, Steele-MacInnis M, Caddick MJ (2014b) QuIB Calc: A MATLAB® script for geobarometry based on elastic modeling of quartz inclusions in garnet. Comp and Geosci 60:155–157

Ashley KT, Darling RS, Bodnar RJ, Law RD (2015) Significance of "stretched" mineral inclusions for reconstructing *P–T* exhumation history. Contrib Mineral Petrol 169:1–9

Atherton MP (1968) The variation of garnet, biotite and chlorite composition in medium grade pelitic rocks from the Dalradian, Scotland, with particular reference to the zonation in garnet. Contrib Mineral Petrol 18:347–371

Atherton MP, Edmunds WM (1965) An electron microprobe study of some zoned garnets from metamorphic rocks. Earth Planet Sci Lett 1:185–193

Baldwin JA, Powell R, White RW, Štípská P (2015) Using calculated chemical potential relationships to account for replacement of kyanite by symplectite in high pressure granulites. J Metamorph Geol 33:311–330

Barrow G (1893) On an intrusion of muscovite–biotite gneiss in the east Highlands of Scotland, and its accompanying metamorphism. Quart J Geol Soc London 49:330–358

Barrow G (1912) On the geology of lower Deeside and the southern Highland border. Proc Geol Assoc 23:268–284

Bast R, Scherer EE, Sprung P, Fischer-Godde M, Stracke A, Mezger K (2015) A rapid and efficient ion-exchange chromatography for Lu–Hf, Sm–Nd, and Rb–Sr geochronology and the routine isotope analysis of sub-ng amounts of Hf by MC-ICP-MS. J Anal At Spectrom 30:2323–2333

Baumgartner LP, Valley JW (2001) Stable isotope transport and contact metamorphic fluid flow. Rev Mineral Geochem 43:415–467

Baumgartner LP, Floess D, Podladchikov Y, Foster CT (2010) Pressure gradients in garnets induced by diffusion relaxation of major element zoning. Geol Soc Denver Ann Meeting

Baxter EF, DePaolo D (2002a) Field measurement of high temperature bulk reaction rates II: Interpretation of results from a field site near Simplon Pass, Switzerland. Am J Sci 302:465–516

Baxter EF, DePaolo DJ (2002b) Field measurement of high temperature bulk reaction rates I: Theory and technique. Am J Sci 302:442–464
Baxter EF, Caddick MJ (2013) Garnet growth as a proxy for progressive subduction zone dehydration. Geology 41:643–646
Baxter EF, Scherer EE (2013) Garnet Geochronology: Timekeeper of Tectonometamorphic Processes. Elements 9:433–438
Baxter EF, Ague JJ, Depaolo DJ (2002) Prograde temperature–time evolution in the Barrovian type-locality constrained by Sm/Nd garnet ages from Glen Clova, Scotland. J Geol Soc London 159:71–82
Baxter EF, Caddick MJ, Ague JJ (2013) Garnet: common mineral, uncommonly useful. Elements 9:415–419
Bebout GE, Tsujimori T, Ota T, Shimaki Y, Kunihiro T, Carlson WD, Nakamura E (2015) Lithium in UHP metasedimentary garnets from Lago Di Cignana, Italy: Coupled substitutions and the role of accessory phases. Geol Soc Am Ann Meeting
Bell TH (1985) Deformation partitioning and porphyroblast rotation in metamorphic rocks: a radical reinterpretation. J Metamorph Geol 3:109–118
Berman RG (1990) Mixing properties of Ca–Mg–Fe–Mn garnets. Am Mineral 75:328–344
Berman RG, Aranovich LY (1996) Optimized standard state and solution properties of minerals. I. Model calibration for olivine, orthopyroxene, cordierite, garnet, and ilmenite in the system FeO–MgO–CaO–Al_2O_3–TiO_2–SiO_2. Contrib Mineral Petrol 126:1–24
Bickle MJ, Baker J (1990) Advective diffusive transport of isotopic fronts—an example from Naxos, Greece. Earth Planet Sci Lett 97:78–93
Bloch E, Ganguly J (2015) ^{176}Lu–^{176}Hf geochronology of garnet II: numerical simulations of the development of garnet–whole-rock ^{176}Lu–^{176}Hf isochrons and a new method for constraining the thermal history of metamorphic rocks. Contrib Mineral Petrol 169:1–16
Bloch E, Ganguly J, Hervig R, Cheng W (2015) ^{176}Lu–^{176}Hf geochronology of garnet I: experimental determination of the diffusion kinetics of Lu^{3+} and Hf^{4+} in garnet, closure temperatures and geochronological implications. Contrib Mineral Petrol 169:1–18
Bohlen SR, Essene EJ (1980) Evaluation of coexisting garnet–biotite, garnet–clinopyroxene and other Mg–Fe exchange thermometers in Adirondack granulites. Geol Soc Am Bull 91:685–719
Bohlen SR, Liotta JJ (1986) A barometer for garnet amphibolites and garnet granulites. J Petrol 27:1025–1034
Bohlen SR, Wall VJ, Boettcher AL (1983) Experimental investigations and gelogical applications of equilibria in the system FeO–TiO_2–Al_2O_3–SiO_2–H_2O. Am Mineral 68:1049–1058
Brady JB, Cherniak DJ (2010) Diffusion in minerals: an overview of published experimental diffusion data. Rev Mineral Geochem 72:899–920
Burton KW, Onions RK (1991) High-resolution garnet chronometry and the rates of metamorphic processes. Earth Planet Sci Lett 107:649–671
Burton KW, Kohn MJ, Cohen AS, Onions RK (1995) The relative diffusion of Pb, Nd, Sr and O in garnet. Earth Planet Sci Lett 133:199–211
Caddick MJ, Thompson AB (2008) Quantifying the tectono-metamorphic evolution of pelitic rocks from a wide range of tectonic settings: Mineral compositions in equilibrium. Contrib Mineral Petrol 156:177–195
Caddick MJ, Bickle MJ, Harris NBW, Holland TJB, Horstwood MSA, Ahmad T (2007) Burial and exhumation history of a Lesser Himalayan schist: Recording the formation of an inverted metamorphic sequence in NW India. Earth Planet Sci Lett 264:375–390
Caddick MJ, Konopásek J, Thompson AB (2010) Preservation of garnet growth zoning and the duration of prograde metamorphism. J Petrol 51:2327–2347
Cahalan RC, Kelly ED, Carlson WD (2014) Rates of Li diffusion in garnet: Coupled transport of Li and Y + REEs. Am Mineral 99:1676–1682
Carlson WD (1989) The significance of intergranular diffusion to the mechanisms and kinetics of porphyroblast crystallization. Contrib Mineral Petrol 103:1–24
Carlson WD (1999) The case against Ostwald ripening of porphyroblasts. Can Mineral 37:403–414
Carlson WD (2002) Scales of disequilibrium and rates of equilibration during metamorphism. Am Mineral 87:185–204
Carlson WD (2006) Rates of Fe, Mg, Mn and Ca diffusion in garnet. Am Mineral 91:1–11
Carlson WD (2011) Porphyroblast crystallization: linking processes, kinetics, and microstructures. Int Geol Rev 53:406–445
Carlson WD (2012) Rates and mechanism of Y REE, and Cr diffusion in garnet. Am Mineral 97:1598–1618
Carlson WD, Denison C, Ketcham RA (1995) Controls on the nucleation and growth of porphyroblasts: Kinetics from natural textures and numerical models. Geol J 30:207–225
Carlson WD, Gale JD, Wright K (2014) Incorporation of Y and REEs in aluminosilicate garnet: Energetics from atomistic simulation. Am Mineral 99:1022–1034
Carlson WD, Hixon JD, Garber JM, Bodnar RJ (2015a) Controls on metamorphic equilibration: the importance of intergranular solubilities mediated by fluid composition. J Metamorph Geol 33:123–146

Carlson WD, Pattison DR, Caddick MJ (2015b) Beyond the equilibrium paradigm: How consideration of kinetics enhances metamorphic interpretation. Am Mineral 100:1659–1667
Cashman KV, Ferry JM (1988) Crystal size distribution (CSD) in rocks and the kinetics and dynamics of crystallization. 3. Metamorphic crystallization. Contrib Mineral Petrol 99:401–415
Castro AE, Spear FS (2016) Reaction overstepping and re-evaluation of peak *P–T* conditions of the blueschist unit Sifnos, Greece: implications for the Cyclades subduction zone. Int Geol Rev:1–15
Chacko T, Cole DR, Horita J (2001) Equilibrium oxygen, hydrogen and carbon isotope fractionation factors applicable to geologic systems. Rev Mineral Geochem 43:1–81
Chakraborty S, Ganguly J (1991) Compositional zoning and cation diffusion in garnets. *In:* Diffusion, Atomic Ordering, and Mass Transport. Ganguly J (ed) Springer-Verlag, New York, p 120–175
Chakraborty S, Anczkiewicz R, Gaidies F, Rubatto D, Sorcar N, Faak K, Mukhopadhyay D, Dasgupta S (2016) A review of thermal history and timescales of tectonometamorphic processes in Sikkim Himalaya (NE India) and implications for rates of metamorphic processes. J Metamorph Geol 34:785–803
Chambers J, Caddick M, Argles T, Horstwood M, Sherlock S, Harris N, Parrish R, Ahmad T (2009) Empirical constraints on extrusion mechanisms from the upper margin of an exhumed high-grade orogenic core, Sutlej valley, NW India. Tectonophysics 477:77–92
Cheng H, Cao D (2015) Protracted garnet growth in high-Peclogite: constraints from multiple geochronology and *P–T* pseudosection. J Metamorph Geol 33:613–632
Cheng H, King RL, Nakamura E, Vervoort JD, Zhou Z (2008) Coupled Lu–Hf and Sm–Nd geochronology constrains garnet growth in ultra-high-pressure eclogites from the Dabie orogen. J Metamorph Geol 26:741–758
Cheng H, Zhang C, Vervoort JD, Zhou Z (2013) New Lu–Hf and Sm–Nd geochronology constrains the subduction of oceanic crust during the Carboniferous–Permian in the Dabie orogen. J Asian Earth Sci 63:139–150
Chen YX, Zheng YF, Li L, Chen RX (2014) Fluid–rock interaction and geochemical transport during protolith emplacement and continental collision: A tale from Qinglongshan ultrahigh-pressure metamorphic rocks in the Sulu orogen. Am J Sci 314:357–399
Cheng H, Liu XC, Vervoort JD, Wilford D, Cao DD (2016) Micro-sampling Lu–Hf geochronology reveals episodic garnet growth and multiple high-*P* metamorphic events. J Metamorph Geol 34:363–377
Chernoff CB, Carlson WD (1997) Disequilibrium for Ca during growth of pelitic garnet. J Metamorph Geol 15:421–438
Chernoff CB, Carlson WD (1999) Trace element zoning as a record of chemical disequilibrium during garnet growth. Geology 27:555–558
Chopin C (1984) Coesite and pure pyrope in high-grade blueschists of the Western Alps: a first record and some consequences. Contrib Mineral Petrol 86:107–118
Christensen JN, Rosenfeld JL, Depaolo DJ (1989) Rates of tectonometamorphic processes from rubidium and strontium isotopes in garnet. Science 244:1465–1469
Christensen JN, Selverstone J, Rosenfeld JL, DePaolo DJ (1994) Correlation by Rb–Sr geochronology of garnet growth histories from different structural levels within the Tauern Window, Eastern Alps. Contrib Mineral Petrol 118:1–12
Chu X, Ague JJ (2015) Analysis of experimental data on divalent cation diffusion kinetics in aluminosilicate garnets with application to timescales of peak Barrovian metamorphism, Scotland. Contrib Mineral Petrol 170
Clayton RN, Goldsmith JR, Mayeda TK (1989) Oxygen isotope fractionation in quartz, albite, anorthite and calcite. Geochim Cosmochim Acta 53:725–733
Clechenko CC, Valley JW (2003) Oscillatory zoning in garnet from the Willsboro Wollastonite Skarn, Adirondack Mts, New York: a record of shallow hydrothermal processes preserved in a granulite facies terrane. J Metamorph Geol 21:771–784
Coghlan RAN (1990) Studies in diffusional transport: grain boundary transport of oxygen in feldspars, diffusion of oxygen, REE's in garnet. Doctoral dissertation, Brown Univ.
Cohen AS, O'Nions RK, Siegenthaler R, Griffin WL (1988) Chronology of the pressure–temperature history recorded by a granulite terrain. Contrib Mineral Petrol 98:303–311
Connolly JAD (1990) Multivariable phase diagrams: an algorithm based on generalized thermodynamics. Am J Sci 290:666–718
Connolly JAD (2005) Computation of phase equilibria by linear programming: A tool for geodynamic modeling and its application to subduction zone decarbonation. Earth Planet Sci Lett 236:524–541
Connolly JAD (2009) The geodynamic equation of state: What and how. Geochem Geophys Geosystem 10
Corrie SL, Kohn MJ (2008) Trace-element distributions in silicates during prograde metamorphic reactions: implications for monazite formation. J Metamorph Geol 26:451–464
Crank J (1975) The Mathematics of Diffusion, 2nd Edition. Clarendon Press, Oxford
Crowe DE, Riciputi LR, Bezenek S, Ignatiev A (2001) Oxygen isotope and trace element zoning in hydrothermal garnets: Windows into large-scale fluid-flow behavior. Geology 29:479–482

Cruz-Uribe AM, Hoisch TD, Wells ML, Vervoort JD, Mazdab FK (2015) Linking thermodynamic modelling, Lu–Hf geochronology and trace elements in garnet: new *P–T–t* paths from the Sevier hinterland. J Metamorph Geol 33:763–781

Cutts K, Kinny P, Strachan R, Hand M, Kelsey D, Emery M, Friend C, Leslie A (2010) Three metamorphic events recorded in a single garnet: Integrated phase modelling, in situ LA-ICPMS and SIMS geochronology from the Moine Supergroup, NW Scotland. J Metamorph Geol 28:249–267

D'Errico ME, Lackey JS, Surpless BE, Loewy SL, Wooden JL, Barnes JD, Strickland A, Valley JW (2012) A detailed record of shallow hydrothermal fluid flow in the Sierra Nevada magmatic arc from low-^{18}O skarn garnets. Geology 40:763–766

Dachs E, Proyer A (2002) Constraints on the duration of high-pressure metamorphism in the Tauern Window from diffusion modelling of discontinuous growth zones in eclogite garnet. J Metamorph Geol 20:769–780

Daniel CG, Spear FS (1998) Three-dimensional patterns of garnet nucleation and growth. Geology 26:503–506

Dasgupta S, Chakraborty S, Neogi S (2009) Petrology of an inverted Barrovian sequence of metapelites in Sikkim Himalaya, India: Constraints on the tectonics of inversion. Am J Sci 309:43–84

de Capitani C, Brown TH (1987) The computation of chemical equilibrium in complex systems containing non-ideal solutions. Geochim Cosmochim Acta 51:2639–2652

de Capitani C, Petrakakis K (2010) The computation of equilibrium assemblage diagrams with Theriak/Domino software. Am Mineral 95:1006–1016

DePaolo DJ, Getty SR (1996) Models of isotopic exchange in reactive fluid–rock systems: Implications for geochronology in metamorphic rock. Geochim Cosmochim Acta 60:3933–3947

DeWolf CP, Zeissler CJ, Halliday AN, Mezger K, Essene EJ (1996) The role of inclusions in U–Pb and Sm–Nd garnet geochronology: Stepwise dissolution experiments and trace uranium mapping by fission track analysis. Geochim Cosmochim Acta 60:121–134

Diener J, Powell R (2012) Revised activity–composition models for clinopyroxene and amphibole. J Metamorph Geol 30:131–142

Dodson MH (1973) Closure temperature in cooling geochronological and petrological systems. Contrib Mineral Petrol 40:259–274

Dorfler KM, Tracy RJ, Caddick MJ (2014) Late-stage orogenic loading revealed by contact metamorphism in the northern Appalachians, New York. J Metamorph Geol 32:113–132

Dragovic B, Samanta LM, Baxter EF, Selverstone J (2012) Using garnet to constrain the duration and rate of water-releasing metamorphic reactions during subduction: An example from Sifnos, Greece. Chem Geol 314–317:9–22

Dragovic B, Baxter EF, Caddick MJ (2015) Pulsed dehydration and garnet growth during subduction revealed by zoned garnet geochronology and thermodynamic modeling, Sifnos, Greece. Earth Planet Sci Lett 413:111–122

Dragovic B, Guevara VE, Caddick MJ, Baxter EF, Kylander-Clark AR (2016) A pulse of cryptic granulite-facies metamorphism in the Archean Wyoming Craton revealed by Sm–Nd garnet and U–Pb monazite geochronology. Precambrian Res 283:24–49

Droop GTR, Bucher-Nurminen K (1984) Reaction textures and metamorphic evolution of sapphirine-bearing granulites from the Gruf Complex, Italian Central Alps. J Petrol 25:766–8031

Ducea MN, Ganguly J, Rosenberg EJ, Patchett PJ, Cheng WJ, Isachsen C (2003) Sm–Nd dating of spatially controlled domains of garnet single crystals: a new method of high-temperature thermochronology. Earth Planet Sci Lett 213:31–42

Duchene S, BlichertToft J, Luais B, Telouk P, Lardeaux JM, Albarede F (1997) The Lu–Hf dating of garnets and the ages of the Alpine high-pressure metamorphism. Nature 387:586–589

Eiler JM (2001) Oxygen isotope variations of basaltic lavas and upper mantle rocks. Rev Mineral Geochem 43:319–364

Elphick SC, Ganguly J, Loomis TP (1981) Experimental study of Fe–Mg interdiffusion in aluminosilicate garnet. Trans Am Geophys Union 62:411

Enami M, Nishiyama T, Mouri T (2007) Laser Raman microspectrometry of metamorphic quartz: A simple method for comparison of metamorphic pressures. Am Mineral 92:1303–1315

Engi M (2017) Petrochronology based on REE–minerals: monazite, allanite, xenotime, apatite. Rev Mineral Geochem 83:365–418

Engi M, Wersin P (1987) Derivation and application of a solution model for calcic garnet. Schweiz Mineral Petrograph Mitteil 67:53–73

Errico JC, Barnes JD, Strickland A, Valley JW (2013) Oxygen isotope zoning in garnets from Franciscan eclogite blocks: evidence for rock-buffered fluid interaction in the mantle wedge. Contrib Mineral Petrol 166:1161–1176

Essene EJ (1982) Geologic thermometry and barometry. Rev Mineral Geochem 10:153–206

Essene EJ (1989) The current status of thermobarometry in metamorphic rocks. *In:* Evolution of Metamorphic Belts. Daly JS, Cliff, RA and Yardley BWD (eds) Geological Society of London, p 1–44

Evans BW (1966) Microprobe study of zoning in eclogite garnet. Geol Soc Am Spec Pap 87:54

Evans BW, Guidotti CV (1966) The sillimanite–potash feldspar isograd in Western Maine, USA. Contrib Mineral Petrol 12:25–62

Faryad SW, Chakraborty S (2005) Duration of Eo-Alpine metamorphic events obtained from multicomponent diffusion modeling of garnet: a case study from the Eastern Alps. Contrib Mineral Petrol 150:306–318

Fernando G, Hauzenberger CA, Baumgartner LP, Hofmeister W (2003) Modeling of retrograde diffusion zoning in garnet: evidence for slow cooling of granulites from the Highland Complex of Sri Lanka. Mineral Petrol 78:53–71

Ferry JM, Spear FS (1978) Experimental calibration of the partitioning of Fe and Mg between biotite and garnet. Contrib Mineral Petrol 66:113–117

Ferry JM, Kitajima K, Strickland A, Valley JW (2014) Ion microprobe survey of the grain-scale oxygen isotope geochemistry of minerals in metamorphic rocks. Geochim Cosmochim Acta 144:403–433

Florence FP, Spear FS (1991) Effects of diffusional modification of garnet growth zoning on *P–T* path calculations. Contrib Mineral Petrol 107:487–500

Florence FP, Spear FS (1993) Influences of reaction history and chemical diffusion on *P–T* calculations for staurolite schists from the Littleton Formation, northwestern New Hampshire. Am Mineral 78:345–359

Foster GL, Parrish RR, Horstwood MSA, Chenery S, Pyle JM, Gibson HD (2004) The generation of prograde *P–T–t* points and paths; a textural, compositional, and chronological study of metamorphic monazite. Earth Planet Sci Lett 228:125–142

Frost MJ (1962) Metamorphic grade and iron–magnesium distribution between coexisting garnet–biotite and garnet–hornblende. Mineral Mag 99:427–438

Gaidies F, Abart R, De Capitani C, Schuster R, Connolly JAD, Reusser E (2006) Characterization of polymetamorphism in the Austroalpine basement east of the Tauern Window using garnet isopleth thermobarometry. J Metamorph Geol 24:451–475

Gaidies F, De Capitani C, Abart R (2008a) THERIA_G: a software program to numerically model prograde garnet growth. Contrib Mineral Petrol 155:657–671

Gaidies F, De Capitani C, Abart R, Schuster R (2008b) Prograde garnet growth along complex *P–T–t* paths: results from numerical experiments on polyphase garnet from the Wölz Complex (Austroalpine basement). Contrib Mineral Petrol 155:673–688

Gaidies F, Pattison DRM, de Capitani C (2011) Toward a quantitative model of metamorphic nucleation and growth. Contrib Mineral Petrol 162:975–993

Gaidies F, Petley-Ragan A, Chakraborty S, Dasgupta S, Jones P (2015) Constraining the conditions of Barrovian metamorphism in Sikkim, India: *P–T–t* paths of garnet crystallization in the Lesser Himalayan Belt. J Metamorph Geol 33:23–44

Galli A, Le Bayon B, Schmidt MW, Burg, J-P, Caddick MJ, Reusser E (2011) Granulites and charnockites of the Gruf Complex: evidence for Permian ultra-high temperature metamorphism in the Central Alps. Lithos 124:17–45

Galli A, Le Bayon B, Schmidt MW, Burg JP, Reusser E, Sergeev SA, Larionov A (2012) U–Pb zircon dating of the Gruf Complex: disclosing the late Variscan granulitic lower crust of Europe stranded in the Central Alps. Contrib Mineral Petrol 163:353–378

Galli A, Le Bayon B, Schmidt MW, Burg, J-P, Reusser E (2013) Tectonometamorphic history of the Gruf complex (Central Alps): exhumation of a granulite–migmatite complex with the Bergell pluton. Swiss J Geosci 106:33–62

Galwey AK, Jones KA (1966) Crystal size frequency distribution of garnets in some analysed metamorphic rocks from Mallaig Inverness Scotland. Geol Mag 103:143-and

Ganguly J (2002) Diffusion kinetics in minerals: Principles and applications to tectono- metamorphic processes. *In:* EMU Notes in Mineralogy: Energy Modelling in Minerals. Gramaccioli CMO (ed) Eur Mineral Union, p 271–309

Ganguly J (2010) Cation diffusion kinetics in aluminosilicate garnets and geological applications. Rev Mineral Geochem 72:559–601

Ganguly J, Saxena SK (1984) Mixing properties of aluminosilicate garnets: constraints from natural and experimental data, and applications to geothermo-barometry. Am Mineral 69:88–97

Ganguly J, Tirone M (1999) Diffusion closure temperature and age of a mineral with arbitrary extent of diffusion: theoretical formulation and applications. Earth Planet Sci Lett 170:131–140

Ganguly J, Tirone M (2001) Relationship between cooling rate and cooling age of a mineral: Theory and applications to meteorites. Meteorit Planet Sci 36:167–175

Ganguly J, Cheng WJ, Tirone M (1996) Thermodynamics of aluminosilicate garnet solid solution: New experimental data, an optimized model, and thermometric applications. Contrib Mineral Petrol 126:137–151

Ganguly J, Cheng W, Chakraborty S (1998a) Cation diffusion in aluminosilicate garnets: experimental determination in pyrope-almandine diffusion couples. Contrib Mineral Petrol 131:171–180

Ganguly J, Tirone M, Hervig RL (1998b) Diffusion kinetics of samarium and neodymium in garnet, and a method for determining cooling rates of rocks. Science 281:805–807

Ganguly J, Dasgupta S, Cheng W, Neogi S (2000) Exhumation history of a section of the Sikkim Himalayas, India: records in the metamorphic mineral equilibria and compositional zoning of garnet. Earth Planet Sci Lett 183:471–486

Gatewood MP, Dragovic B, Stowell HH, Baxter EF, Hirsch DM, Bloom R (2015) Evaluating chemical equilibrium in metamorphic rocks using major element and Sm–Nd isotopic age zoning in garnet, Townshend Dam, Vermont, USA. Chem Geol 401:151–168

Gauthiez-Putallaz L, Rubatto D, Hermann J (2016) Dating prograde fluid pulses during subduction by in situ U–Pb and oxygen isotope analysis. Contrib Mineral Petrol 171:1–20

Gessmann CK, Spiering B, Raith M (1997) Experimental study of the Fe–Mg exchange between garnet and biotite: Constraints on the mixing behavior and analysis of the cation-exchange mechanisms. Am Mineral 82:1225–1240

Getty SR, Selverstone J, Wernicke BP, Jacobsen SB, Aliberti E, Lux DR (1993) Sm–Nd dating of multiple garnet growth events in an arc-continent collision zone, northwestern United-States Cordillera. Contrib Mineral Petrol 115:45–57

Ghent ED (1976) Plagioclase–garnet–Al_2SiO_5–quartz: a potential geothermometer–geobarometer. Am Mineral 61:710–714

Ghent ED (1977) Applications of activity-composition relations to displacement of a solid-solid equilibrium anorthite = grossular + kyanite + quartz. *In:* Short Course in Application of Thermodynamics to Petrology and Ore Deposits. Greenwood HJ (ed) Mineral Assoc Canada, p 99–108

Ghent ED, Stout MZ (1981) Geobarometry and geothermometry of plagioclase–biotite–garnet–muscovite assemblages. Contrib Mineral Petrol 76:92–97

Gieré R, Rumble D, Gunther D, Connolly J, Caddick MJ (2011) Correlation of growth and breakdown of major and accessory minerals in metapelites from Campolungo, Central Alps. J Petrol 52:2293–2334

Goldman DS, Albee AL (1977) Correlation of Mg/Fe partitioning between garnet and biotite with O^{18}/O^{16} partitioning between quartz and magnetite. Am J Sci 277:750–761

Goldsmith JR (1980) Melting and breakdown reactions of anorthite at high pressures and temperatures. Am Mineral 65:272–284

Gordon SM, Luffi P, Hacker B, Valley J, Spicuzza M, Kozdon R, Kelemen P, Ratshbacher L, Minaev V (2012) The thermal structure of continental crust in active orogens: insight from Miocene eclogite and granulite xenoliths of the Pamir Mountains. J Metamorph Geol 30:413–434

Grew ES, Locock AJ, Mills SJ, Galuskina IO, Galuskin EV, Halenius U (2013) Nomenclature of the garnet supergroup. Am Mineral 98:785–810

Griffin WL, Brueckner HK (1980) Caledonian Sm–Nd ages and a crustal origin for Norwegian eclogites. Nature 285:319–321

Guevara VE, Caddick MJ (2016) Shooting at a moving target: phase equilibria modeling of high-temperature metamorphism. J Metamorph Geol 34:209–235

Guiraud M, Powell R (2006) *P–V–T* relationships and mineral equilibria in inclusions in minerals. Earth Planet Sci Lett 244:683–694

Guiraud M, Powell R, Rebay G (2001) H_2O in metamorphism and unexpected behaviour in the preservation of metamorphic mineral assemblages. J Metamorph Geol 19:445–454

Hallett BW, Spear FS (2011) Insight into the cooling history of the Valhalla complex, British Columbia. Lithos 125:809–824

Hackler RT, Wood BJ (1989) Experimental determination of Fe and Mg exchange between garnet and olivine and estimation of Fe–Mg mixing properties in garnet. Am Mineral 74:994–999

Hallett BW, Spear FS (2014a) The *P–T* history of anatectic pelites of the Northern East Humboldt Range, Nevada: Evidence for tectonic loading, decompression, and anatexis. J Petrol 55:3–36

Hallett BW, Spear FS (2015) Monazite, zircon, and garnet growth in migmatitic pelites as a record of metamorphism and partial melting in the East Humboldt Range, Nevada. Am Mineral 100:951–972

Harte B, Henley KJ (1966) Occurence of compositionally zoned almanditic garnets in regionally metamorphosed rocks. Nature 210:689–692

Harvey J, Baxter EF (2009) An improved method for TIMS high precision neodymium isotope analysis of very small aliquots (1–10 ng). Chem Geol 258:251–257

Hemley RJ (1987) Pressure dependence of Raman spectra of SiO_2 polymorphs; α-quartz, coesite and stishovite. *In:* High-Pressure Research in Mineral Physics. Murli, HM and Syono Y (eds) Am Geophys Union, Washington DC, p 347–359

Hensen BJ (1971) Theoretical phase relations involving cordierite and garnet in the system MgO–FeO–Al_2O_3–SiO_2. Contrib Mineral Petrol 33:191–214

Hermann J, Rubatto D (2003) Relating zircon and monazite domains to garnet growth zones: age and duration of granulite facies metamorphism in the Val Malenco lower crust. J Metamorph Geol 21:833–852

Herwartz D, Nagel TJ, Munker C, Scherer EE, Froitzheim N (2011) Tracing two orogenic cycles in one eclogite sample by Lu–Hf garnet chronometry. Nat Geosci 4:178–183

Hickmott DD, Shimizu N (1990) Trace-element zoning in garnet from the Kwoiek area, British-Columbia—disequilibrium partitioning during garnet growth. Contrib Mineral Petrol 104:619–630

Hickmott D, Spear FS (1992) Major-element and trace-element zoning in garnets from calcareous pelites in the NW Shelburne Falls quadrangle, Massachusetts—garnet growth histories in retrograded rocks. J Petrol 33:965–1005

Hickmott DD, Shimizu N, Spear FS, Selverstone J (1987) Trace-element zoning in a metamorphic garnet. Geology 15:573–576

Hodges KV, Crowley PD (1985) Error estimation and empirical geothermobarometry for pelitic systems. Am Mineral 70:702–709

Hodges KV, McKenna LW (1987) Realistic propagation of uncertainties in geologic thermobarometry. Am Mineral 72:671–680

Hoisch TD (1990) Empirical calibration of six geobarometers for the mineral assemblage quartz + muscovite + biotite + plagioclase + garnet. Contrib Mineral Petrol 104:225–234

Hoisch TD (1991) Equilibria within the mineral assemblage quartz + muscovite + biotite + garnet + plagioclase, and implications for the mixing properties of octahedrally-coordinated cations in muscovite and biotite. Contrib Mineral Petrol 108:43–54

Holdaway MJ (2000) Application of new experimental and garnet Margules data to the garnet–biotite geothermometer. Am Mineral 85:881–892

Holdaway MJ (2001) Recalibration of the GASP geobarometer in light of recent garnet and plagioclase activity models and versions of the garnet–biotite geothermometer. Am Mineral 86:1117–1129

Holdaway MJ, Mukhopadhyay B, Dyar MD, Guidotti CV, Dutrow BL (1997) Garnet–biotite geothermobarometry revised: New Margules parameters and a natural specimen data set from Maine. Am Mineral 82:582–595

Holland TJB, Powell R (1985) An internally consistent thermodynamic dataset with uncertainties and correlations: 2. Data and results. J Metamorph Geol 3:343–370

Holland TJB, Powell R (1990) An enlarged and updated internally consistent thermodynamic dataset with uncertainties and correlations—the system K_2O–Na_2O–CaO–MgO–MnO–FeO–Fe_2O_3–Al_2O_3–TiO_2–SiO_2–C–H_2–O_2. J Metamorph Geol 8:89–124

Holland TJB, Powell R (1998) An internally consistent thermodynamic data set for phases of petrological interest. J Metamorph Geol 16:309–343

Holland TJB, Powell R (2011) An improved and extended internally consistent thermodynamic dataset for phases of petrological interest, involving a new equation of state for solids. J Metamorph Geol 29:333–383

Hollister LS (1966) Garnet zoning: an interpretation based on the Rayleigh fractionation model. Science 154:1647–1651

Ikeda T, Shimobayashi N, Wallis SR, Tsuchiyama A (2002) Crystallographic orientation, chemical composition and three-dimensional geometry of sigmoidal garnet: evidence for rotation. J Struct Geol 24:1633–1646

Indares AD, Martignole J (1985) Biotite–garnet geothermometry in the granulite facies: the influence of Ti and Al in biotite. Am Mineral 70:272–278

Izraeli ES, Harris JW, Navon O (1999) Raman barometry of diamond formation. Earth Planet Sci Lett 173:351–360

Jamtveit B, Hervig RL (1994) Constraints on transport and kinetics in hydrothermal systems from zoned garnet crystals. Science 263:505–508

Jamtveit B, Wogelius RA, Fraser DG (1993) Zonation patterns of skarn garnets—records of hydrothermal system evolution. Geology 21:113–116

Jedlicka R, Faryad SW, Hauzenberger C (2015) Prograde Metamorphic History of UHP Granulites from the Moldanubian Zone (Bohemian Massif) Revealed by Major Element and Y + REE Zoning in Garnets. J Petrol 56:2069–2088

John T, Gussone N, Podladchikov YY, Bebout GE, Dohmen R, Halama R, Klemd R, Magna T, Seitz HM (2012) Volcanic arcs fed by rapid pulsed fluid flow through subducting slabs. Nat Geosci 5:489–492

Johnson SE (1993) Testing models for the development of spiral-shaped inclusion trails in garnet porphyroblasts—to rotate or not to rotate, that is the question. J Metamorph Geol 11:635–659

Kawakami T, Hokada T (2010) Linking *P–T* path with development of discontinuous phosphorus zoning in garnet during high-temperature metamorphism—an example from Lützow-Holm Complex, East Antarctica. J Mineral Petrol Sci 105:175–186

Kelly ED, Carlson WD, Connelly JN (2011) Implications of garnet resorption for the Lu–Hf garnet geochronometer: an example from the contact aureole of the Makhavinekh Lake Pluton, Labrador. J Metamorph Geol 29:901–916

Kelly ED, Carlson WD, Ketcham RA (2013a) Crystallization kinetics during regional metamorphism of porphyroblastic rocks. J Metamorph Geol 31:963–979

Kelly ED, Carlson WD, Ketcham RA (2013b) Magnitudes of departures from equilibrium during regional metamorphism of porphyroblastic rocks. J Metamorph Geol 31:981–1002

Kelsey DE, Hand M (2015) On ultrahigh temperature crustal metamorphism: phase equilibria, trace element thermometry, bulk composition, heat sources, timescales and tectonic settings. Geoscience Frontiers 6:311–356
Ketcham RA, Carlson WD (2012) Numerical simulation of diffusion-controlled nucleation and growth of porphyroblasts. J Metamorph Geol 30:489–512
Kita NT, Ushikubo T, Fu B, Valley JW (2009) High precision SIMS oxygen isotope analysis and the effect of sample topography. Chem Geol 264:43–57
Kleeman U, Reinhardt J (1994) Garnet–biotite thermometry revised: the effect of AlVI and Ti in biotite. Eur J Mineral 6:925–941
Kohn MJ (1993) Modeling of prograde mineral $\delta^{18}O$ changes in metamorphic systems. Contrib Mineral Petrol 113:249–261
Kohn MJ (2004) Oscillatory- and sector-zoned garnets record cyclic (?) rapid thrusting in central Nepal. Geochem Geophys Geosystem 5:9
Kohn MJ (2009) Models of garnet differential geochronology. Geochim Cosmochim Acta 73:170–182
Kohn MJ (2014) "Thermoba-Raman-try": Calibration of spectroscopic barometers and thermometers for mineral inclusions. Earth Planet Sci Lett 388:187–196
Kohn MJ, Penniston–Dorland SC (2017) Diffusion: Obstacles and opportunities in petrochronology. Rev Mineral Geochem 83:103–152
Kohn MJ, Spear FS (1991) Error propagation in barometers: 2. Application to rocks. Am Mineral 76:138–147
Kohn MJ, Spear FS (2000) Retrograde net transfer reaction insurance for pressure–temperature estimates. Geology 28:1127–1130
Kohn MJ, Valley JW (1994) Oxygen-isotope constraints on metamorphic fluid-flow, Townshend Dam, Vermont, USA. Geochim Cosmochim Acta 58:5551–5566
Kohn MJ, Valley JW (1998) Obtaining equilibrium oxygen isotope fractionations from rocks: theory and examples. Contrib Mineral Petrol 132:209–224
Kohn MJ, Valley JW, Elsenheimer D, Spicuzza MJ (1993) O isotope zoning in garnet and staurolite—evidence for closed-system mineral growth during regional metamorphism. Am Mineral 78:988–1001
Kohn MJ, Spear FS, Valley JW (1997) Dehydration-melting and fluid recycling during metamorphism: Rangeley Formation, New Hampshire, USA. J Petrol 38:1255–1277
Konrad-Schmolke M, Babist J, Handy MR, O'Brien PJ (2006) The physico-chemical properties of a subducted slab from garnet zonation patterns (Sesia Zone, Western Alps). J Petrol 47:2123–2148
Konrad-Schmolke M, O'Brien PJ, Heidelbach F (2007) Compositional re-equilibration of garnet: the importance of sub-grain boundaries. Eur J Mineral 19:431–438
Konrad-Schmolke M, O'Brien PJ, De Capitani C, Carswell DA (2008) Garnet growth at high- and ultra-high pressure conditions and the effect of element fractionation on mineral modes and composition. Lithos 103:309–332
Korsakov AV, Zhukov VP, Vandenabeele P (2010) Raman-based geobarometry of ultrahigh-pressure metamorphic rocks: applications, problems, and perspectives. Anal Bioanal Chem 397:2739–2752
Korhonen FJ, Brown M, Grove M, Siddoway CS, Baxter EF, Inglis JD (2012) Separating metamorphic events in the Fosdick migmatite–granite complex, West Antarctica. J Metamorph Geol 30:165–191
Kouketsu Y, Nishiyama T, Ikeda T, Enami M (2014) Evaluation of residual pressure in an inclusion-host system using negative frequency shift of quartz Raman spectra. Am Mineral 99:433–442
Koziol AM, Newton RC (1988) Redetermination of the anorthite breakdown reaction and improvement of the plagioclase– garnet–Al_2SiO_5–quartz geobarometer. Am Mineral 73:216–223
Koziol AM, Newton RC (1989) Grossular activity-composition relationships in ternary garnets determined by reversed displaced-equilibrium experiments. Contrib Mineral Petrol 103:423–433
Kretz R (1959) Chemical study of garnet, biotite and hornblende from gneisses of southwestern Quebec, with emphasis on distri- bution of elements in coexisting minerals. J Geol 67:371–403
Kretz R (1964) Analysis of equilibrium in garnet–biotite–sillimanite gneisses from Quebec. J Petrol 5:1–20
Kretz R (1966) Interpretation of the shape of mineral grains in metamorphic rocks. J Petrol 7:68–94
Kretz R (1973) Kinetics of the crystallization of garnet at two localities near Yellowknife. Can Mineral 12:1–20
Kretz R (1974) Some models for the rate of crystallization of garnet in metamorphic rocks. Lithos 7:123–131
Kylander-Clark ARC, Hacker BR, Johnson CM, Beard BL, Mahlen NJ, Lapen TJ (2007) Coupled Lu–Hf and Sm–Nd geochronology constrains prograde and exhumation histories of high- and ultrahigh-pressure eclogites from western Norway. Chem Geol 242:137–154
Lagos M, Scherer EE, Tomaschek F, Munker C, Keiter M, Berndt J, Ballhaus C (2007) High precision Lu–Hf geochronology of eocene eclogite-facies rocks from syros, cyclades, Greece. Chem Geol 243:16–35
Lanari P, Engi M (2017) Local bulk composition effects on mineral assemblages. Rev Mineral Geochem v. 83
Lanari P, Giuntoli F, Loury C, Burn M, Engi M (2017) An inverse modeling approach to obtain *P–T* conditions of metamorphic stages involving garnet growth and resorption. Eur J Mineral in press:doi:10.1127/ejm/2017/0029–2597

Lancaster PJ, Fu B, Page FZ, Kita NT, Bickford ME, Hill BM, McLelland JM, Valley JW (2009) Genesis of metapelitic migmatites in the Adirondack Mountains, New York. J Metamorph Geol 27:41–54

Lanzirotti A (1995) Yttrium zoning in metamorphic garnets. Geochim Cosmochim Acta 59:4105–4110

Lapen TJ, Johnson CM, Baumgartner LP, Mahlen NJ, Beard BL, Amato JM (2003) Burial rates during prograde metamorphism of an ultra-high-pressure terrane: an example from Lago di Cignana, western Alps, Italy. Earth Planet Sci Lett 215:57–72

Lasaga AC (1979) Multicomponent exchange and diffusion in silicates. Geochim Cosmochim Acta 43:455–469

Lasaga AC (1983) Geospeedometry: An extension of geothermometry. *In:* Kinetics and Equilibrium in Mineral Reactions. Saxena SK (ed) Springer-Verlag, New York, p 81–114

Loomis TP (1975) Reaction zoning of garnet. Contrib Mineral Petrol 52:285–305

Loomis TP, Ganguly J, Elphick SC (1985) Experimental determination of cation diffusivities in aluminosilicate garnets II. Multicomponent simulation and tracer diffusion coefficients. Contrib Mineral Petrol 90:45–51

Mahar E, Powell R, Holland TJB, Howell N (1997) The effect of Mn on mineral stability in metapelites. J Metamorph Geol 15:223–238

Malaspina N, Poli S, Fumagalli P (2009) The oxidation state of metasomatized mantle wedge: insights from C–O–H-bearing garnet peridotite. J Petrol 50:1533–1552

Manzotti P, Ballevre M (2013) Multistage garnet in high-pressure metasediments: Alpine overgrowths on Variscan detrital grains. Geology 41:1151–1154

Marmo BA, Clarke GL, Powell R (2002) Fractionation of bulk rock composition due to porphyroblast growth: effects on eclogite facies mineral equilibria, Pam Peninsula, New Caledonia. J Metamorph Geol 20:151–165

Martin AJ (2009) Sub-millimeter heterogeneity of yttrium and chromium during growth of semi-pelitic garnet. J Petrol 50:1713–1727

Martin L, Duchene S, Deloule E, Vanderhaeghe O (2006) The isotopic composition of zircon and garnet: A record of the metamorphic history of Naxos, Greece. Lithos 87:174–192

Martin LAJ, Ballevre M, Boulvais P, Halfpenny A, Vanderhaeghe O, Duchene S, Deloule E (2011) Garnet re-equilibration by coupled dissolution-reprecipitation: evidence from textural, major element and oxygen isotope zoning of 'cloudy' garnet. J Metamorph Geol 29:213–231

Martin LAJ, Rubatto D, Crépisson C, Hermann J, Putlitz B, Vitale-Brovarone A (2014) Garnet oxygen analysis by SHRIMP-SI: Matrix corrections and application to high-pressure metasomatic rocks from Alpine Corsica. Chem Geol 374–375:25–36

Masago H, Rumble D, Ernst WG, Parkinson CD, Maruyama S (2003) Low $\delta^{18}O$ eclogites from the Kokchetav massif, northern Kazakhstan. J Metamorph Geol 21:579–587

McKenna LW, Hodges KV (1988) Accuracy versus precision in locating reaction boundaries: Implications for the garnet–plagioclase–aluminum silicate–quartz geobarometer. Am Mineral 73:1205–1205

Menard T, Spear FS (1993) Metamorphism of calcic pelitic schists, Strafford Dome, Vermont: Compositional zoning and reaction history. J Petrol 34:977–1005

Menard T, Spear FS (1996) Interpretation of plagioclase zonation in calcic pelitic schist, south Strafford, Vermont, and the effects on thermobarometry. Can Mineral 34:133–146

Meth CE, Carlson WD (2005) Diffusion-controlled synkinematic growth of garnet from a heterogeneous precursor at Passo del Sole, Switzerland. Can Mineral 43:157–182

Mezger K, Hanson GN, Bohlen SR (1989) U–Pb systematics of garnet—dating the growth of garnet in the late Archean Pikwitonei Granulite Domain at Cauchon and Natawahunan lakes, Manitoba, Canada. Contrib Mineral Petrol 101:136–148

Mezger K, Essene EJ, Halliday AN (1992) Closure temperatures of the Sm–Nd system in metamorphic garnets. Earth Planet Sci Lett 113:397–409

Moecher DP, Essene EJ, Anovitz LM (1988) Calculation and application of clinopyroxene–garnet–plagioclase–quartz geobarometers. Contrib Mineral Petrol 100:92–106

Moore SJ, Carlson WD, Hesse, Ma (2013) Origins of yttrium and rare earth element distributions in metamorphic garnet. J Metamorph Geol 31:663–689

Moscati RJ, Johnson CA (2014) Major element and oxygen isotope geochemistry of vapour-phase garnet from the Topopah Spring Tuff at Yucca Mountain, Nevada, USA. Mineral Mag 78:1029–1041

Mottram CM, Parrish RR, Regis D, Warren CJ, Argles TW, Harris NB, Roberts NM (2015) Using U–Th–Pb petrochronology to determine rates of ductile thrusting: Time windows into the Main Central Thrust, Sikkim Himalaya. Tectonics 34:1355–1374

Moynihan DP, Pattison DRM (2013) An automated method for the calculation of *P–T* paths from garnet zoning, with application to metapelitic schist from the Kootenay Arc, British Columbia, Canada. J Metamorph Geol 31:525–548

Mukhopadhyay B, Holdaway MJ, Koziol AM (1997) A statistical model of thermodynamic mixing properties of Ca–Mg–Fe^{2+} garnets. Am Mineral 82:165–181

Nesheim TO, Vervoort JD, McClelland WC, Gilotti JA, Lang HM (2012) Mesoproterozoic syntectonic garnet within Belt Supergroup metamorphic tectonites: Evidence of Grenville-age metamorphism and deformation along northwest Laurentia. Lithos 134:91–107

Newton RC, Haselton HT (1981) Thermodynamics of the garnet–plagioclase–Al_2SiO_5–quartz geobarometer. *In:* Thermodynamics of Minerals and Melts. Newton RC, Navrotsky, A and Wood BJ (eds) Springer-Verlag, New York, p 129–145

O'Brien PJ, Vrána S (1995) Eclogites with a short-lived granulite facies overprint in the Moldanubian Zone, Czech Republic: Petrology, geochemistry and diffusion modelling of garnet zoning. Geol Rundsch 84:473–488

Otamendi JE, de la Rosa JD, Douce AEP, Castro A (2002) Rayleigh fractionation of heavy rare earths and yttrium during metamorphic garnet growth. Geology 30:159–162

Page FZ, Kita NT, Valley JW (2010) Ion microprobe analysis of oxygen isotopes in garnets of complex chemistry. Chem Geol 270:9–19

Page FZ, Essene EJ, Mukasa SB, Valley JW (2014) A garnet–zircon oxygen isotope record of subduction and exhumation fluids from the Franciscan Complex, California. J Petrol 55:103–131

Palin RM, Weller OM, Waters DJ, Dyck B (2016) Quantifying geological uncertainty in metamorphic phase equilibria modelling; a Monte Carlo assessment and implications for tectonic interpretations. Geosci Frontiers 7:591–607

Parkinson C, Katayama I (1999) Present-day ultrahigh-pressure conditions of coesite inclusions in zircon and garnet: Evidence from laser Raman microspectroscopy. Geology 27:979–982

Pattison D (2015) Challenges in phase diagram modelling, focusing on metapelites. Geological Society of America

Pattison DRM, Chacko T, Farquhar J, McFarlane CRM (2003) Temperatures of granulite-facies metamorphism: constraints from experimental phase equilibria and thermobarometry corrected for retrograde exchange. J Petrol 44:867–900

Pattison DRM, De Capitani C, Gaidies F (2011) Petrological consequences of variations in metamorphic reaction affinity. J Metamorph Geol 29:953–977

Peck W, Valley J (2004) Quartz–garnet isotope thermometry in the southern Adirondack Highlands (Grenville Province, New York). J Metamorph Geol 22:763–773

Penniston-Dorland SC, Sorensen SS, Ash RD, Khadke SV (2010) Lithium isotopes as a tracer of fluids in a subduction zone melange: Franciscan Complex, CA. Earth Planet Sci Lett 292:181–190

Perchuk LL, Lavrent'eva IV (1983) Experimental investigation of exchange equilibria in the system cordierite–garnet–biotite. *In:* Kinetics and Equilibrium in Mineral Reactions. Saxena SK (ed) Springer-Verlag, New York, p 199–239

Perchuk A, Philippot P, Erdmer P, Fialin M (1999) Rates of thermal equilibration at the onset of subduction deduced from diffusion modeling of eclogitic garnets, Yukon–Tanana terrane, Canada. Geology 27:531–534

Peterman EM, Hacker BR, Baxter EF (2009) Phase transformations of continental crust during subduction and exhumation: Western Gneiss Region, Norway. Eur J Mineral 21:1097–1118

Pogge von Strandmann PAE, Dohmen R, Marschall HR, Schumacher JC, Elliott T (2015) Extreme magnesium isotope fractionation at outcrop scale records the mechanism and rate at which reaction fronts advance. J Petrol 56:33–58

Pollington AD, Baxter EF (2010) High resolution Sm–Nd garnet geochronology reveals the uneven pace of tectonometamorphic processes. Earth Planet Sci Lett 293:63–71

Pollington AD, Baxter EF (2011) High precision microsampling and preparation of zoned garnet porphyroblasts for Sm–Nd geochronology. Chem Geol 281:270–282

Powell R, Holland TJB (1988) An internally consistent dataset with uncertainties and correlations. 3. Applications to geobarometry, worked examples and a computer-program. J Metamorph Geol 6:173–204

Powell R, Holland TJB, Worley B (1998) Calculating phase diagrams involving solid solutions via non-linear equations, with examples using THERMOCALC. J Metamorph Geol 16:577–588

Prince C, Harris N, Vance D (2001) Fluid-enhanced melting during prograde metamorphism. J Geol Soc London 158:233–241

Putlitz B, Matthews A, Valley JW (2000) Oxygen and hydrogen isotope study of high-pressure metagabbros and metabasalts (Cyclades, Greece): implications for the subduction of oceanic crust. Contrib Mineral Petrol 138:114–126

Pyle J, Spear F (1999) Yttrium zoning in garnet: Coupling of major and accessory phases during metamorphic reactions. Geol Mater Res 1:1–49

Pyle JM, Spear FS (2000) An empirical garnet (YAG)–xenotime thermometer. Contrib Mineral Petrol 138:51–58

Pyle JM, Spear FS (2003) Four generations of accessory-phase growth in low-pressure migmatites from SW New Hampshire. Am Mineral 88:338–351

Pyle JM, Spear FS, Rudnick RL, McDonough WF (2001) Monazite–xenotime–garnet equilibrium in metapelites and a new monazite- garnet thermometer. J Petrol 42:2083–2107

Raimondo T, Clark C, Hand M, Cliff J, Harris C (2012) High-resolution geochemical record of fluid–rock interaction in a mid-crustal shear zone: a comparative study of major element and oxygen isotope transport in garnet. J Metamorph Geol 30:255–280

Ramberg H (1952) Chemical bonds and distribution of cations in silicates. J Geol 60:331–355

Ramsay JG (1962) The geometry and mechanics of formation of "similar" type folds. J Geol 70:309–327

Richter R, Spiering B, Hoernes S (1988) Petrology and isotope-geochemistry of granulite-facial marbles and calcium-silicate rocks of Sri-Lanka. Fortschr Mineral 66:134–134

Robyr M, Carlson WD, Passchier C, Vonlanthen P (2009) Microstructural, chemical and textural records during growth of snowball garnet. J Metamorph Geol 27:423–437

Robyr M, Darbellay B, Baumgartner LP (2014) Matrix-dependent garnet growth in polymetamorphic rocks of the Sesia zone, Italian Alps. J Metamorph Geol 32:3–24

Romer RL, Xiao YL (2005) Initial Pb–Sr(Nd) isotopic heterogeneity in a single allanite–epidote crystal: implications of reaction history for the dating of minerals with low parent-to-daughter ratios. Contrib Mineral Petrol 148:662–674

Rosenfeld JL (1968) Garnet rotations due to the major Paleozoic deformations in southeast Vermont. *In:* Studies of Appalachian Geology: Northern and Maritime. Zen E (ed) John Wiley and Sons, Inc., New York, p 185–202

Rosenfeld JL (1969) Stress effects around quartz inclusions in almandine and the piezothermometry of coexisting aluminum silicates. Am J Sci 267:317–351

Rosenfeld JL, Chase AB (1961) Pressure and temperature of crystallization from elastic effects around solid inclusions in minerals? Am J Sci 259:519–541

Rubatto D (2002) Zircon trace element geochemistry: partitioning with garnet and the link between U–Pb ages and metamorphism. Chem Geol 184:123–138

Rubatto D (2017) Zircon: the metamorphic mineral. Rev Mineral Geochem 83

Rubatto D, Angiboust S (2015) Oxygen isotope record of oceanic and high-pressure metasomatism: a *P–T–*time–fluid path for the Monviso eclogites (Italy). Contrib Mineral Petrol 170

Rumble D, Yui TF (1998) The Qinglongshan oxygen and hydrogen isotope anomaly near Donghai in Jiangsu Province, China. Geochim Cosmochim Acta 62:3307–3321

Russell AK, Kitajima K, Strickland A, Medaris LG, Schulze DJ, Valley JW (2013) Eclogite-facies fluid infiltration: constraints from $\delta^{18}O$ zoning in garnet. Contrib Mineral Petrol 165:103–116

Sato K, Santosh M, Tsunogae T (2009) A petrologic and laser Raman spectroscopic study of sapphirine–spinel–quartz–Mg-staurolite inclusions in garnet from Kumiloothu, southern India: Implications for extreme metamorphism in a collisional orogen. J Geodynam 47:107–118

Saxena SK (1968) Distribution of elements between coexisting minerals and the nature of solid solution in garnet. Am Mineral 53:994–1014

Saxena SK (1969) Silicate solid solutions and geothermometry: 3. Distribution of Fe and Mg between coexisting garnet and biotite. Contrib Mineral Petrol 22:259–267

Sayab M, Shah SZ, Aerden D (2016) Metamorphic record of the NW Himalayan orogeny between the Indian plate-Kohistan Ladakh Arc and Asia: Revelations from foliation intersection axis (FIA) controlled *P–T–t–d* paths. Tectonophysics 671:110–126

Scherer EE, Cameron KL, Blichert-Toft J (2000) Lu–Hf garnet geochronology: Closure temperature relative to the Sm–Nd system and the effects of trace mineral inclusions. Geochim Cosmochim Acta 64:3413–3432

Schmidt C, Ziemann MA (2000) *In-situ* Raman spectroscopy of quartz: A pressure sensor for hydrothermal diamond-anvil cell experiments at elevated temperatures. Am Mineral 85:1725–1734

Schmidt C, Steele-MacInnis M, Watenphul A, Wilke M (2013) Calibration of zircon as a Raman spectroscopic pressure sensor to high temperatures and application to water-silicate melt systems. Am Mineral 98:643–650

Schmidt A, Pourteau A, Candan O, Oberhansli R (2015) Lu–Hf geochronology on cm-sized garnets using microsampling: New constraints on garnet growth rates and duration of metamorphism during continental collision (Menderes Massif, Turkey). Earth Planet Sci Lett 432:24–35

Schoene B, Baxter EF (2017) Petrochronology and TIMS. Rev Mineral Geochem 83:231–260

Schwarz JO, Engi M, Berger A (2011) Porphyroblast crystallization kinetics: the role of the nutrient production rate. J Metamorph Geol 29:497–512

Skelton A, Annersten H, Valley J (2002) $\delta^{18}O$ and yttrium zoning in garnet: time markers for fluid flow? J Metamorph Geol 20:457–466

Skora S, Baumgartner LP, Mahlen NJ, Johnson CM, Pilet S, Hellebrand E (2006) Diffusion-limited REE uptake by eclogite garnets and its consequences for Lu–Hf and Sm–Nd geochronology. Contrib Mineral Petrol 152:703–720

Skora S, Baumgartner LP, Mahlen NJ, Lapen TJ, Johnson CM, Bussy F (2008) Estimation of a maximum Lu diffusion rate in a natural eclogite garnet. Swiss J Geosci 101:637–650

Skora S, Lapen TJ, Baumgartner LP, Johnson CM, Hellebrand E, Mahlen NJ (2009) The duration of prograde garnet crystallization in the UHP eclogites at Lago di Cignana, Italy. Earth Planet Sci Lett 287:402–411

Smit MA, Scherer EE, Mezger K (2013) Lu–Hf and Sm–Nd garnet geochronology: Chronometric closure and implications for dating petrological processes. Earth Planet Sci Lett 381:222–233
Sobolev NV, Fursenko BA, Goryainov SV, Shu J, Hemley RJ, Mao A, Boyd FR (2000) Fossilized high pressure from the Earth's deep interior: the coesite-in-diamond barometer. PNAS 97:11875–11879
Sobolev NV, Schertl HP, Valley JW, Page FZ, Kita NT, Spicuzza MJ, Neuser RD, Logvinova AM (2011) Oxygen isotope variations of garnets and clinopyroxenes in a layered diamondiferous calcsilicate rock from Kokchetav Massif, Kazakhstan: a window into the geochemical nature of deeply subducted UHPM rocks. Contrib Mineral Petrol 162:1079–1092
Solva H, Thoni M, Habler G (2003) Dating a single garnet crystal with very high Sm/Nd ratios (Campo basement unit, Eastern Alps). Eur J Mineral 15:35–42
Sorby HC, Butler PJ (1869) On the structure of rubies, sapphires, diamonds, and some other minerals. Proc R Soc London 17:291–302
Sousa J, Kohn MJ, Schmitz MD, Northrup CJ, Spear FS (2013) Strontium isotope zoning in garnet: implications for metamorphic matrix equilibration, geochronology and phase equilibrium modelling. J Metamorph Geol 31:437–452
Spear FS (1993) Metamorphic phase equilibria and pressure–temperature–time paths. Mineral Soc Am, Washington, DC
Spear FS (2004) Fast cooling and exhumation of the Valhalla metamorphic core complex, southeastern British Columbia. Int Geol Rev 46:193–209
Spear FS (2014) The duration of near-peak metamorphism from diffusion modelling of garnet zoning. J Metamorph Geol 32:903–914
Spear FS, Daniel CG (2001) Diffusion control of garnet growth, Harpswell Neck, Maine, USA. J Metamorph Geol 19:179–195
Spear FS, Florence FP (1992) Thermobarometry in granulites: pitfalls and new approaches. Precambr Res 55:209–241
Spear FS, Kohn MJ (1996) Trace element zoning in garnet as a monitor of crustal melting. Geology 24:1099–1102
Spear FS, Selverstone J (1983) Quantitative *P–T* paths from zoned minerals: theory and tectonic applications. Contrib Mineral Petrol 83:348–357
Spear FS, Selverstone J, Hickmott D, Crowley PD, Hodges KV (1984) *P–T* paths from garnet zoning—a new technique for deciphering tectonic processes in crystalline terranes. Geology 12:87–90
Spear FS, Kohn MJ, Florence FP, Menard T (1991) A model for garnet and plagioclase growth in pelitic schists: Implications for thermobarometry and *P–T* path determinations. J Metamorph Geol 8:683–696
Spear FS, Thomas JB, Hallett BW (2014) Overstepping the garnet isograd: a comparison of QuiG barometry and thermodynamic modeling. Contrib Mineral Petrol 168
Spear FS, Pattison DRM, Cheney JT (2015). It's a mad, mad, mmad world. GSA Annual Meeting. Baltimore
Spear FS, Pattison DRM, Cheney JT (2016) The metamorphosis of metamorphic petrology. Geol Soc Am Spec Pap 523:31–73
Spiess R, Peruzzo L, Prior DJ, Wheeler J (2001) Development of garnet porphyroblasts by multiple nucleation, coalescence and boundary misorientation-driven rotations. J Metamorph Geol 19:269–290
Spry A (1963) The origin and significance of snowball structure in garnet. J Petrol 4:211–222
St-Onge MR (1987) Zoned poikiloblasic garnets: *P–T* paths and syn-metamorphic uplift through 30 km of structural depth, Wopmay Orogen, Canada. J Petrol 28:1–21
Stallard A, Ikei H, Masuda T (2002) Numerical simulations of spiral-shaped inclusion trails: can 3D geometry distinguish between end-member models of spiral formation? J Metamorph Geol 20:801–812
Štípská P, Powell R, White RW, Baldwin JA (2010) Using calculated chemical potential relationships to account for coronas around kyanite: an example from the Bohemian Massif. J Metamorph Geol 28:97–116
Stixrude L, Lithgow-Bertelloni C (2005) Thermodynamics of mantle minerals—I. Physical properties. Geophys J Inter 162:610–632
Storm LC, Spear FS (2005) Pressure, temperature and cooling rates of granulite facies migmatitic pelites from the southern Adirondack Highlands, New York. J Metamorph Geol 23:107–130
Stowell HH, Menard T, Ridgway CK (1996) Ca-metasomatism and chemical zonation of garnet in contact-metamorphic aureoles, Juneau Gold Belt, southeastern Alaska. Can Mineral 34:1195–1209
Stowell HH, Taylor DL, Tinkham DL, Goldberg SA, Ouderkirk KA (2001) Contact metamorphic *P–T–t* paths from Sm–Nd garnet ages, phase equilibria modelling and thermobarometry: Garnet Ledge, south-eastern Alaska, USA. J Metamorph Geol 19:645–660
Stowell H, Tulloch A, Zuluaga C, Koenig A (2010) Timing and duration of garnet granulite metamorphism in magmatic arc crust, Fiordland, New Zealand. Chem Geol 273:91–110
Stowell H, Parker KO, Gatewood M, Tulloch A, Koenig A (2014) Temporal links between pluton emplacement, garnet granulite metamorphism, partial melting and extensional collapse in the lower crust of a Cretaceous magmatic arc, Fiordland, New Zealand. J Metamorph Geol 32:151–175

Strickland A, Russell AK, Quintero R, Spicuzza MJ, Valley JW (2011) Oxygen isotope ratios of quartz inclusions in garnet and implications for mineral pair thermometry. Geol Soc Am Abstr with Programs 43:93

Stüwe K (1997) Effective bulk composition changes due to cooling: a model predicting complexities in retrograde reaction textures. Contrib Mineral Petrol 129:43–52

Sutton JR (1921) Inclusions in diamond from South Africa. Mineral Mag 19:208–210

Symmes GH, Ferry JM (1991) Evidence from mineral assemblages for infiltration of pelitic schists by aqueous fluids during metamorphism. Contrib Mineral Petrol 108:419–438

Tajčmanová L, Konopásek J, Connolly JAD (2007) Diffusion-controlled development of silica-undersaturated domains in felsic granulites of the Bohemian Massif (Variscan belt of Central Europe). Contrib Mineral Petrol 153:237–250

Taylor HP, Sheppard SMF (1986) Igneous rocks. 1. Processes of isotopic fractionation and isotope systematics. Rev Miner 16:227–271

Thompson AB (1976a) Mineral reactions in pelitic rocks: I. Prediction of *P*–*T*–X (Fe–Mg) phase relations. Am J Sci 276:401–424

Thompson AB (1976b) Mineral reactions in pelitic rocks: II. Calculation of some *P*–*T*–X (Fe–Mg) phase relations. Am J Sci 276:425–454

Thompson AB, Tracy RJ, Lyttle PT, Thompson JB (1977) Prograde reaction histories deduced from compositional zonation and mineral inclusions in garnet from the Gassetts schist, Vermont. Am J Sci 277:1152–1167

Thoni M (2002) Sm–Nd isotope systematics in garnet from different lithologies (Eastern Alps): age results, and an evaluation of potential problems for garnet Sm–Nd chronometry. Chem Geol 185:255–281

Tinkham DK, Ghent ED (2005) Estimating *P*–*T* conditions of garnet growth with isochemical phase-diagram sections and the problem of effective bulk-composition. Can Mineral 43:33–50

Tinkham DK, Zuluaga CA, Stowell HH (2001) Metapelite phase equilibria modeling in MnNCKFMASH: The effect of variable Al_2O_3 and MgO/(MgO+FeO) on mineral stability. Geol Mater Res 3:1–42

Tirone M, Ganguly J, Dohmen R, Langenhorst F, Hervig R, Becker, H-W (2005) Rare earth diffusion kinetics in garnet: Experimental studies and applications. Geochim Cosmochim Acta 69:2385–2398

Tracy RJ (1982) Compositional zoning and inclusions in metamorphic minerals. Rev Mineral 10:355–397

Tracy RJ, Robinson P, Thompson AB (1976) Garnet composition and zoning in the determination of temperature and pressure of metamorphism, central Massachusetts. Am Mineral 61:762–775

Tracy RJ, Caddick MJ, Thompson AB (2012) Garnet growth zoning in metapelites: not so simple after all, and revealing more than we once thought? GSA Annual Meeting

Valley JW (1986) Stable isotope geochemistry of metamorphic rocks. Rev Mineral 16:445–489

Valley JW (2001) Stable isotope thermometry at high temperatures. Rev Mineral Geochem 43:365–413

Valley JW, Bindeman IN, Peck WH (2003) Empirical calibration of oxygen isotope fractionation in zircon. Geochim Cosmochim Acta 67:3257–3266

van Breemen O, Hawkesworth CJ (1980) Sm–Nd isotopic study of garnets and their metamorphic host rocks. Transactions of the Royal Society of Edinburgh: Earth Sciences 71:97–102

Van der Molen I (1981) The shift of the α–β transition temperature of quartz associated with the thermal expansion of granite at high pressure. Tectonophysics 73:323–342

van Haren JLM, Ague JJ, Rye DM (1996) Oxygen isotope record of fluid infiltration and mass transfer during regional metamorphism of pelitic schist, Connecticut, USA. Geochim Cosmochim Acta 60:3487–3504

Van Orman JA, Grove TL, Shimizu N, Layne GD (2002) Rare earth element diffusion in a natural pyrope single crystal at 2.8 GPa. Contrib Mineral Petrol 142:416–424

Vance D, Harris N (1999) Timing of prograde metamorphism in the Zanskar Himalaya. Geology 27:395–398

Vance D, Holland T (1993) A detailed isotopic and petrological study of a single garnet from the Gassetts Schist, Vermont. Contrib Mineral Petrol 114:101–118

Vance D, Onions RK (1990) Isotopic chronometry of zoned garnets—growth-kinetics and metamorphic histories. Earth Planet Sci Lett 97:227–240

Vance D, Onions RK (1992) Prograde and retrograde thermal histories from the central Swiss Alps. Earth Planet Sci Lett 114:113–129

Vannay JC, Grasemann B (1998) Inverted metamorphism in the High Himalaya of Himachal Pradesh (NW India): Phase equilibria versus thermobarometry. Schweiz Mineral Petrograph Mitteil 78:107–132

Vannay JC, Sharp ZD, Grasemann B (1999) Himalayan inverted metamorphism constrained by oxygen isotope thermometry. Contrib Mineral Petrol 137:90–101

Vielzeuf D, Saúl A (2011) Uphill diffusion, zero-flux planes and transient chemical solitary waves in garnet. Contrib Mineral Petrol 161:638–702

Vielzeuf D, Champenois M, Valley JW, Brunet F, Devidal JL (2005) SIMS analyses of oxygen isotopes: Matrix effects in Fe–Mg–Ca garnets. Chem Geol 223:208–226

Viete DR, Hermann J, Lister GS, Stenhouse IR (2011) The nature and origin of the Barrovian metamorphism, Scotland: diffusion length scales in garnet and inferred thermal time scales. J Geol Soc London 168:115–131

Vorhies SH, Ague JJ (2011) Pressure–temperature evolution and thermal regimes in the Barrovian zones, Scotland. J Geol Soc London 168:1147–1166

Vrijmoed JC, Hacker BR (2014) Determining *P–T* paths from garnet zoning using a brute-force computational method. Contrib Mineral Petrol 167:1–13

Wang X, Planavsky NJ, Reinhard CT, Zou H, Ague JJ, Wu Y, Gill BC, Schwarzenbach EM, Peucker-Ehrenbrink B (2016) Chromium isotope fractionation during subduction-related metamorphism, black shale weathering, and hydrothermal alteration. Chem Geol 423:19–33

Waters D, Martin H (1993) The garnet–clinopyroxene–phengite barometer. Terra Abst 5:410–411

Waters DJ, Lovegrove DP (2002) Assessing the extent of disequilibrium and overstepping of prograde metamorphic reactions in metapelites from the Bushveld Complex aureole, South Africa. J Metamorph Geol 20:135–149

Watson EB, Cherniak DJ (2013) Simple equations for diffusion in response to heating. Chem Geol 335:93–104

Wendt I, Carl C (1991) The statistical distribution of the mean squared weighted deviation Chem Geol 86:275–285

White RW, Powell R, Holland TJB, Worley B (2000) The effect of TiO_2 and Fe_2O_3 on metapelitic assemblages at greenschist and amphibolite facies conditions: mineral equilibria calculations in the system K_2O–FeO–MgO–Al_2O_3–SiO_2–H_2O–TiO_2–Fe_2O_3. J Metamorph Geol 18:497–511

White RW, Pomroy NE, Powell R (2005) An in situ metatexite–diatexite transition in upper amphibolite facies rocks from Broken Hill, Australia. J Metamorph Geol 23:579–602

White RW, Powell R, Baldwin JA (2008) Calculated phase equilibria involving chemical potentials to investigate the textural evolution of metamorphic rocks. J Metamorph Geol 26:181–198

White RW, Powell R, Holland TJB, Johnson TE, Green ECR (2014a) New mineral activity–composition relations for thermodynamic calculations in metapelitic systems. J Metamorph Geol 32:261–286

White RW, Powell R, Johnson TE (2014b) The effect of Mn on mineral stability in metapelites revisited: new *a–X* relations for manganese-bearing minerals. J Metamorph Geol 32:809–828

Whitney DL, Seaton NCA (2010) Garnet polycrystals and the significance of clustered crystallization. Contrib Mineral Petrol 160:591–607

Whitney DL, Goergen ET, Ketcham RA, Kunze K (2008) Formation of garnet polycrystals during metamorphic crystallization. J Metamorph Geol 26:365–383

Williams ML, Jercinovic MJ, Hetherington CJ (2007) Microprobe monazite geochronology: understanding geologic processes by integrating composition and chronology. Ann Rev Earth Planet Sci 35:137

Williams HM, Nielsen SG, Renac C, Griffin WL, O'Reilly SY, McCammon CA, Pearson N, Viljoen F, Alt JC, Halliday AN (2009) Fractionation of oxygen and iron isotopes by partial melting processes: Implications for the interpretation of stable isotope signatures in mafic rocks. Earth Planet Sci Lett 283:156–166

Williams ML, Jercinovic MJ, Mahan KH, Dumond G (2017) Electron microprobe petrochronology. Rev Mineral Geochem 83:153–182

Wing BA, Ferry JM, Harrison TM (2003) Prograde destruction and formation of monazite and allanite during contact and regional metamorphism of pelites: petrology and geochronology. Contrib Mineral Petrol 145:228–250

Wood BJ, Banno S (1973) Garnet–orthopyroxene and orthopyroxene–clinopyroxene relationships in simple and complex systems. Contrib Mineral Petrol 42:109–124

Woodsworth GJ (1977) Homogenization of zoned garnets from pelitic schists. Can Mineral 15:230–242

Wu C-M, Zhao G (2006) Recalibration of the garnet–muscovite (GM) geothermometer and the garnet–muscovite–plagioclase–quartz (GMPQ) geobarometer for metapelitic assemblages. J Petrol 47:2357–2368

Wu C-M, Zhang J, Ren L-D (2004) Empirical garnet–biotite–plagioclase–quartz (GBPQ) geobarometry in medium- to high-grade metapelites. J Petrol 45:1907–1921

Wu C-M, Cheng B-H (2006) Valid garnet–biotite (GB) geothermometry and garnet–aluminum silicate–plagioclase–quartz (GASP) geobarometry in metapelitic rocks. Lithos 89:1–23

Yakymchuk C, Brown M (2014) Consequences of open-system melting in tectonics. J Geol Soc London

Yakymchuk C, Brown M, Clark C, Korhonen FJ, Piccoli PM, Siddoway CS, Taylor RJM, Vervoort JD (2015) Decoding polyphase migmatites using geochronology and phase equilibria modelling. J Metamorph Geol 33:203–230

Yakymchuk C, Clark C, White RW (2017) Phase relations, reaction sequences and petrochronology. Rev Mineral Geochem 83:13–53

Yang PS, Pattison D (2006) Genesis of monazite and Y zoning in garnet from the Black Hills, South Dakota. Lithos 88:233–253

Yang P, Rivers T (2001) Chromium and manganese zoning in pelitic garnet and kyanite: Spiral, overprint, and oscillatory (?) zoning patterns and the role of growth rate. J Metamorph Geol 19:455–474

Yang P, Rivers T (2002) The origin of Mn and Y annuli in garnet and the thermal dependence of P in garnet and Y in apatite in calc- pelite and pelite. Gagnon terrane, western Labrador. Geol Mater Res 4:1–35

Yardley BWD (1977) An empirical study of diffusion in garnet. Am Mineral 62:793–800

Young ED, Rumble D (1993) The origin of correlated variations in insitu $^{18}O/^{16}O$ and elemental concentrations in metamorphic garnet from southeastern Vermont, USA. Geochim Cosmochim Acta 57:2585–2597

Zack T, John T (2007) An evaluation of reactive fluid flow and trace element mobility in subducting slabs. Chem Geol 239:199–216

Zack T, Tomascak PB, Rudnick RL, Dalpe C, McDonough WF (2003) Extremely light Li in orogenic eclogites: The role of isotope fractionation during dehydration in subducted oceanic crust. Earth Planet Sci Lett 208:279–290

Zeng L, Asimow PD, Saleeby JB (2005) Coupling of anatectic reactions and dissolution of accessory phases and the Sr and Nd isotope systematics of anatectic melts from a metasedimentary source. Geochim Cosmochim Acta 69:3671–3682

Zhang Y (1998) Mechanical and phase equilibria in inclusion–host systems. Earth Planet Sci Lett 157:209–222

Zheng YF (1991) Calculation of oxygen isotope fractionation in metal-oxides. Geochim Cosmochim Acta 55:2299–2307

Zheng YF (1993) Calculation of oxygen-isotope fractionation in hydroxyl-bearing silicates. Earth Planet Sci Lett 120:247–263

Zheng Y-F, Fu B, Li Y, Xiao Y, Li S (1998) Oxygen and hydrogen isotope geochemistry of ultrahigh-pressure eclogites from the Dabie Mountains and the Sulu terrane. Earth Planet Sci Lett 155:113–129

Zheng YF, Zhao ZF, Wu YB, Zhang SB, Liu XM, Wu FY (2006) Zircon U–Pb age, Hf and O isotope constraints on protolith origin of ultrahigh-pressure eclogite and gneiss in the Dable orogen. Chem Geol 231:135–158

Zhou B, Hensen BJ (1995) Inherited Sm/Nd isotope components preserved in monazite inclusions within garnets in leucogneiss from East Antarctica and implications for closure temperature studies. Chem Geol 121:317–326

Zhukov VP, Korsakov AV (2015) Evolution of host-inclusion systems: a visco-elastic model. J Metamorph Geol 33:815–828.